PERFORMANCE ENHANCEMENT OF VAPOR COMPRESSION REFRIGERATION SYSTEM

Thesis submitted in

partial fulfilment of the requirements for the degree of

DOCTOR OF PHILOSOPHY

in

MECHANICAL ENGINEERING

Submitted

By

Naveen Solanki

(2K16/PHD/ME/51)

Under the Supervision

Of

Dr. Akhilesh Arora
(Professor)
Mechanical Engineering

Dr. Raj Kumar Singh
(Professor)
Mechanical Engineering

Department of Mechanical Engineering,
Delhi Technological University, Shahabad Daulatpur, Delhi- 110042, India

2024

CERTIFICATE OF THE SUPERVISOR

It is certified that **Mr. Naveen Solanki** has worked for his Doctoral Thesis on the topic entitled **"Performance Enhancement of Vapor Compression Refrigeration System"** under our supervision. This is an original work and all the help taken during the course of the study has been duly acknowledged. We find it worthy of submission for Ph.D. degree and recommend that the same may be sent for evaluation.

To the best of our knowledge, this work has not been submitted in part or full for any Degree or Diploma to this University or elsewhere, and it is free from plagiarism.

Dr. Akhilesh Arora
(Professor)
Department of Mechanical Engineering

Dr. Raj Kumar Singh
(Professor)
Department of Mechanical Engineering

Date:

Place:

STUDENT DECLARATION

I, hereby declare that the Thesis entitled **"Performance Enhancement of Vapor Compression Refrigeration System"** being submitted to Delhi Technological University, Shahabad Daulatpur, Delhi- 110042, India, is an original piece of work done by me and has not been published or submitted elsewhere for any other degree in full or in part.

I, declare that I have faithfully acknowledged, given credit, and referenced the authors/researchers whenever their works have been cited in the text and throughout the body of this thesis. I further certify that I have not willfully lifted up some other's work, para, text, data, results, figures etc. reported in the journals, books, magazines, reports, dissertations, thesis etc., or available at web-sites and included them in this Ph.D. Dissertation/Thesis and cited as my own work.

Date: Name: **Naveen Solanki**

Place: Enrolment No: **2K16/Ph.D/ME/51**

Verification

This is to certify that the above statement made by **Mr. Naveen Solanki** is correct to the best of our knowledge. Certified that a check for plagiarism has been made on the software available in the University and the contents of thesis have been found free from plagiarism.

Dr. Akhilesh Arora
(Professor)
Department of Mechanical Engineering

Dr. Raj Kumar Singh
(Professor)
Department of Mechanical Engineering

ACKNOWLEDGEMENTS

I am profoundly grateful to my supervisors, **Prof. (Dr.) Akhilesh Arora** and **Prof. (Dr.) Raj Kumar Singh**, from the Department of Mechanical Engineering at Delhi Technological University, Delhi, India. Their consistent guidance, support, and extensive knowledge have been invaluable. Throughout my research, **Prof. (Dr.) Akhilesh Arora** stood by me like a generous mentor, offering support, assistance, and valuable guidance. I extend my sincere thanks to **Prof. (Dr.) Raj Kumar Singh**, who has been with me since the beginning of my research, guiding me through every phase and the thesis writing process. I feel fortunate to have mentors who not only granted me the freedom to explore and research independently but also provided guidance for crucial decisions. They have helped me explore this vast topic in an organized manner and provided me with all the ideas on how to work towards a research oriented venture.

I would like to express my sincere thanks to **Dr. Vaibhav Jain,** HOD Department of Mechanical Engineering, MAIT, Delhi, who consistently supported me whenever I needed help and guided me through all the highs and lows to finish my research work and write my thesis, and **Dr. V. N. Mathur**, HOD Department of Mechanical and Automation Engineering, MAIT, Delhi, for their support and encouragement throughout this period.

I am grateful to **Dr. Ramakant Rana**, Instructional Designer, Holmesglen, Melbourne, Australia who was always there when I needed a help and boosted me to complete my research work. I am also thankful to **Dr. Anupam Thakur**, Assistant Professor, MAIT who was always there to help me and give a positive motivation throughout my journey of this research work. I would like to thank **Dr. Naushad Ahmad Ansari (DTU)** and **Dr. Deshdeep Gambhir (MAIT)** for their technical support.

I am always in debt to my parents **Mr. Phool Kumar Solanki** and **Mrs. Santosh Devi,** for providing me with all the energy booster thoughts, opportunities, and motivation that helped me to complete my Ph.D.

I am truly grateful for the immense love, encouragement, and unwavering support from my wife, **Mrs. Deepika**, throughout the entirety of my research journey. Her understanding and encouragement allowed me to fully concentrate on my work, and without her support, completing my Ph.D. would not have been possible. I also want to express my heartfelt appreciation to my kids, **Avisha Solanki** and **Avyaan Solanki**, for their patience and understanding during this challenging period. Their presence and positivity added immeasurable strength to complete my Ph.D.

Last but not the least; I would like to thank the almighty for showing me the right direction out of the blue, to help me stay calm in the oddest of the times and keep moving even at times when there was no hope.

Naveen Solanki

Enrolment No: 2K16/Ph.D/ME/51

ABSTRACT

This thesis presents a comprehensive exploration of dedicated mechanical subcooled vapor compression refrigeration (DMS-VCR) system, focusing on their performance, optimization, and environmental implications in commercial chiller applications. The research aims to conduct a thorough analysis of the DMS-VCR system, considering aspects such as energy, exergy, environment and economic (4E analysis).

The findings reveal promising prospects for the DMS-VCR system in enhancing environmental sustainability and energy efficiency in refrigeration applications. Notably, significant reductions in power consumption and CO_2 emissions are observed compared to equivalent vapor compression refrigeration system, suggesting its potential to mitigate environmental impacts associated with traditional cooling technologies. Specifically, the proposed system reduces compressor power consumption by 10.45% and CO_2 emissions by 10.43%. Moreover, thermoeconomic optimization demonstrates that the DMS-VCR system offers lower annual operating costs, being 6.72% more cost effective than conventional VCR system. Optimization further yield additional cost reductions of 1.88% (in Case-I) and 16.36% (in Case-II), highlighting its economic viability.

The thesis incorporates advanced exergy analysis (AEA) methodologies, including coefficient of structural bond (CSB) analysis, to further investigate the DMS-VCR system's performance. CSB values for various system components provide insights into their efficiency and contributions to irreversibility rates. Additionally, AEA techniques identify the system's potential performance and areas for optimization. By enhancing component parameter efficiency, it is possible to reduce irreversibility rates and improve system performance significantly.

Furthermore, while the DMS-VCR system may require slightly higher initial investment due to additional heat exchanger area requirements, the long-term operational cost savings and environmental benefits outweigh the initial capital expenditure. Thermoeconomic optimization allows for independent optimization of key components, resulting in lower annual operating costs compared to equivalent vapor compression systems.

The present work majorly is based on the theoretical investigation of DMS-VCR system; however, a prototype experimental test facility has been developed for the

preliminary analysis of DMS-VCR system to provide confidence in the theoretical finding. The experimental result showed that the COP of the VCR system is improved in the range of 3.05 to 3.69 (for different Sets of reading) due to subcooling with inclusion of DMS technique.

In summary, this thesis offers a comprehensive overview of multiple studies conducted on the DMS-VCR system, highlighting its potential to revolutionize the refrigeration industry by offering more energy-efficient, environmentally responsible, and economically viable cooling solutions.

CONTENTS

LIST OF FIGURES

LIST OF TABLES

NOMENCULATURE

a^c	recovery factor of capital
C_{env}	annual environment damage cost ($/year)
C_{co_2}	penalty cost of CO_2 emissions ($/tonnes of CO_2 emission)
C_i^{el}	cost per kilowatt-hour of electricity ($/kWh)
$\dot{C}_t$	the overall annual cost of the system ($/year)
C	thermal capacitance rate (kW. K^{-1})
c_p	specific heat (kJ.kg^{-1}.K^{-1})
F_i, F_o	interior and exterior fouling factors (m^2.K/kW)
h	enthalpy (specific, kJ.kg^{-1})
h_i, h_o	inner and outer convective coefficient of heat transfer (kW/m^2.K)
i_{rate}	rate of interest (%)
$\dot{I}$	irreversibility (rate, kW)
k	thermal conductivity of material (kW/m^2. K)
$\dot{m}$	flow rate of mass (kg/s)
m_{co_2}	annual emission of carbon dioxide (ton)
P	state point pressure (kPa)
PR	pressure ratio between high and low pressure side
N_y	time frame for repayment (years)
$\dot{Q}$	heat transfer(kW)
S	entropy (specific, kJ. kg^{-1}.K^{-1})
t_{oper}	annual operational hours (h)
T	temperature (K)
ΔT_m	mean temperature difference in logarithmic scale (LMTD, in Kelvin)
U	coefficient of overall heat transfer (kW/m^2. K)
VCRS	vapor compression refrigeration system
$\dot{W}$	power input rate (kW)
x	quality
Z_k	capital cost of K subsystem ($)
Z_t	the overall cost of the system

Greek Symbols

$\in$	effectiveness
η	efficiency
λ	conversion factor of Co_2 emission (kg/kWh)
ϕ	the maintenance factor
Ψ	chemical, potential, kinetic, and physical exergy of matter

Superscripts

in	inlet
out	outlet
Q	heat
W	Work
AVO	avoidable
END	endogenous
EXO	exogenous
UNA	unavoidable

Subscripts

k	k^{th} element of a system
ref	refrigerant
o	environment condition
EoS	element or subsystem
comp	compressor
cond	condenser
dl	discharge line
EoE	element or subsystem
ef	external fluid
ev	expansion valve
evap	evaporator
isen	isentropic
in	inlet condition
mod	current model
n	n^{th} element of system

out	outlet condition
o	environment condition
ol	overlap
sc	subcooling
sl	suction line
t	total
z_i	system efficiency parameter
II	second law
1,2,3…..	state points

Abbreviations

AEA	advance exergy analysis
CSB	coefficient of structural bonds
COP	coefficient of performance
DMS	dedicated mechanical subcooled
DOS	degree of subcooling
DOO	degree of overlap
EES	engineering equation solver
ED	Exergy Destruction
VCRS	vapor compression refrigeration system
VCRC	vapor compression refrigeration cycle

CHAPTER 1

INTRODUCTION

This chapter provides an in-depth introduction to the vapor compression refrigeration system and the techniques utilized to improve its performance while minimizing power consumption.

1.1 INTRODUCTION

Refrigeration, a process that involves transferring heat from a low-temperature region to a high-temperature region, plays a crucial role in various aspects of modern life. This thermal management process is commonly executed through a cycle that employs a specific refrigerant or working fluid. Among the various refrigeration cycles, the vapor compression refrigeration cycle (VCRC) stands out as the most widely used in applications such as refrigerators, air-conditioning systems, and heat pumps. The vapor compression refrigeration system (VCRS) is a significant consumer of energy globally, finding applications in commercial, residential, and industrial sectors for purposes like cooling, heating, and food preservation.

Refrigeration and air conditioning have played vital roles in enhancing human living conditions over time, closely linked to the development of diverse refrigerants and system components. Energy consumption significantly affects economic development, especially during high-demand periods like hot summers. Escalating fuel costs and global environmental concerns highlight the need for analyzing refrigeration systems. The temperature difference between the evaporator and condenser in VCRS leads to higher compressor power usage and reduced cooling efficiency per unit, particularly challenging in extreme weather conditions. Scientists are thus investigating sustainable and energy-efficient solutions to address these challenges and mitigate costs and environmental impact. The global environmental challenges, including environmental degradation, rising energy needs, global warming, and ozone layer depletion, underscore the urgency for efficient energy use in practical applications. Researchers, faced with the substantial costs associated with traditional refrigeration system, are investigating alternative solutions to meet the demands for thermal comfort in both industrial and domestic sectors. Achieving higher efficiency in vapor compression refrigeration is paramount, and various methods are employed to increase the Coefficient of Performance (COP). Advanced subcooling techniques, such as optimizing liquid suction heat exchangers and fine-tuning with mechanical subcooling systems (e.g. Dedicated mechanical subcooled system and Integrated mechanical subcooled system),

directly contribute to enhance the COP. Incorporating enhanced heat exchanger designs, variable-speed compressors, and improved refrigerants with superior thermodynamic properties further elevates system efficiency. Smart control strategies, dynamically adjust parameters, synchronization and efficiency of both cycles in mechanical subcooling systems are crucial. Collectively, these strategies promote a higher COP, ensuring that vapor compression refrigeration systems operate at their optimal level of performance while minimizing energy consumption and environmental impact. Reducing power consumption for refrigeration applications is a key goal to enhance efficiency and environmental friendliness. Numerous studies have demonstrated performance improvements through the mechanical subcooling of vapor compression refrigeration system (VCRS). Refrigeration plays a vital role in our lives and global energy usage, from its historical importance to current challenges and sustainable advancements. The pursuit of mechanical subcooling represents progress towards energy-efficient and eco-friendly refrigeration systems, meeting present needs and fostering a sustainable future.

The process of analyzing refrigeration systems to determine their energy efficiency is another matter that requires consideration. The conventional approach to evaluate refrigeration systems is energy analysis. Only energy conservation is covered by the first law of thermodynamics; it gives no details on the extent, mode, or location of system performance degradation. Energy analysis ignores the idea of energy quality. Therefore, exergy analysis, which is based on the second law of thermodynamics, overcomes the limitations of energy analysis. Exergy analysis is an important tool in the design, optimization and performance evaluation of refrigeration systems. In order to enhance operation, it is often meant to determine the system's maximum performance as well as the locations, reasons, and actual amounts of available energy losses. Complex cooling systems ask for larger initial investment costs since they incorporate a larger number of components. As a result, it requires economic analysis, especially when their thermodynamic parameters change. In order to give refrigeration system designers information which is not available through conventional energy analysis and economic evaluation, thermoeconomic integrates thermodynamics with economics. This knowledge is essential for the design and operation of a cost-effective system.

1.2 MOTIVATION OF THE RESEARCH

The motivation for the research stems from the global challenge of balancing the escalating demand for refrigeration with the crucial to reduce energy consumption. In many parts of the world, a significant portion of the population faces limited access to electricity, intensifying

the need for innovative solutions in refrigeration technology. The refrigeration sector, known for its substantial power consumption, contributes significantly to operational costs in various industries. High energy demands, coupled with concerns about environmental sustainability, prompt us to explore novel approaches to enhance the efficiency of refrigeration systems.

This research represents a critical response to the escalating energy crisis, which demands innovative solutions to mitigate its impact. It aims to address this energy crisis by focusing on the implementation of a dedicated mechanical subcooled vapor compression refrigeration system. This innovative approach seeks to amplify the cooling effect while minimizing electricity consumption, presenting a promising avenue for more sustainable and economically viable refrigeration solutions. By introducing a subcooling loop into the existing VCR system, this work aspires to revolutionize the energy efficiency of refrigeration systems on a global scale. This research is not only about the advancing technology but also about contributing to a more sustainable and energy-efficient future.

1.3 OBJECTIVES AND SCOPE OF THE THESIS

The specific objectives of the present thesis are as follows:

i) To carry out energy & exergy analysis of the DMS-VCR system for a pair of refrigerants such as R134a, R410A and other combination, i.e. theoretical analysis.
ii) To carry out the thermoeconomic and environmental analysis of the dedicated mechanical subcooled vapor compression refrigeration system.
iii) To carry out the thermodynamic and coefficient of structural bond analysis of actual dedicated mechanical subcooled vapor compression refrigeration system.
iv) To carry out the advance exergy and coefficient of structural bond analysis of dedicated mechanical subcooled vapor compression refrigeration system.
v) To design and develop prototype of dedicated mechanical subcooled vapor compression refrigeration system.
vi) To carry out the experimental analysis of dedicated mechanical subcooled vapor compression refrigeration system.

1.4 ORGANIZATION OF THE THESIS

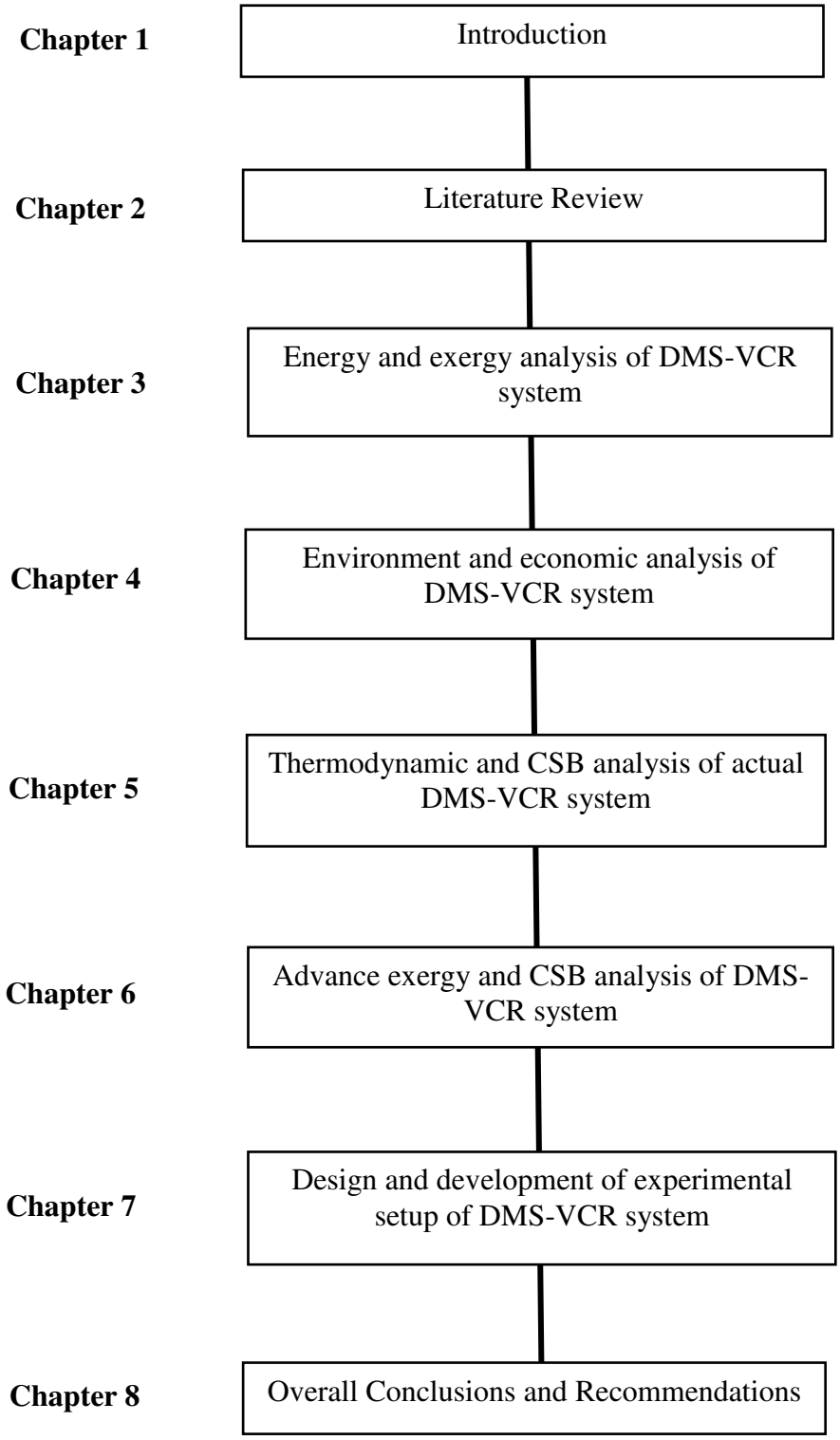

Figure 1.1 Structure of thesis

The thesis consists of eight Chapters which are summarized as follow:

Chapter 1: Introduction

This Chapter presents an overview of dedicated mechanical subcooled vapor compression refrigeration system. It delves into the pivotal role of refrigeration in modern life, highlighting the importance of vapor compression refrigeration cycle's (VCRC). It underscores the energetic and exergetic intensive nature of vapor compression refrigeration systems (VCRS) and explores its past evolution. This Chapter emphasizes the connection between energy consumption, economic development, and environmental concerns. Focusing on sustainability, it introduces mechanical subcooling as a key strategy to enhance system efficiency. Additionally, it advocates for exergy analysis, integrating thermodynamics and economics, to optimize the energy efficiency of refrigeration systems for cost-effectiveness. Further, the objectives of the thesis along with Chapter wise organization of the thesis are presented in this Chapter.

Chapter 2: Literature review

This Chapter thoroughly explores various aspects concerning vapor compression refrigeration systems. It covers both theoretical and experimental studies, providing insight into their academic and practical operation. Special attention is given to subcooling and the thermodynamic properties of refrigerants. Advanced exergy and coefficient of structural bond analysis are also discussed, offering insight into recent advancements. Key findings from the literature survey are highlighted, along with identified research gaps, setting the stage for further investigation. Lastly, this Chapter outlines specific objectives for the current work, aiming to address the gaps and enhance understanding within the field of vapor compression refrigeration systems.

Chapter 3: Energy and exergy analysis of dedicated mechanical subcooled vapor compression refrigeration system

This Chapter delves into the crucial role of energy and exergy analysis in optimizing dedicated mechanical subcooled vapor compression refrigeration (DMS-VCR) systems, widely used for cooling in various applications. This Chapter explores the complex thermodynamic cycles of DMS-VCR system, emphasizing the significance of energy and exergy analysis for assessing system efficiency. The research, comparing DMS-VCR system with traditional systems for water chiller applications, reveals a 19°C optimum subcooling degree, yielding a 11.67% higher Coefficient of Performance (COP) and a 10.45% reduction

in compressor power consumption. Exergy analysis indicates a 15.71% reduction in total irreversibility and a 10.38% increase in exergetic efficiency for DMS-VCRS. Parametric analysis underscores the influence of evaporator and condenser temperatures, degree of overlap, and subcooling on system performance. In conclusion, the study highlights the need to consider both the energy and exergy aspects for designing efficient cooling systems, providing valuable insights for achieving optimal system performance.

Chapter 4: Environment and economic analysis of dedicated mechanical subcooled vapor compression refrigeration system

This Chapter explore the environmental and economic analysis of dedicated mechanical subcooled vapor compression refrigeration (DMS-VCR) system for 100 kW water chiller applications, addressing the rising global demand for efficient and environment friendly refrigeration. The study reveals a 19°C optimum subcooling degree, leading to a 10.45% reduction in compressor power consumption, substantial cost savings, and a 10.43% decrease in CO_2 emissions. Despite a 6.07% increase in heat exchanger area, the DMS-VCRS proves more cost-effective, reducing overall operational costs by 6.72% and CO_2 production mass by 10.43%. Parametric analysis emphasizes the significance of degree of overlap and subcooling for optimal performance and cost-effectiveness. In summary, the research underscores the need for a holistic approach considering thermodynamics, economics, and environmental impact for designing efficient and cost-effective cooling systems.

Chapter 5: Thermodynamic and coefficient of structural bond analysis of actual dedicated mechanical subcooled vapor compression refrigeration system

This Chapter addresses the energy efficiency of vapor compression refrigeration (VCR) systems, widely used for heating and cooling. To enhance performance and mitigate energy consumption, dedicated mechanical subcooled (DMS) systems are explored, focusing on energy, exergy, and Coefficient of Structural Bond (CSB) analysis. The results, obtained at constant condenser temperature and variable evaporator temperatures, demonstrate that the actual DMS-VCR system outperforms a simple VCR system. At 0°C evaporator temperature, DMS-VCR system reduces compressor-1 work input by 8.65%, increases COP and exergetic efficiency by 4.60% and 4.38%, respectively, leading to lower operating costs. Exergy analysis reveals a 4.68% decrease in total irreversibility compared to the VCR system. CSB analysis identifies evaporator and condenser-1 as crucial components for improving system efficiency and increasing exergetic efficiency.

Chapter 6: Advance exergy and coefficient of structural bond analysis of dedicated mechanical subcooled vapor compression refrigeration system

This Chapter explores the innovative application of advanced exergy analysis and Coefficient of Structural Bond (CSB) analysis to dedicated mechanical subcooled vapor compression refrigeration (DMS-VCR) system, an evolving technology in heating and cooling applications. Distinguished by its comprehensive approach, the study surpasses previous works by integrating advanced exergy and CSB analysis, providing unique insights into system performance. Results show that a 15°C subcooling level optimizes overall COP and minimizes total irreversibility. In comparison to conventional VCR systems, the DMS system exhibits a 7.6% reduction in compressor work input, an 8.2% increase in COP, and an 11% decrease in overall irreversibility. Further, CSB and advanced exergy analysis identify areas for potential improvements, emphasizing the significance of enhancing component efficiency for overall system performance. This Chapter offers valuable contributions towards designing energy-efficient and environmentally sustainable vapor compression refrigeration systems.

Chapter 7: Design and development of experimental setup of dedicated mechanical subcooled vapor compression refrigeration system

This Chapter go through into the design and development of an experimental setup customized for dedicated mechanical subcooled vapor compression refrigeration (DMS-VCR) system. Amidst the escalating demand for energy-efficient and environmentally friendly refrigeration system, this innovation holds promise in revolutionizing the industry. Vapor compression refrigeration systems, connected to various sectors, face challenges of efficiency and environmental impact. Subcooling emerges as a solution, offering improved system performance and adaptability, crucial in regions with high ambient temperatures. This C hapter outlines the objectives, emphasizing efficiency improvement, enhanced cooling capacity, environmental impact assessment, component optimization, and system reliability. The experimental setup reflects a commitment to advancing refrigeration technology for a more sustainable and energy efficient future.

Chapter 8: Overall Conclusions and Recommendations

In this Chapter, overall conclusions of the present investigations are presented. The appropriate suggestions and recommendations for further work are also mentioned in the Chapter.

CHAPTER 2

LITERATURE REVIEW

This chapter presents a detailed literature survey about the vapor compression refrigeration system and development of mechanical subcooling using different parameters with simulations of different ideas on multiple refrigerants.

2.1 INTRODUCTION

Vapor compression refrigeration systems play a foundational role in various applications spanning industrial processes to household cooling solutions. This literature survey is designed to thoroughly explore both theoretical frameworks and experimental studies related to vapor compression refrigeration systems, setting the stage for a well-informed and substantiated thesis. In this Chapter, a comprehensive review of the literature on vapor compression refrigeration systems is presented, with a specific focus on dedicated mechanical subcooled vapor compression refrigeration systems. Additionally, advanced exergy and coefficient of structural bond analysis of refrigeration systems are discussed, providing a holistic understanding of the current state of research in this field.

2.2 LITERATURE SURVEY ON THEORETICAL AND EXPERIMENTAL STUDIES OF VAPOR COMPRESSION REFRIGERATION SYSTEM

Chen and Lin [1] presented a fundamental principle and approach for attaining efficient matching to minimize energy consumption in small-scale refrigeration systems through systems analysis. A thorough grasp of the dynamic features of a refrigeration system is essential for accurate performance prediction. To showcase optimal matching, a simulation model of a refrigeration system, including a compressor, evaporator, condenser, and capillary tube, has been developed. Mathematical models have been developed for each component, incorporating the concept of transient and distributive parameters. Through dynamic simulation, a recommended method of optimal matching is proposed to minimize power consumption. An experiment on a small-scale refrigeration system was conducted to validate the reliability of the theoretical models.

Wang et al. [2] explored ways to enhance the efficiency of compressors in cooling systems, given their substantial power consumption. Two primary strategies were investigated for various cooling liquids (R22, R134a, R410A, and R744). The first involved exploring the potential benefits of cooling the motor externally, especially for R22, R410A, and R744, indicating potential advantages in refrigeration applications. The second approach focused on

achieving a more uniform compression process by transferring heat from the compression chamber. By combining different air compression methods, this approach showed a potential 14% reduction in compressor workload, leading to an overall system efficiency improvement. When applied to the entire cooling system, these innovations could potentially result in energy savings of approximately 16%, contingent on operating conditions and the chosen cooling liquid.

Arora and Kaushik [3] conducted a theoretical analysis of a vapor compression refrigeration system utilizing R502, R404A, and R507A. This study provides a thorough examination of the exergy aspects within an actual vapor compression refrigeration (VCR) cycle. A computational model was developed to assess crucial parameters, including coefficient of performance (COP), exergy destruction, exergetic efficiency, and efficiency defects for the specified refrigerants—R502, R404A, and R507A. The investigation considered evaporator temperatures ranging from -50°C to 0°C and condenser temperatures from 40°C to 55°C. The results indicate that, among the examined refrigerants, R507A emerges as a more suitable alternative to R502 compared to R404A. Significantly, the efficiency defect is highest in the condenser and lowest in the liquid-vapor heat exchanger for the analyzed refrigerants.

Khan and Zubair [4] evaluated the effectiveness of a vapor compression system by studying performance curves that illustrate the relationship between the inverse coefficient of performance (1/COP) and the inverse cooling capacity ($1/Q_{evap}$). They employed a finite-time thermodynamic model to replicate actual system operations, uncovering linear performance curves attributed to losses arising from irreversibilities in heat transfer, non-isentropic compression, and expansion. The model's versatility extends to study variable-speed refrigeration systems and predicting optimal heat-exchanger area distribution. Additionally, the analysis explores the impact of subcooling and superheating on system performance.

Winkler et al. [5] conducted a comprehensive investigation into numerical methods for simulating steady-state vapor compression systems, focusing on three distinct algorithms designed for modular/component-based systems. The enthalpy marching solver stood out as superior in both robustness and computational efficiency, successfully solving 97% of test cases. The study emphasized the importance of investing computational effort in obtaining accurate initial guess values for improved overall efficiency. Additionally, the impact of different closure equations on numerical performance was explored, providing insights into algorithm efficacy across a test matrix.

Cabello et al**.** [6] presented a simplified model for a single-stage vapor compression system, using fundamental physical equations and empirical correlations. The model outputs key

parameters like refrigerant mass flow rate, cooling capacity, compression power consumption, and COP based on operating variables. Its utility lies in analyzing how major factors influence energy performance. Validation against experimental data for R134a, R407C, and R22 revealed model predictions within ±5% for mass flow rate and specific refrigerating effect, and within ±10% for other energy parameters.

Aprea and Greco [7] addressed the challenge of replacing R22 in refrigeration plants by exploring R407C as a potential alternative. Experimental tests in a vapor compression plant with a reciprocating compressor compared the performance of R407C to R22, with a focus on assessing both compressor and overall plant energy efficiency. The consistent findings indicate that R22 outperforms R407C due to varying irreversibilities in system components, particularly in compressor irreversibilities. Performance indices highlight R22's superiority, attributed to a more efficient compression process, including better isentropic and volumetric efficiencies of the semi-hermetic compressor.

Chakravarthy et al. [8] extensively reviewed the refrigeration methods across a temperature range of 4 K to 300 K. It covers steady-state and periodic systems, summarizes current technology and challenges, and provides comparisons. The key message is that selecting the right refrigeration method depends on factors like capacity, temperature, and application environment, considering cost, reliability, size, and power. The paper aims to offer detailed insights into engineering, serve as a practical resource for industry designers, and provide guidance on method selection.

Yao et al. [9] presented a transient response model for a vapor compression refrigeration system, consisting of four sub-models. Using a moving-boundary approach, the condenser and evaporator models are formulated, and linearization transforms them into a state-space matrix. The compressor and electronic expansion valve (EEV) utilize steady models. Experimental validation shows good agreement, with simulation errors mostly below 10%. The state-space matrix format enhances portability and computational efficiency, making it suitable for studying thermal dynamics and developing control schemes under various conditions.

Nunes et al. [10] presented a simple mathematical model designed to enhance the responsiveness of a vapor compression refrigeration system. The model integrates thermodynamic principles, heat and mass transfer, and empirical correlations to formulate a set of ordinary differential equations. Validated through experiments with an industrial chiller, the model identifies optimal parameters. The research investigates heat exchanger area inventory optimization to minimize pull-down time and compares the performance of three refrigerants (R12, R134a, R1234yf). Results show that R1234yf performs closer to R12 than R134a. The

study identifies the optimal heat transfer area distribution for maximum system efficiency. Emphasizing the importance of a second-law assessment for realistic results, especially in optimizing for pull-down time versus coefficient of performance (COP), the study notes significant variations in maxima and minima with changes in heat exchanger coefficients.

Sayyaadi and Nejatolahi [11] They introduces an innovative method for optimizing a cooling tower-assisted vapor compression refrigeration system, considering both thermodynamic and economic factors in system design and component selection. It calculates irreversibility and develops an economic model using the total revenue requirement (TRR) method. Utilizing a multi-objective evolutionary algorithm, the optimization involves eight decision variables with engineering constraints. Three optimization scenarios - thermodynamic, economic, and multi-objective are explored. The multi-objective optimization, addressing both thermodynamic and economic objectives simultaneously, proves more comprehensive than single-objective designs. Results indicate that the multi-objective approach better satisfies both criteria, offering a more balanced solution. Deviation percentages from ideal values provide a comprehensive evaluation of the system's performance.

2.3 LITERATURE SURVEY ON SUBCOOLING OF VAPOR COMPRESSION REFRIGERATION SYSTEM

Selbas et al. [12] **c**onducted a study on optimizing vapor compression refrigeration cycles using exergy analysis, considering both subcooled and superheated conditions. The exergy method allows for the individual optimization of key components like condensers, evaporators, sub-cooling, and superheating heat exchangers. The research focused on determining the optimal heat exchanger areas and corresponding sub-cooling and superheating temperatures, establishing a cost function for these conditions. Three refrigerants—R22, R134a, and R407c—were analyzed using thermodynamic properties derived from the artificial neural network methodology.

Park et al. [13] presented a comprehensive overview of recent studies on advanced vapor compression cycle technologies, classifying them into three groups: subcooling cycles, expansion loss recovery cycles, and multi-stage cycles. Subcooling cycle research focuses on suction-line heat exchangers, thermoelectric subcoolers, and mechanical subcoolers, while expansion loss recovery cycles explore the use of expanders and ejectors. Multi-stage cycle research includes vapor or liquid refrigerant injection cycles and two-phase refrigerant injection cycles. The paper reviews these technologies, discusses their effects, and highlights improvements in vapor compression cycle performance achieved through recent research and development. The findings suggest potential areas for future research.

Agarwal et al. [14] they evaluated the exergy performance of a dedicated mechanical subcooled vapor compression refrigeration system with, and compares it with alternative cycles employing various refrigerants. The study employs computational models to assess key parameters and investigates the influence of subcooler effectiveness and compressor isentropic efficiency on cycle performance. Results show that the dedicated mechanically subcooled cycle outperforms the simple cycle, and HFO-R1234ze proves to be an environmentally friendly alternative to HFC-R134a and R1234yf. Condenser-1 is identified as the most sensitive component in the dedicated mechanically subcooled cycle.

Gil et al. [15] examined the energy efficiency improvements of dedicated and integrated mechanical subcooling systems within CO_2 booster systems for supermarkets. Utilizing realistic thermodynamic models and focusing on a specific supermarket with defined thermal loads, the study found that both systems can reduce energy consumption. However, their effectiveness is strongly influenced by environmental conditions. The dedicated mechanical subcooling system showed annual energy savings ranging from 1.5% to 5.1%, depending on the climate, while the integrated subcooling system achieved reductions between 1.3% and 4.0% across different temperature regions.

Wang and Zhang [16] examines the different subcooling methods for the transcritical CO_2 vapor compression cycle in district heating and cooling. It considers the trade-off between efficiency and cost, using a dual-objective algorithm. Optimal subcooling methods vary with ambient temperatures, favouring dry coolers at lower temperatures and cooling towers at higher temperatures. Expansion work recovery minimizes performance differences, with internal heat exchangers suitable for winter and cooling towers for summer.

She et al. [17] theoretically analyzed that the expander is used for additional compression work considerations to drive the mechanical subcooling cycle. They claim that the hybrid VCR system outperforms the conventional VCR system, the conventional expansion power recovery system, and the conventional mechanical subcooling system in terms of COP, with maximum COP increases of 67.76%, 17.73%, and 19.27%, respectively, in systems using R744 as the main cycle refrigerant.

Pottker and Hrnjak [18] examined the impact of increasing condenser subcooling in vapor-compression systems on maximizing the Coefficient of Performance (COP) by balancing refrigerating effect and compression work. The research reveals that refrigerants with higher latent heat of vaporization benefit less from subcooling. Among air conditioning systems, R1234yf demonstrates the most significant improvement (8.4%), followed by R410A (7.0%), R134a (5.9%), and R717 (2.7%), primarily due to its smaller latent heat of vaporization. The

optimal subcooling value for maximizing COP is not strongly dependent on thermodynamic properties.

Pottker and Hrnjak [19] presented experimental results investigating the influence of condenser subcooling on air conditioning systems employing R134a and R1234yf as refrigerants. The study indicates that both refrigerants exhibit a peak Coefficient of Performance (COP) as a result of a trade-off between increased refrigerating effect and specific compression work. Under a given operating condition, the system COP experienced an increase of up to 18% for R1234yf and 9% for R134a. The findings affirm that R1234yf benefits more from condenser subcooling. Despite potential interference between an internal heat exchanger and condenser subcooling, simultaneous utilization of both leads to a more efficient air conditioning system, particularly for R1234yf.

Koeln and Alleyne [20] experimentally and theoretically addresses the significant energy consumption of vapor compression systems in the U.S. and the ongoing efforts to optimize system efficiency for cooling needs. Current control strategies often overlook a crucial factor—condenser subcooling, related to the amount of refrigerant in the system. The paper proposes innovative system architecture with a receiver and an additional electronic expansion valve, allowing independent control of condenser subcooling. Simulation and experimental results reveal an optimal subcooling level that maximizes system efficiency, varying with operating conditions. To adapt to this variability, the study employs extremum seeking control, achieving a noteworthy 9% improvement in efficiency compared to conventional methods.

Yang and Yeh [21] numerically analyzed the vapor-compression refrigeration systems using various refrigerants. It considered factors like condensation and evaporation temperatures, cooling water in a subcooler, and refrigerant pressure drop. Two key parameters, representing cost savings and total exergy destruction, were introduced to determine the optimal subcooling degree. Results showed that condensation temperature is crucial for maximizing initial cost savings, and subcooling degrees based on the second law of thermodynamics consistently exceeded those from the first law.

Yang and Zhang [22] analyzed the energy-saving potential in supermarket HVAC and refrigeration systems by strategically placing multiple subcoolers. The approach involves the higher COP system generating more cooling capacity to reduce power consumption in lower COP systems. Various scenarios with one, two, and three subcoolers are explored, considering factors like load ratio, COP, and HVAC system duty time. The paper also proposes an optimal sequence for adding subcoolers.

Qureshi and Zubair [23] they investigated the impact of different refrigerant combinations in vapor compression cycles with dedicated mechanical sub-cooling. R134a in both cycles yields the best results in scratch designs. In retrofit cases, dedicated sub-cooling may be more suitable for R134a cycles than for R717 due to COP sensitivity. Changing the sub-cooler cycle refrigerant has minimal impact on performance parameters when R134a is the main refrigerant.

Qureshi et al. [24] experimentally explored the impact of incorporating a dedicated mechanical subcooling cycle into a 1.5-ton residential vapor compression refrigeration system. By comparing the system's performance with and without the dedicated subcooler and maintaining room temperature between 18°C and 22°C, the research aims to quantify the percentage increase in efficiency resulting from the dedicated subcooling loop. Using R22 as the main refrigerant and R12 in the dedicated subcooling cycle, the results indicate a notable improvement of approximately 0.5 kW in the evaporator's load-carrying capacity when R22 is subcooled by 5°C–8 °C in the main cycle. Additionally, the second-law efficiency experiences an average enhancement of 21% with the implementation of subcooling. This work highlights the potential of dedicated subcooling to enhance both the cooling capacity and efficiency of residential vapor compression refrigeration systems.

Qureshi and Zubair [25] analyzed the mechanical sub-cooling systems to improve the coefficient of performance (COP) in vapor compression cycles is a recognized method for energy savings. Recent progress, both numerically and experimentally, focuses on various aspects such as simulating performance with different refrigerant combinations, analyzing performance variations due to fouling, and studying the effects of dedicated sub-cooling cycles in simple vapor compression systems and subcoolers in two-stage refrigeration cycles. The results showcase important findings, with the paper concluding by suggesting future research directions to implement these advancements effectively.

Ansari et al. [26] Examined the thermodynamic efficiency of a vapor compression refrigeration system incorporating dedicated mechanical subcooling, employing environmentally friendly refrigerants R1243zf and R1233zd(E), and comparing them with R134a. Parameters including Coefficient of Performance (COP) and exergetic efficiency were calculated, revealing that R1233zd(E) surpasses R134a in performance. In contrast, R1243zf, another low-GWP refrigerant, exhibits slightly lower COP and exergetic efficiency compared to R134a. The study underscores the substantial impact of subcooling temperature on system performance and identifies an optimal subcooling temperature.

Llopis et al. [27] they conducted experiments to explore the potential enhancement in the performance of a transcritical CO_2 refrigeration plant by incorporating a dedicated mechanical subcooling system with zeotropic refrigerant mixtures. Theoretical and experimental analysis involved three blends (R-32, R-600, or CO_2 with R-152a). Theoretical simulations indicated higher Coefficient of Performance (COP) values compared to pure fluids, identifying the R-600/R-152a blend [60/40%] as the most effective, with theoretical COP improvements of up to 0.46%. Experimental tests, conducted at three heat rejection levels, demonstrated that the R-600/R-152a blend could enhance COP by 1.1 to 1.4%, and the R-152a/CO_2 blend [90/10%] also showed improved performance with subcooler resizing. The utilization of zeotropic blends in the subcooler was found to reduce irreversibilities.

Agaro et al. [28] suggests that employing dedicated mechanical subcooling (DMS) is a well-researched and efficient strategy for improving the performance of transcritical CO_2 commercial refrigeration systems. This research delves into crucial parameters—DMS cooling capacity, subcooling degree, and gas cooler pressure—during the design and operation of such systems. Using a validated model, the study evaluates the impact of these parameters on the annual energy consumption of the plant in warm and hot climate conditions. DMS is then compared to parallel compression and subcooling through a dedicated HVAC water chiller. The findings emphasize DMS as the most effective solution, revealing that optimized design and operational parameters can lead to additional energy savings and cost reduction compared to other approaches.

Andres et al. [29] observed that recent research has concentrated on enhancing transcritical CO_2 plant performance through subcooling systems, with the dedicated mechanical subcooling system (DMS) emerging as a notable contributor to significant improvements in overall Coefficient of Performance (COP) and cooling capacity. This experimental investigation focuses on a transcritical CO_2 plant incorporating an R-152a DMS. Through tests conducted under various pressure and subcooling conditions, optimal operational conditions are identified for different ambient and cold sink temperatures. The measured values range from 6.5 kW to 9.8 kW for different glycol inlet temperatures, while the optimum COP varies from 1.51 to 2.52. The study puts forth correlations to establish optimal pressure and subcooling for CO_2 plants utilizing DMS, based on gas-cooler outlet temperature and evaporation level.

Chen et al. [30] explored the relationship between subcooling power and enhanced cooling capacity in refrigeration systems. Conducting experiments with two electronic expansion valve modes, the paper introduces the Rise of Cooling Capacity to Subcooling Power

(RICOSP) as a critical parameter. Results reveal contrasting RICOSPs for different conditions with the two expansion valve modes, and in the fixed opening mode, enhanced cooling capacity can surpass subcooling power. The research contributes to a better understanding of the conversion of subcooling power to improved cooling capacity in subcooling refrigeration systems.

Thornton et al. [31] described that dedicated mechanical subcooling cycles incorporate a secondary, compact mechanical vapor-compression cycle linked to the primary cycle after the condenser to supply subcooling. The efficiency of the entire cycle is influenced by factors such as the extent of subcooling and the thermal lift of the subcooling cycle, which is directly associated with the evaporator temperature of the subcooling cycle. This study anticipates the optimal subcooling evaporator temperature utilizing an ideal dedicated subcooling cycle and compares the outcomes with a model dependent on properties. The results establish a design guideline for optimizing the distribution of heat exchange area in the dedicated subcooling cycle.

Llopis et al. [32] examined how CO_2 subcooling has emerged as a crucial technique for enhancing the efficiency of CO_2 refrigeration plants, leading to substantial overall improvements. Recent research indicates performance enhancements of up to 12% with internal heat exchangers, 22% with economizers, 25.6% with thermoelectric systems, and 30.3% with dedicated subcooling methods. This review specifically focuses on recent developments in CO_2 refrigeration cycles incorporating accumulation receivers for commercial applications, excluding air conditioning or mobile air conditioning systems. The paper addresses thermodynamic aspect, analysis findings from recent investigations into both internal and external subcooling methods, and concludes highlighting current trends and proposing areas for future research.

Llopis et al. [33] investigated the potential enhancement in the energy efficiency of CO_2 transcritical refrigeration systems by incorporating a dedicated mechanical subcooling cycle. The theoretical analysis involves examining the modification of optimal operating conditions for the CO_2 transcritical cycle and assessing energy performance improvements across various evaporating levels. Propane is utilized as the refrigerant for the subcooling cycle. The findings reveal a maximum increase of 20% in Coefficient of Performance (COP) and a maximum increase of 28.8% in cooling capacity, with higher increments observed at elevated evaporating levels. The cycle demonstrates greater benefits for environmental temperatures exceeding 25 ºC. Results using different refrigerants for the mechanical subcooling cycle show no significant differences

Llopis et al. [34] conducted experiments to investigate the energy enhancements achieved by integrating a mechanical subcooling cycle with a CO_2 transcritical refrigeration plant. The experiment entails testing a combination of an R1234yf single-stage refrigeration cycle with a semi-hermetic compressor for the mechanical subcooling cycle and a single-stage CO_2 transcritical refrigeration plant with a semi-hermetic compressor. The assessment covers two evaporating levels of the CO_2 cycle and three heat rejection temperatures. The findings reveal capacity improvements of up to 55.7% and Coefficient of Performance (COP) improvements of up to 30.3%.

Ochoa et al. [35] investigated when mechanical subcooling is employed for increasing the coefficient of the performance in low temperature applications and if comes to dedicated mechanical subcooling, retrofitting allows great flexibility with the system point of view because the same capacity the system takes less run time, many cases can be run on simulation for finding the best case for the optimum design, taking all the restrictions into account.

2.4 LITERATURE SURVEY ON THE THERMODYNAMIC PROPERTIES OF REFRIGERANTS

F. de Monte [36] explored the thermodynamic properties of R407C and R410A in their superheated vapor states through theoretical modeling, using the Martin-Hou equation of state. The study focused on unpublished properties such as compressibility factor, isothermal compressibility, volume expansion, exponents, speed of sound, and Joule–Thomson coefficient. These findings provide a theoretical foundation for research on optimal HFC mixtures for compressor efficiency and cycle calculations in vapor-phase systems with R407C and R410A.

Kucuksille et al. [37] uutilized ten diverse modeling techniques in the data mining process to predict thermo-physical properties of refrigerants (R134a, R404A, R407A, R410A). These methods involved linear regression, multi-layer perception, pace regression, simple linear regression, sequential minimal optimization, KStar, additive regression, M5 model tree, decision table, and M5'Rules models. Established relationships based on temperature and pressure to determine properties like specific heat capacity, viscosity, heat conduction coefficient, and density. Comparative analysis of model results revealed the most effective approach for each refrigerant. The study suggests that employing these derived formulations will simplify the design and optimization of heat exchangers, particularly in vapor compression refrigeration systems.

Arora and Kaushik [38] presented a comparative analysis of R422 series refrigerants as potential alternatives to HCFC22 in vapor compression refrigeration. Utilizing Refprop version 7.0 and Engineering Equation Solver (EES) software, it evaluates parameters like volumetric cooling capacity, COP, and exergetic efficiency. Results indicate that while HCFC22 outperforms R422 series refrigerants in these metrics, significant efficiency deficits are observed in the condenser.

Calm [39] **t**he article reviews the historical progression of refrigerants, dividing it into four generations based on selection criteria. It discusses the displacement of earlier working fluids, the renewed interest in natural refrigerants, and examines the outlook for current options in the context of international agreements such as the Montreal and Kyoto Protocols. The paper also considers other environmental concerns and regulatory measures. It emphasizes the importance of addressing multiple environmental issues collectively and identifies potential policy changes that could significantly impact the next generation of refrigerants.

McLinden et al. [40] the study presented thermodynamic properties of the hydro-fluoro-olefin (HFO) refrigerant R1234ze (E). Measurements were conducted using a two-sinker densimeter, covering the p-ρ-T behaviour from 240 K to 420 K and pressures up to 15 MPa. The research encompassed various states, including low-density vapor to compressed-liquid phases, with additional vapor pressure measurements. The equation of state (EOS) for R1234ze (E) was formulated in terms of the Helmholtz energy, applicable across the entire fluid range for calculating all thermodynamic properties. Validation was established through comparisons with experimental data.

Reasor et al. [41] explored the increasing significance of refrigerants with low global warming impact in response to environmental concerns in the refrigeration industry. R1234yf, with a low Global Warming Potential (GWP) of 4 compared to R134a's 1430, exhibits thermodynamic properties similar to R134a, making it a promising choice for future automotive refrigerants. R1234yf has the potential to serve as a drop-in replacement for R134a. The study also compares R1234yf with the commonly used refrigerant R410A to assess its compatibility as a replacement. Comparisons between R1234yf, R134a, and R410A are made, and simulations are conducted to evaluate the feasibility of using R1234yf as a substitute for either R134a or R410A. The paper focuses on comparing the thermo-physical properties of R1234yf, R134a, and R410A, presenting simulation results in tube-fin and micro channel heat exchangers.

Pearson [42] examined the historical progression of older carbon dioxide systems, analyzed the factors contributing to their slow development and eventual decline, including technical,

commercial, and social reasons. The study investigated the recent resurgence of interest in these systems, which is evident across a diverse range of applications, such as transcritical car air conditioners and low-temperature industrial freezer plants.

Karber et al. [43] examined the refrigerants R-1234yf and R-1234ze as replacements for R134a in household refrigerators. Experimental data shows R-1234yf to be a feasible drop-in replacement with slightly increased energy consumption compared to R134a. However, R-1234ze demonstrates energy savings potential, albeit with issues regarding its lower capacity. This suggests R-1234yf as a practical alternative for immediate adoption, while further adjustments may be needed for R-1234ze to become a suitable replacement.

Saleh and Wendland [44] discussed the growing interest in alternative refrigerants to mitigate environmental impact, particularly focusing on fluorinated ethers and cyclic hydrocarbons as potential replacements for high GWP hydro-fluoro-carbons (HFCs). It highlights the challenge of limited data availability for evaluating these alternatives and introduces backone equations as a method for accurately describing their thermodynamic properties with minimal parameters. This approach facilitates the assessment of various refrigerants, indicating promising options among hydrocarbons and fluorinated ethers for sustainable refrigeration applications.

Brown et al. [45] provided estimates for various properties of R-1234ze(Z) and its potential as a replacement for R-114 in high-temperature heat pumping applications. The provided estimates include critical temperature, pressure, density, acentric factor, and ideal gas specific heat. Simulation results indicate comparable performance between R-1234ze(Z) and R-114 in terms of coefficient of performance and volumetric heating capacity, reinforcing the former suitability as a replacement. The paper suggests that R-1234ze(Z) warrants further investigation as a viable alternative refrigerant.

Brown et al. [46] discussed the use of group contribution methods to predict various properties of eight fluorinated olefins, including critical temperatures, pressures, densities, acentric factors, and ideal gas specific heats. Additionally, the Peng-Robinson equation of state is employed to forecast thermodynamic properties, illustrated through pressure-enthalpy and temperature-entropy state diagrams. The methodology's predictive capability is assessed by comparing property predictions for R-134a with known data and for R-1234yf with available literature, providing valuable insights into the accuracy and reliability of the predictive techniques employed.

Makhnatcha and Khodabandeh [47] evaluated three key environmental metrics - GWP, TEWI, and LCCP - to guide the selection of low GWP refrigerants for a 30 kW air/water heat

pump system, while addressing uncertainties associated with their use. The study concludes with a recommended refrigerant choice and suggests avenues for further research to improve the identification of low GWP refrigerants with minimal global warming contribution.

Mora et al. [48] explored the use of Artificial Neural Networks (ANNs) for predicting thermodynamic properties of refrigerants in vapor-liquid equilibrium, aiming to simplify equipment operation and design. ANNs offer a promising alternative to traditional equations of state (EoS) by learning complex input-output relationships. Employing multilayer perceptron ANNs with back-propagation algorithms, accurate property prediction models are developed without the need for EoS. This approach not only accurately predicts refrigerant properties but also holds potential for process optimization and the development of intelligent devices, leading to cost and energy savings.

Devecioglu and Oruc [49] explored the potential of new-generation low GWP gases as alternatives to commonly used refrigerants in refrigeration and air conditioning systems. By comparing various HFO-based mixed gases, such as R450A, R513A, R1234yf, and R1234ze(E), against traditional refrigerants like R134a, R404A, R410A, and R22, the research identifies promising alternatives with lower GWP values and favorable energy characteristics. Notably, R1234yf, L40, DR-5, and R444B emerge as particularly viable replacements. However, it emphasizes the importance of thorough testing before commercial implementation to ensure optimal performance and environmental impact.

Sulaiman et al. [50] investigated low global warming potential (GWP) refrigerants for high-temperature heat pumps (HTHPs) to comply with F-gas regulations. Through theoretical simulations, it evaluates replacements for HFC-245fa and HFC-365mfc, focusing on system performance and efficiency. HCFO-1233zd(E) and HFO-1336mzz(Z) emerge as promising replacements, with HC-601 showing low exergetic destruction. The study underscores the importance of regulating superheat and validates theoretical results with empirical data, offering insights for optimizing refrigerant selection in HTHPs for enhanced overall efficiency.

2.5 LITERATURE SURVEY ON ADVANCE EXERGY AND COEFFICIENT OF STRUCTURAL BOND ANALYSIS

To enhance the performance of the mechanical subcooled system, above mentioned researchers conducted energy and exergy study but, neglected to take into account advanced exergy and coefficient of structural bond analysis factors, which are crucial when choosing how to use energy resources responsibly.

Tsatsaronis and Park [51] assessed the possibility of enhancing system component performance and examined the exergy destruction and investment costs associated with compressors, turbines, heat exchangers, and combustion chambers. The exergy destruction was categorized into endogenous/exogenous and unavoidable/avoidable components for a comprehensive analysis.

Morosuk and Tsatsaronis [52] presented a new method of splitting exergy destruction into endogenous/exogenous and unavoidable/avoidable parts, improving accuracy in energy system analysis. Using an absorption refrigeration machine as a case study, it demonstrates how this approach enhances understanding of system thermodynamics and offers insights for optimization. The study hints at potential applications in exergoeconomic evaluation for a comprehensive understanding of system performance and cost-effectiveness.

Kelly et al. [53] improved the researchers understanding regarding four different approaches, endogenous and exogenous with the concept of avoidable and unavoidable exergy destruction parts. They also discuss the concept of overall system optimization.

Morosuk and Tsatsaronis [54] This literature survey introduces the concept of splitting exergy destruction into endogenous/exogenous and unavoidable/avoidable parts, enhancing the analysis of energy conversion systems. It demonstrates this concept in vapor-compression refrigeration machines using different refrigerants, including R125, R134a, R22, R717, azeotropic (R500), and zeotropic (R407C). Endogenous exergy destruction occurs within a component's real efficiency, while exogenous destruction is influenced by system-wide irreversibilities. Unavoidable destruction is inherent to a component, while avoidable destruction could potentially be reduced, providing valuable insights for system optimization.

An advanced exergy study of an air conditioning system including LHTS (latent heat thermal storage) and VCR (vapor compression refrigeration) was examined by Mosaffa et al. [55] Additionally, they determined exergy destruction (overall) by the system, both during the day and at night.

Utilizing advanced exergy analysis, Gong and Boulama [56] evaluated an absorption refrigeration unit. The exergy destruction at the evaporator and condenser was found to be primarily endogenous and avoidable, and at the evaporator section, it was determined that internal inefficiencies were entirely responsible for the exergy destruction.

Based on an advanced exergy method a sensitivity study of a real combined cycle power plant was conducted by Boyaghchi and Molaie [57] they discovered that an increase in

compressor pressure ratio and turbine inlet temperature had a beneficial impact on most of the components' efficiency and exergy destruction.

A single-stage heat transformer's advanced exergy analysis was used by Colorado [58] to determine the sensitivity of the energy destruction. His research showed that the cycle's overall reversibility (base case), which was 14.78%, could be lowered by changing its design and configuration, while the avoidable endogenous component of the evaporator's exergy destruction stayed unchanged.

A sophisticated exergy analysis was used by Liao et al. [59] to examine the organic rankine cycle in order to recover flue gas waste heat. According to their findings, 25.65% of the total exergy destruction can be avoided and endogenous exergy rates are higher than exogenous exergy rates in all system components.

Misra et al. [60] the study employed thermo-economics to optimize a LiBr/H_2O absorption chiller for air-conditioning, aiming to minimize product cost. Using the structural coefficient, the methodology simplifies optimization by sequentially refining subsystems. Findings reveal a 33.3% increase in capital cost for the optimized configuration, offset by a notable 47.2% reduction in plant irreversibilities. Ultimately, this leads to improved efficiency and reduced fuel costs. Overall, the research highlights the importance of integrating economic factors for effective system optimization.

Boer et al. [61] conducted an energy, exergy, and structural analysis of a single effect vapor absorption cooling cycle that utilized ammonia and water. Through exergy analysis, they were able to assess the level of irreversibility within each component of the cycle as well as the overall system. The CSB analysis was also performed to access the impact that how any change in irreversibility within one component of the system would affect the rest of the components and the system as a whole.

To assess the actual thermodynamic efficiency of chemical processes and the distribution of irreversibility in a plant, Tekin and Bayramoglu [62] carried out an exergy and CSB analysis. They reported the decrease in total exergy loss is equal to 4.21%in sugar manufacturing plants.

Nikolaidis and Probert [63] investigated a two-stage compound compression-cycle with flash inter-cooling, using refrigerant R22. The analysis reveals that changes in condenser and evaporator temperatures significantly affect the plant's irreversibility rate. Employing the coefficient of structural bond demonstrates the interconnectedness of plant components, with reductions in individual component irreversibility rates leading to greater reductions in the plant's overall irreversibility. Optimizing condenser and evaporator conditions is crucial for

enhancing overall plant efficiency, underscoring the importance of careful design and operation in achieving optimal performance.

2.6 CONCLUSIONS OF LITERATURE SURVEY

In conclusion, the inclusion of these recent papers augments the depth and relevance of the literature survey, ensuring that the theoretical and experimental landscape of vapor compression refrigeration systems is portrayed in a current and comprehensive manner. The relationship among theoretical advancements, experimental methodologies, and multidisciplinary approaches clarifies the path of this field and establishes the foundation for future research endeavours. The following key points are addressed in the literature survey:

1. Extensive literature exists on the topic of vapor compression refrigeration systems and researchers have a variety of thermodynamic models. These models serve the purpose of analyzing and evaluating the performance of vapor compression refrigeration systems, providing valuable insights into their efficiency and functionality.
2. Literature survey covers theoretical and experimental studies of vapor compression refrigeration systems.
3. Literature survey emphasis on selecting the right vapor compression refrigeration method based on factors like cooling capacity, temperature, and application environment.
4. Various refrigerants exhibit distinct impacts on the performance of vapor compression systems, each possessing unique physical and atmospheric properties.
5. A sizable literature is available on diverse methods employed to measure the thermodynamic properties of various refrigerants.
6. Exploration of advanced vapor compression cycle technologies, subcooling methods, and impact of refrigerant combinations.
7. Studies on dedicated mechanical subcooling systems highlight environmental benefits and efficiency improvements.
8. Introduction of advanced exergy and coefficient of structural bond analysis adds a comprehensive dimension in literature survey.

2.7 GAPS IN LITERATURE SURVEY

1. There is very less work on experimental analysis of DMS-VCR system in open literature. Most of the work is based on theoretical analysis. Researchers have done some basic parametric study to evaluate the performance of the system. The detailed

integrated designs of system components and performance evaluation for wide range of operating parameters have not been done so far.

2. An existing subcooled vapor compression system using R22 and R12 as a refrigerant which can be replaced by alternative environmental friendly refrigerants. Further, the effect of losses, superheating, subcooling, degree of overlap, cooling capacity, size of heat exchanger and fouling in DMS-VCR system has not been taken into consideration.
3. There has been limited study on the economic and thermo-economic analysis of dedicated subcooled vapor compression refrigeration system.
4. There has been very less work on the environment analysis of dedicated refrigeration system.
5. No research has been conducted on the advanced exergy analysis of a dedicated mechanical subcooled vapor compression refrigeration system.
6. The coefficient of structural bond analysis for a dedicated mechanical subcooled vapor compression refrigeration system has not been explored in existing literature.

2.8 OBJECTIVES OF PRESENT WORK

1. To carryout energy & exergy analysis of the DMS-VCR system with alternative refrigerants and other combinations, i.e. theoretical analysis of system.
2. To carryout the thermo-economic and environmental analysis of DMS-VCR system.
3. To design a dedicated mechanical subcooled VCR system. (i.e. Thermodynamically)
4. To fabricate the experimental setup of DMS-VCR system and carryout the experimental analysis.

CHAPTER 3

ENERGY AND EXERGY ANALYSIS OF DEDICATED MECHANICAL SUBCOOLED VAPOR COMPRESSION REFRIGERATION SYSTEM

This chapter offers an in-depth analysis of the energy and exergy aspects of vapor compression refrigeration systems, with a particular focus on the dedicated subcooled vapor compression refrigeration approach. Employing this method is targeted at enhancing the Coefficient of Performance while simultaneously reducing power consumption.

3.1 INTRODUCTION

The energy and exergy analysis of dedicated mechanical subcooled vapor compression refrigeration (DMS-VCR) system plays a pivotal role in optimizing the performance and efficiency of these systems, which are widely employed in various industrial, commercial, and residential applications for cooling and air conditioning purposes. As concerns about energy conservation and environmental impact continue to grow, there is an increasing emphasis on understanding and improving the thermodynamic performance of refrigeration systems.

The dedicated mechanical subcooled vapor compression refrigeration systems are complex thermodynamic cycles that involve the compression, condensation, subcooling, expansion, and evaporation of a refrigerant fluid. While energy analysis focuses on the overall energy transfers within the system, exergy analysis takes a more detailed approach by evaluating the quality of energy and its potential for doing useful work. Therefore, the combined study of energy and exergy provides a comprehensive support for assessing the efficiency and effectiveness of refrigeration systems.

The global demand for cooling and refrigeration is rising, driven by factors such as population growth, urbanization, and the expansion of various industries. Consequently, the energy consumption associated with these systems has become a critical consideration. Researchers and engineers are increasingly turning to advanced analytical tools, including energy and exergy analysis, to identify areas of inefficiency and to develop strategies for enhancing the overall performance of dedicated mechanical subcooled vapor compression refrigeration systems.

This Chapter aims to explore the principles and methodologies of energy and exergy analysis in the context of dedicated mechanical subcooled vapor compression refrigeration systems. By delving into the fundamental thermodynamics governing these systems, it seeks to uncover insights that can inform the design, operation, and maintenance of more sustainable

and energy-efficient refrigeration technologies. Through a systematic examination of energy and exergy flows, this research contributes to the ongoing efforts to mitigate environmental impact, reduce energy consumption, and advance the state of the art in refrigeration technology.

The analysis of systems based on combined first and second laws of thermodynamics is a better approach. Many researchers are focusing on the analysis of thermal systems based on this approach. The analysis based on second approach is also known as exergy analysis. The exergy analysis helps to quantify the irreversibility occurring in the system components and thus proves itself better than energy analysis. Presently, greater emphasis is being laid upon energy efficient systems. Many studies involving energy and exergy analysis of refrigeration systems such as Arora and Kaushik [3], Arora and Sachdev [38] and Arora et al. [64], have been reported in recent past. In one of the notable study, Arora and Kaushik [3] extensively evaluated the energy and exergy performance of R502, R404A, and R507A in a vapor compression cycle. Notably, R507A demonstrates superior COP and exergetic efficiency compared to R404A within the 40°C to 55°C condenser temperature range, yet both fall short by 4–17% compared to R502. The condenser emerges as the most irreversible component, with the liquid vapor heat exchanger being the most efficient. R507A consistently outperforms R404A in various scenarios, such as with increasing dead state temperature, subcooling, and pressure drops in the evaporator and condenser. Consequently, the study concludes that R507A stands as a more promising alternative to R502 than R404A in practical vapor compression applications.

Ahamed et al. [65] explored the potential for exergy analysis in vapor compression refrigeration systems, emphasizing factors like evaporating and condensing temperatures, sub-cooling, and compressor pressure. The focus on environmentally friendly hydrocarbons, particularly R407a, R600a, R410a, and R134a, is highlighted for their low environmental impact. The study identifies the compressor as a major source of exergy losses, with ongoing research suggesting potential reductions through the use of nano-fluids and nano-lubricants.

Agarwal et al. [14] presented an exergy analysis of a dedicated mechanically subcooled vapor compression refrigeration system, comparing its performance with various cycles using HFO-R1234ze, R1234yf, and HFC-R134a. The computational model evaluates key parameters and explores the impact of subcooler effectiveness and compressor isentropic efficiency on cycle performance. The dedicated mechanically subcooled VCR cycle outperforms the simple VCR cycle, with HFO-R1234ze proving to be a competitive and environmentally friendly

alternative to HFC-R134a, surpassing R1234yf. Condenser1 is identified as the most sensitive component in this cycle for the considered refrigerants.

Moles et al. [66] focused on the energy and exergy analysis of vapor compression systems using R1234yf and R1234ze(E) as alternatives to R134a with lower GWP. Despite an initial decrease in performance upon substitution, configurations with an expander or an ejector as an expansion device demonstrate superior energy and exergy efficiency. The introduction of an internal heat exchanger enhances cooling capacity, but its impact on the Coefficient of Performance (COP) varies when replacing the expansion valve with an expander or an ejector.

Menlik et al. [67] conducted energy and exergy analysis and compares the performance of R22 and its alternatives, R407C and R410A, in a vapor compression refrigeration system (VCR system). The analysis involves a detailed examination of the first law (energy) and second law (exergy) for these refrigerants under various conditions, including different evaporator, condenser, subcooling/superheating, and dead state temperatures. The findings indicate that R407C is a more favorable alternative to R22 compared to R410A. Furthermore, the condenser is identified as the least efficient component in the VCR system based on the analysis

Most DMS-VCR system studies are introductory in nature and give attention to an energy and exergy study of the system without in depth parametric explanation. The system's energy and exergy performance are predicted by the suggested model and the DMS-VCR system concept is used for water chiller application. After creating a model, a system's first and second laws are examined for a variety of operating factors i.e. evaporator temperature, condenser temperature, degree of overlap and degree of subcooling. The appropriate degree of subcooling, which is the uniqueness of this analysis, is determined by the overall COP, second law efficiency, total irreversibility, and total work consumption.

3.2 SYSTEM DESCRIPTION

The key components of a dedicated mechanical subcooled vapor compression refrigeration (DMS-VCR) system including two condensers, two compressors, two expansion valves, one evaporator, and one subcooler, as are shown in schematically diagram of the system in Figure 3.1. The pressure-enthalpy (P-h) diagram of the cycle is shown in Figure 3.2. It illustrates various processes taking place in the VCR system and DMS-VCR system. The cycle works between the condensers and evaporator temperatures, respectively.

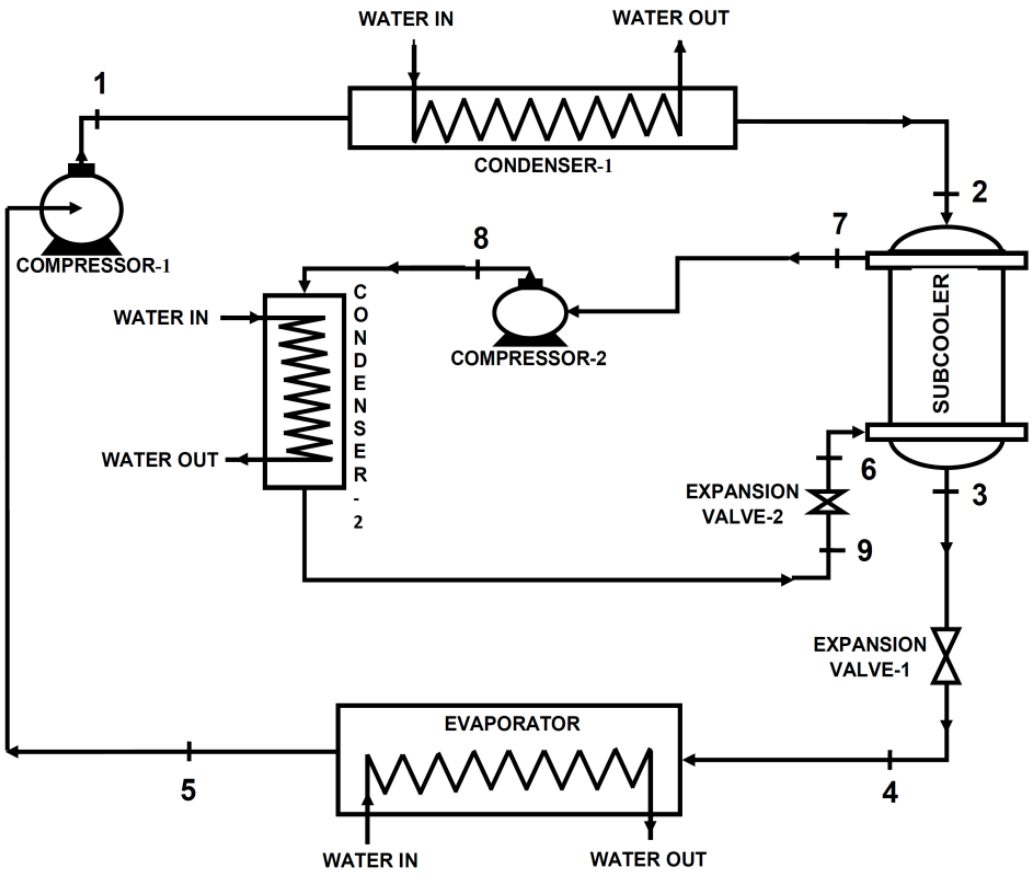

Figure 3.1 Schematic diagram of DMS-VCR system

The subcooling DMS cycle (6–7–8–9) is attached with the VCR cycle (1–2–3–4–5) at the condenser-1 outlet. These components of the two cycles (VCR and DMS) are attached through a piping system in a folded loop with a provision for heat transfer to the environment. This designed system can use the same or different refrigerants in two cycles.

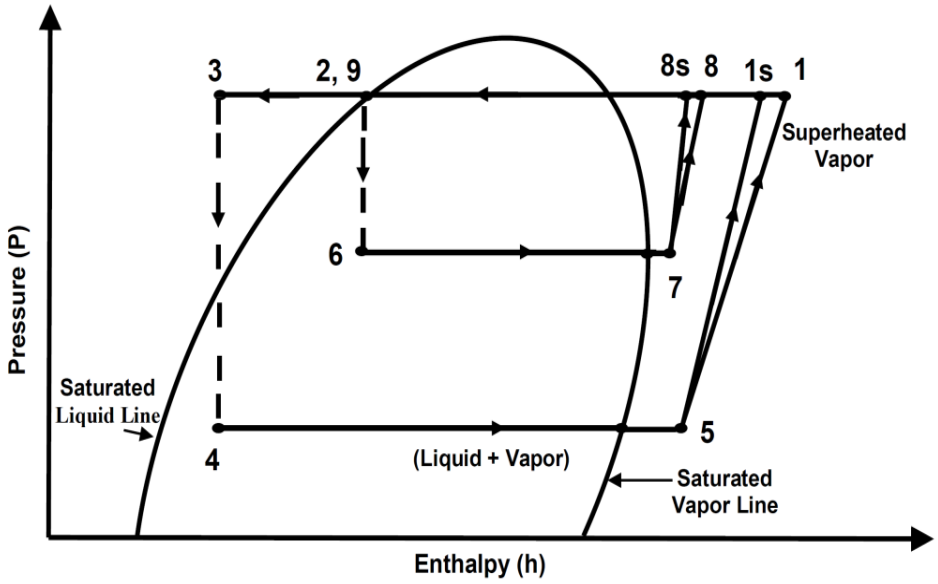

Figure 3.2 Pressure – enthalpy diagram of DMS-VCR cycle

3.3 THERMODYNAMIC MODELING OF DMS-VCRS

Thermodynamic modeling of DMS-VCRS involves energetic analysis for evaluating performance of the system and exergetic analysis to identify irreversibilities and second law efficiency.

3.3.1. Energetic and exergetic analysis

In Engineering Equation Solver (EES) software, the DMS-VCR system is thermodynamically simulated for energy and exergy analysis based on the first and second laws, respectively. The mass, energy, and exergy balance concept is applied to each component of the system as the thermo-physical refrigerant parameters are derived from built-in EES functions at different state points. The following equations treat the system's components as control volumes with inlet and output streams, heat transfer, and work interactions by Nag [68].

(i) $\sum \dot{m}_i - \sum \dot{m}_o = 0$ (Mass balance) (3.1)

(ii) $\sum \dot{Q} - \sum \dot{W} = \sum \dot{m}_{out} h_{out} - \sum \dot{m}_{in} h_{in}$ (Energy balance) (3.2)

(iii) $\dot{S}_{gen} = \sum \dot{m}_{out} s_{out} - \sum \dot{m}_{in} s_{in} - \sum \frac{\dot{Q}}{T} \geq 0$ (Entropy generation) (3.3)

The rate of heat transmission is significantly influenced by the specific heat and mass flow rate of the fluid streams moving within heat exchangers, specifically the evaporator, condenser-1, condenser-2, and subcooler. The rate of heat transmission particularly in the evaporator is depicted in Eq. (3.4).

$$\dot{Q}_{evap} = (\dot{m}_{ef} . c_{sp})_{evap}(T_{in,evap} - T_{out,evap}) = \dot{m}_{ref1}(h_5 - h_4) \quad (3.4)$$

$T_{in,evap}$, as shown in Eq. (4), represents the temperature of the fluid coming from outside and entering the evaporator and Eqs. (3.5) and (3.6) shows the compressor's work in the compressor-1 and compressor-2 sections.

$$\dot{W}_{comp1} = \frac{\dot{W}_{comp1,isen}}{\eta_{isen1}} \quad \text{and} \quad \dot{W}_{comp1,isen} = \dot{m}_{ref1}(h_{1s} - h_5) \quad (3.5)$$

$$\dot{W}_{comp2} = \frac{\dot{W}_{comp2,isen}}{\eta_{isen2}} \quad \text{and} \quad \dot{W}_{comp2,isen} = \dot{m}_{ref2}(h_{8s} - h_7) \quad (3.6)$$

Points 1s and 8s represent the isentropic condition of the refrigerant vapor at the compressor's outlet. A steady-state flow equation is used to calculate the work input needed by the compressor. Furthermore, the coefficient of performance (COP) is determined as the refrigerant effect to compressor power ratio

$$COP = \frac{\dot{Q}_{evap}}{\dot{W}_{comp1} + \dot{W}_{comp2}} \quad (3.7)$$

In both commercial and residential systems, fan power consumption is quite low. Therefore, it is not taken into account while calculating COP.

By modifying the design parameters, second law-based analysis aims to improve system performance by identifying energy losses. Exergy analysis is the most accurate way for determining actual losses because the process is irreversible. The irreversibility ($\dot{I}$) of a process indicates the potential loss of useful work (W_{useful}) compared to reversible work.

The following governing equations are part of thermodynamic modelling for a specific system component:

Exergy balance, $\dot{I} = E^{in} - E^{out} + E^{Q} - E^{W}$ (3.8)

Thus, E^{Q} and E^{W} are the exergy flows connected to heat and work transfer, respectively, and $\dot{I}$ is the total irreversibility or exergy destruction (loss). In $E = \dot{m} * \psi$, ψ is the chemical, potential, kinetic, and physical exergy of matter, and E^{in} and E^{out}, which are matter exergies at the control volume's input and output. The physical specific exergy is calculated after removing chemical, potential, and kinetic exergies.

$$\psi = (h - T_o s) - (h_o - T_o s_o) \quad (3.9)$$

$$\dot{E}D = \sum \dot{E}_{in} - \sum \dot{E}_{out} + \sum \dot{Q}\left(1 - \frac{T_o}{T}\right) - \sum \dot{W} \quad (3.10)$$

Here, the temperature of the reference environment is referred to as T_o.

By employing the above fundamental equations to all the elements of the DMS-VCR system, the system's entire exergy destruction is indicated by the Eq. (3.11).

$$\dot{E}D_t = \dot{E}D_{evap} + \dot{E}D_{cond1} + \dot{E}D_{cond2} + \dot{E}D_{sc} + \dot{E}D_{comp1} + \dot{E}D_{comp2} + \dot{E}D_{ev1} + \dot{E}D_{ev2} \quad (3.11)$$

Aminyavari et al. [69] calculated the exergetic efficiency of the VCR system.

$$\eta_{ex} = \left(1 - \frac{\dot{E}D_t}{\dot{W}_t}\right) \quad (3.12)$$

3.4 ASSUMPTIONS

The assumptions considered in the thermodynamic modeling of the system are:

i) The system component is in a steady-state.

ii) At the exit, the refrigerants in the evaporator and condenser are in a saturated

vapor and saturated liquid state.

iii) The pressure losses in connecting pipelines and other system components are neglected.

iv) Isentropic efficiency is assumed to be constant for the compressors.

v) The changes in kinetic energy and potential energy are neglected.

3.5 MODEL VALIDATION

A program is developed in the EES software based on the model presented above, considering the thermophysical characteristics of the R134a refrigerant. The results of the present work are compared with that of Agarwal et al. [70]. The input data used by Agarwal et al. [70] are $\dot{Q}_{evap}$ = 3.5167kW, T_{evap}, = -10°C, DOS = 5°C, T_{cond1}, T_{cond2} = 50 °C, η_{comp1}, η_{comp2} = 80%, ϵ_{sc} = 0.8, T_o = 25°C, P_o = 101.325 kPa. The same is used in the current program and the computed results are compared with that of Agarwal et al. [70]. The results depicts that all relevant quantities (COP and exergetic efficiency) are anticipated by EES software effectively with a maximum encountered error of 3.45% but most of the errors are less than 2% (see Figure 3.3 and Figure 3.4).

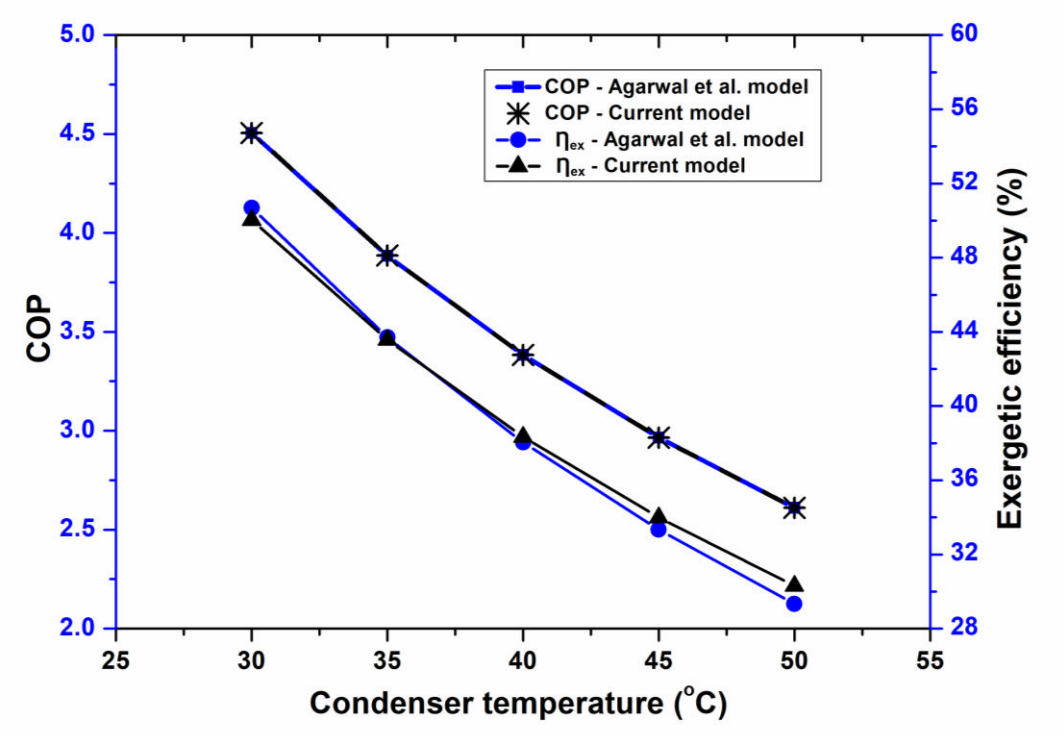

Figure 3.3 Performance comparison of Agarwal et al. [70] for effect of condenser temperature with refrigerant R134a (T_{evap} = -10°C)

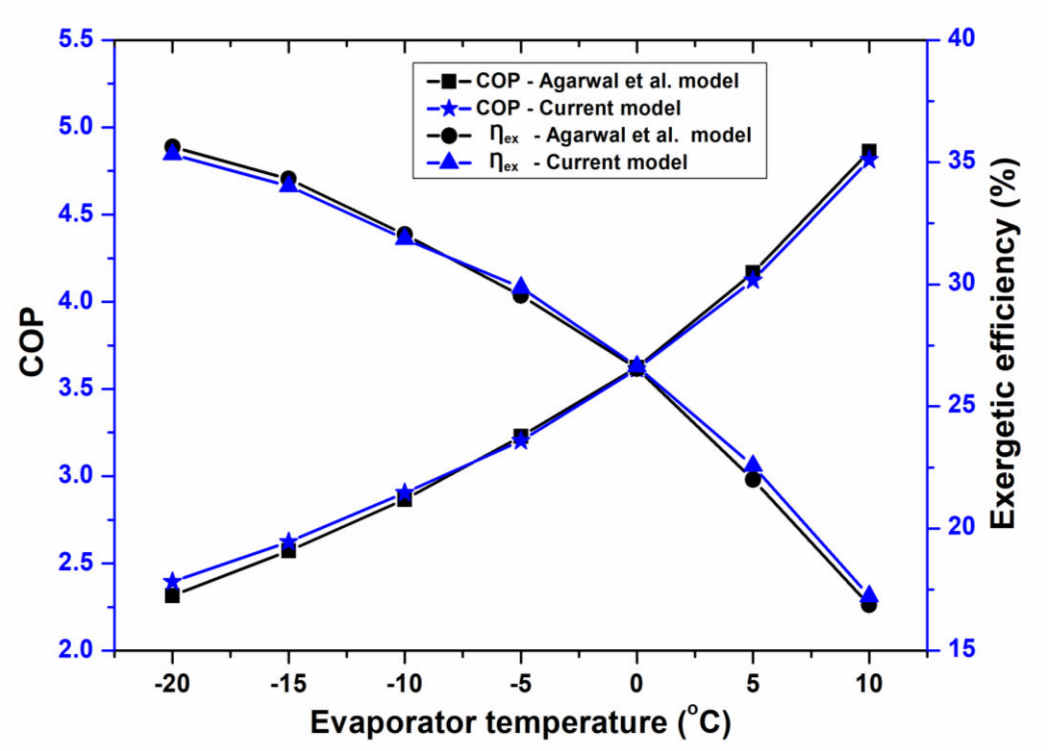

Figure 3.4 Performance comparison of Agarwal et al. [70] for effect of evaporator temperature with refrigerant R134a (T_{cond} = 50°C)

3.6 INPUT PARAMETERS

A comprehensive comparison is conducted between the DMS-VCR system and an equivalent VCR system, designed for industrial water chiller applications. Both systems operate with refrigerant R134a under identical conditions. This assessment encompasses various aspects, including energy and exergy considerations. The operational parameters for implementing water cooling within the DMS-VCR system were obtained through research papers [69] and are detailed in Table 3.1.

Table 3.1 Process data of DMS-VCR system (for Refrigerant R134a)

	Parameters	**Values**
Thermal parameters (Aminyavari et al. [69])	Evaporator cooling capacity ($\dot{Q}_{evap}$, kW)	100
	Evaporator temperature (T_{evap} °C)	0
	Inlet temperature of evaporator coolant ($T_{in,evap}$ °C)	10
	Outlet temperature of evaporator coolant ($T_{out,\ evap}$ °C)	5
	Temperature of Condenser (T_{cond} °C)	45
	Coolant inlet temperature at condenser ($T_{in,\ cond}$ °C)	35
	Coolant outlet temperature at condenser ($T_{out,\ cond}$ °C)	40
	Overlap degree ($T_{overlap}$, °C)	5

	Degree of subcooling ($T_{subcooling}$ ^oC)	5, 19 (optimal)
	Isentropic efficiency of compressors (η_{isen})	0.66, 0.76
	Environment temperature (T_o ^oC)	25
	Environment pressure (P_o, kPa)	101.325
	Refrigerants (for both the cycles)	R134a

3.7 RESULTS AND DISCUSSION

The efficiency of the DMS-VCR system is analysed and improved using a thermodynamic model that has been verified as effective. The effectiveness of a dedicated mechanical subcooled vapor compression refrigeration system is assessed and compared to that of a refrigeration system with an equivalent vapor compressor that uses R134a as a refrigerant.

3.7.1 Results of energy analysis

Table 3.2 displays the outcomes of an energy analysis, which compares the performance of R134a in DMS-VCR system with an equivalent VCR system, both operating under identical conditions. The primary objective of this is to determine COP and electricity consumption in the DMS-VCR system.

As indicated in Table 3.2, the DMS-VCR system achieves a substantial reduction (17.20%) in electricity consumption while maintaining the same cooling capacity as that in VCR system. Consequently, this reduction leads to decreased compressor-1 work and heat load on the condenser-1. Additionally, the mass flow rate of the refrigerant experienced a reduction of 17.22%. Simultaneously, the COP of the DMS-VCR system shows a noteworthy improvement of 11.67%.

Table 3.2 Energy analysis results for refrigerant R134a

Performance Parameters	**R134a**		**Percentage Change /% [(Y-X)/X*100]**
	VCR system (X)	**DMS-VCR system (Y)**	
COP	3.128	3.493	(+) 11.67
$\dot{Q}_{cond1}$ (kW)	131.97	109.28	(-) 17.19
$\dot{Q}_{cond2}$ (kW)	-	19.35	-
$\dot{Q}_{cond,t}$ (kW)	131.97	128.63	(-) 2.53
$\dot{Q}_{sc}$ (kW)	-	17.19	-
$\dot{Q}_{evap}$ (kW)	100	100	-

$\dot{W}_{comp1}$ (kW)	31.97	26.47	(-) 17.20
$\dot{W}_{comp2}$ (kW)	-	2.16	-
$\dot{W}_{comp,t}$ (kW)	31.97	28.63	(-) 10.45
$\dot{m}_{ref1}$ (kg s^{-1})	0.743	0.615	(-) 17.23
$\dot{m}_{ref2}$ (kg s^{-1})	-	0.117	-
$\dot{m}_{ref,t}$ (kg s^{-1})	0.743	0.732	(-) 1.48
$\dot{m}_{ef,evap}$ (kg s^{-1}	4.762	4.762	-
$\dot{m}_{ef,cond1}$ (kg s^{-1})	6.315	5.230	(-) 17.18
$\dot{m}_{ef,cond2}$ (kg s^{-1})	-	0.926	-
$\dot{m}_{ef,t}$ (kg s^{-1})	6.315	6.156	(-) 2.52

3.7.2 Results of exergy analysis

The findings of an exergy study performed on the equivalent VCR system and the DMS-VCR system are shown in Table 3.3. The study under Section 3.7.1 indicates that DMS-VCR system experiences a decrease in compressor work, cooling load of condenser, and mass flow rate of refrigerants, resulting in a 15.71% reduction in the rate of total irreversibility in the DMS-VCR system. Furthermore, the DMS-VCR system exergetic efficiency increases by 10.38%, which shows the effectiveness of using DMS system for subcooling in VCR system.

Table 3.3 Exergy analysis results for the refrigerants R134a

Performance Parameters	**R134a**		**Percentage Change /% [(Y-X)/X*100]**
	VCR system (X)	**DMS-VCR system (Y)**	
η_{II} (%)	36.10	39.85	(+) 10.38
$\dot{I}_t$ (kW)	20.43	17.22	(-) 15.71
$\dot{I}_{cond,1}$ (kW)	3.43	2.84	(-) 17.20
$\dot{I}_{cond,2}$ (kW)	-	0.46	-
$\dot{I}_{cond,t}$ (kW)	3.43	3.30	(-) 3.79
$\dot{I}_{evap}$ (kW)	2.85	2.85	-
$\dot{I}_{comp,1}$ kW)	9.69	8.02	(-) 17.23
$\dot{I}_{comp,2}$ (kW)	-	0.48	-
$\dot{I}_{comp,t}$ (kW)	9.69	8.50	(-) 12.28

$\dot{I}_{sc}$	(kW)	-	0.82	-
$\dot{I}_{ev,1}$	(kW)	4.46	1.53	(-) 65.70
$\dot{I}_{ev,2}$	(kW)	-	0.22	-
$\dot{I}_{ev,t}$	(kW)	4.46	1.75	(-) 60.76

3.8 PARAMETRIC ANALYSIS OF DMS-VCR SYSTEM

In order to make the DMS-VCR system more feasible, it's important to control the design parameter of the system. This can be achieved by choosing appropriate operating parameters such as evaporator and condenser temperatures, degree of subcooling, and degree of overlap, which can lead to improvements in the system's energy and exergy analysis. In this Section a parametric study is carried out to examine the effect of these factors.

3.8.1 Effect of evaporator temperature (T_{evap})

Figure 3.5 depicts how changes in evaporator temperature impact COP and the overall irreversibility rate. As the evaporator temperature increases from -4°C to 4°C, the refrigerant's specific volume decreases, leading to a 26.03% reduction in compressor power. Moreover, as evaporator temperature increases by 8°C the system COP improves from 3.0 to 4.1 leading to an increase of 36.67%. This rise in evaporator temperature results in a reduction of heat load on condenser-1 and condenser-2 by 7.12% and 2.85% respectively, which in turn, decrease the mass flow rate of the external fluid.

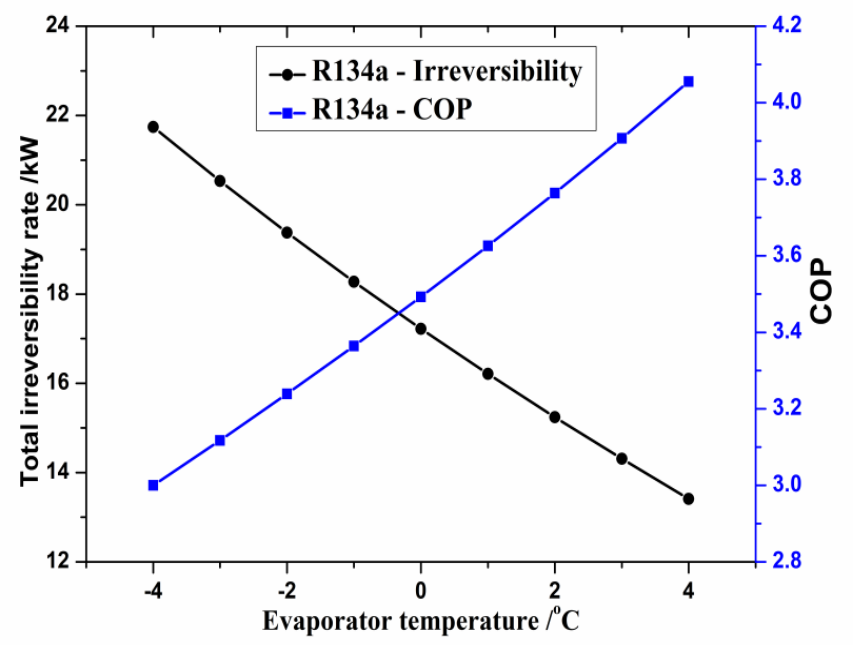

Figure 3.5 Effect of evaporator temperature on total irreversibility rate and COP of the system

As the evaporator temperature increases, the rate of irreversibility in the evaporator section decreases significantly, dropping from 4.5 kW to 1.3 kW. This reduction occurs due to a decrease in the average temperature gradient between the chilled water and the evaporator section. Additionally, the irreversibility rate of the remaining components within the system also decreases, leading to an overall reduction of 38.32% in the irreversibility rate. Consequently, the exergetic efficiency experiences a 31.17% improvement. Hence, a higher evaporator temperature is deemed preferable from both energy and exergy perspectives.

3.8.2 Effect of condenser temperature (T_{cond})

In Figure 3.6, it is observed that altering the condenser temperature has a significant effect on both total irreversibility rates and the COP of the system. By increasing the condenser temperature while keeping other conditions constant, the work done by the compressor goes up by 34.7%. This, in turn, leads to a 60.55% increase in total irreversibility rates and a 25.81% decrease in the COP of the system. Additionally, the system's exergetic efficiency drops from 44.97% to 34.42%. Therefore, from the perspectives of energy and exergy analysis, it is more advantageous to maintain a lower temperature in the condenser.

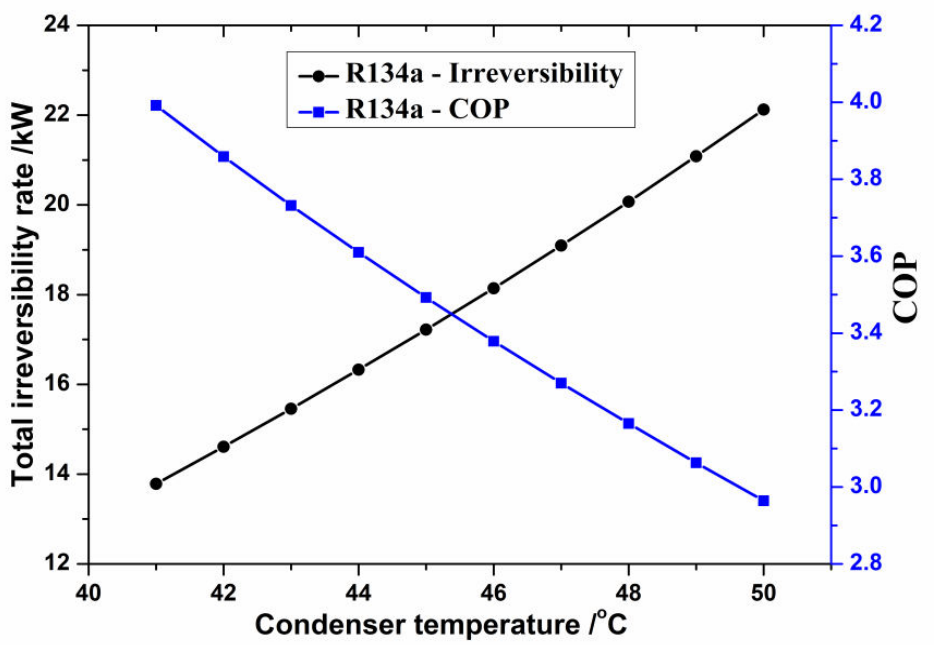

Figure 3.6 Effect of condenser temperature on total irreversibility rate and COP of the system

3.8.3 Effect of degree of overlap

The difference in temperature between the fluid exiting the VCR cycle (state 3) after subcooling and the fluid exiting the DMS system (state 7) from the subcooler is referred to as the degree of overlap. Increasing the degree of overlap from 1°C to 10°C (with an

effectiveness variation from 95% to 65%) results in a 5.8% increase in heat load over the DMS cycle condenser (condenser-2) while keeping other design factors constant. Figure 3.7 shows how the degree of overlap affects the system's COP and total irreversibility rate. The performance of compressor of VCR system remains unchanged, while the overall compressor work increases from 28.19 kW to 29.24 kW as the DMS cycle compressor work increases by nearly 62%. This leads to a 6% increase in total irreversibility and the system's overall COP decreases from 3.547 to 3.420. Hence, considering energy and exergy, it is recommended to have modest degree of overlap values.

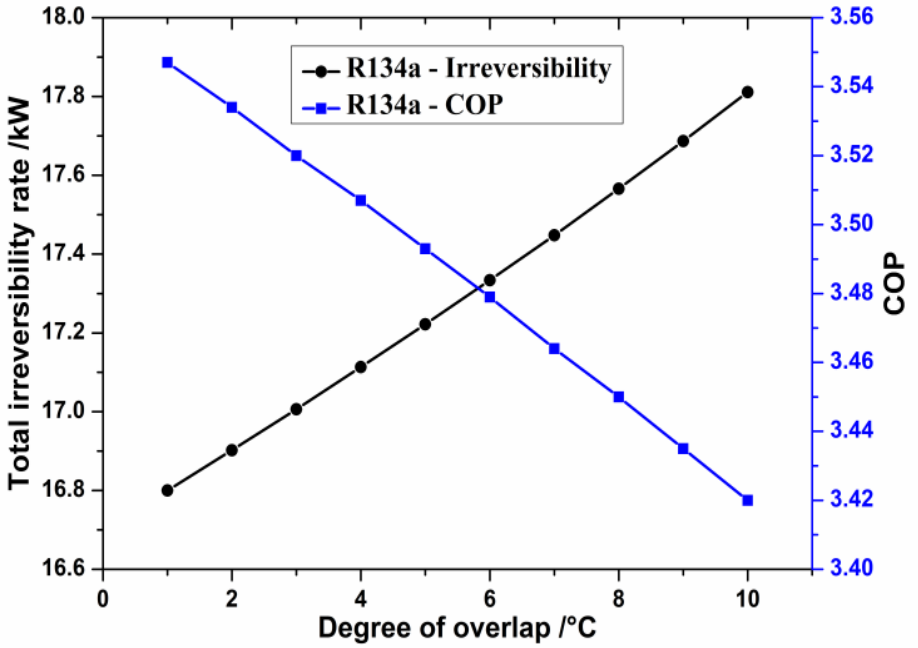

Figure 3.7 Effect of overlap degree on total irreversibility rate and COP of the system

3.8.4 Effect of degree of subcooling

Figure 3.8 shows the variation of total irreversibiblity and COP with degree of subcooling in DMS-VCR system. It is observed that optimal degree of subcooling is 19°C as total irreversibilty is minimum and COP is maximum for this value of DOS. Consequently, 19°C as degree of subcooling is considered for computation of above mentioned results for enhancing the enegy and exergy performance of the DMS-VCR system. This innovative approach is a notable contribution of this study to the field.

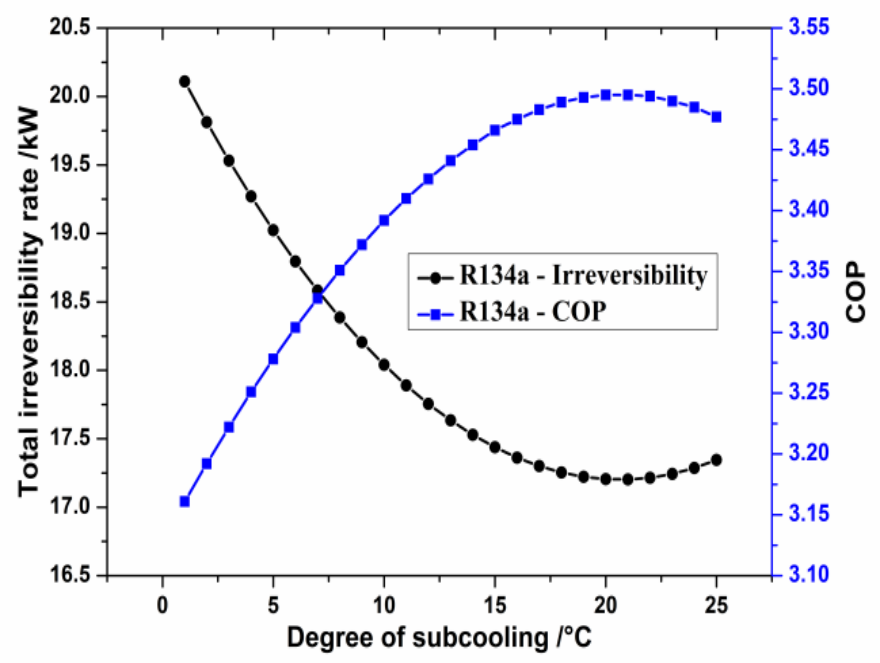

Figure 3.8 Effect of degree of subcooling on system's total irreversibility rate and COP

3.9 CONCLUSIONS

In this Chapter the emphasis is laid on energy and exergy analysis of DMS-VCR system and its comparison with VCR system for water chiller applications. The following conclusions can be drawn from the present study: The optimum value of degree of subcooling for DMS-VCR system is 19°C. The energy analysis shows that the COP of DMS-VCR system is 11.67% higher than that of equivalent VCR system. Moreover, the power consumption of compressors is also reduced by 10.45%, which indicates huge cost savings in terms of electricity consumption cost. The exergy analysis shows reduction in total irreversibility of the system by 15.71 % and an increase of 10.38% in exergetic efficiency of DMS-VCR system in comparison to VCR system. The parametric analysis shows that with increase in evaporator temperature COP increases whereas irreversibility decreases and the increase in condenser temperature gives opposite results for COP and irreversibility in comparison to evaporator temperature increase. The evaporator temperature at 1°C and the condenser temperature at 44°C optimize the DMS-VCR system energy and exergy. The parametric analysis further shows that the degree of overlap and degree of subcooling significantly influence the performance of the DMS-VCR system. Increasing the DOO leads to a decrease in the system's COP and an increase in total irreversibility whereas opposite trends are observed with variation of DOS. A modest degree of overlap around 5°C, and for the degree of subcooling, a value of 19°C is crucial to achieve optimal performance of the system.

In summary, this research highlights the significance of considering energy and exergy aspects when designing efficient cooling systems. It is worth noting that while striving for a high evaporator temperature or low condenser temperature can reduce irreversibility. Similarly, raising the subcooler's (evaporator of DMS system) temperature can improve the COP. So in order to have a feasible and optimum system, it is important to combine energy and exergy aspects.

CHAPTER 4

ENVIRONMENT AND ECONOMIC ANALYSIS OF DEDICATED MECHANICAL SUBCOOLED VAPOR COMPRESSION REFRIGERATION SYSTEM

This chapter explores the environmental and economic considerations on dedicated mechanical subcooled vapor compression refrigeration system. The analysis examines the system's impact on the environment and its economic implications, providing insights into both aspects for a comprehensive understanding.

4.1 INTRODUCTION

As the worldwide demand for efficient and environmentally responsible refrigeration solutions continues to grow, dedicated mechanical subcooled vapor compression refrigeration system have emerged as promising candidates for meeting these dual objectives. This advanced refrigeration technology involves a careful instrumentation of various components, including the evaporator, condenser, compressor, expansion valve, and subcooler, each playing a crucial role in the overall system performance.

The economic and environmental analysis of dedicated mechanical subcooled vapor compression refrigeration systems represents a comprehensive examination of the cost and carbon footprint associated with each system component. One key focal point in this analysis is the concept of reducing compressor work, particularly concerning the high-grade energy required for compression. The compressor, as a major energy consumer in vapor compression systems, significantly influences both operational costs and the carbon footprint. By investigating strategies to minimize the compressor work, such as through advanced technologies, and system optimization, this study aims to demonstrate the potential for substantial energy and cost savings.

This research seeks to contribute to the ongoing communication on sustainable refrigeration practices by shedding light on the economic and environmental intricacies of dedicated mechanical subcooled vapor compression systems. Through a holistic analysis that considers the costs and benefits associated with each system component, as well as the crucial to reduce high-grade energy consumption i.e. electricity, it aim to provide insights that not only advance the adoption of efficient refrigeration technologies but also promote financially viable and environmentally friendly practices. The ultimate goal is to pave the way for a new era of refrigeration systems that strike a harmonious balance between economic viability, energy efficiency, and environmental operation. Qureshi and Zubair [71] examined the

thermoeconomic considerations of heat exchanger inventory allocation in vapor compression cycles with mechanical subcooling. The investigation covers constant work rate, heat rejection, and cooling rates, as well as subcooler heat transfer. Findings indicate no minima for cost functions concerning absolute temperature and average subcooling temperature ratios. Derivatives for the integrated subcooling cycle can be derived from those of the dedicated subcooling cycle. The study concludes that the cost optimization for the integrated mechanical subcooling system is qualitatively similar to that of the dedicated subcooling system. Zare et al. [72] revealed that ammonia-water cogeneration cycle's economic optimization via thermodynamic and thermoeconomic models, emphasizing product unit costs. Parametric analysis optimizes thermal, exergetic efficiencies alongside unit costs. Their findings indicate thermoeconomic optimization reduces product costs by up to 25.9% compared to thermodynamic optimization. Dai et al. [73] examined a residential CO_2 heat pump system with direct mechanical subcooling, considering annual energy and economic performance with frosting effects. Optimal COP achieved at specific discharge pressure and subcooling, enhancing COP by 24.4% and reducing discharge pressure. In severe cold regions, seasonal performance factor (SPF) notably improves, with floor-coil radiators or fan-coil units yielding a 32.0% increase. Employing small temperature difference fan-coil units achieves the highest SPF. Additionally, the CO_2 HP with DMS demonstrates superior economic efficiency, reducing annual total cost by 7.51–15.27% compared to traditional systems. Dai et al. [74] Introduced a CO_2 heat pump-air conditioning system with dedicated subcooling for yearly heating and cooling needs. Assessments cover energetic, exergetic, and exergoeconomic aspects, comparing to traditional CO_2 setups. Results show notable enhancements in annual performance factor (APF) and annual exergy efficiency (AEE). Introducing dedicated subcooling proves cost-effective, reducing total costs by up to 16.96% for heating and 4.52% for cooling. Recommendations include reducing compressor prices and enhancing building insulation for broader CO_2 system adoption. Dai et al. [75] presented an environmental and economic model for assessing transcritical CO_2 heat pump with dedicated subcooling. Integrating DMS reduces energy consumption, particularly with small temperature difference fan-coil units. CO_2 heat pump systems for space heating offer eco-friendly alternatives, with lower initial and operating costs compared to traditional methods. Payback periods for CO_2 HP_{DMS} systems are generally under 9 years, and with reduced compressor and electricity prices, competitiveness with coal-fired boilers is achievable. In China, subsidizing electricity prices and reducing compressor costs could facilitate widespread adoption of CO_2 HP_{DMS} for space heating. Miran et al. [76] investigated

transcritical refrigeration cycles with dedicated mechanical subcooling, assessing energy, exergy, and exergoeconomic aspects with CO_2 (R744), N_2O (R744A), and ethane (R170),. Results show N_2O with the highest COP and exergy performance, while CO_2 exhibits superior economic performance. Subcooling improves system performance with minimal increase in unit product cost, making it an effective and economical enhancement. Application of subcooling leads to significant COP enhancement for all refrigerants with moderate unit product cost increments. Mofrad et al. [77] investigated thermodynamic analysis of cascade and heat recovery cascade refrigeration cycles, utilizing R744 and R744A refrigerants. Advanced analysis highlight superior performance of the heat recovery cascade refrigeration system, employing exergoeconomic and exergoenvironmental approaches. Optimization via genetic algorithm reveals significant improvements in coefficient of performance and exergy efficiency with the heat recovery cascade refrigeration cycle. Tsimpoukis et al. [78] examined a supermarkets' refrigeration and HVAC systems contribute significantly to industrialized countries' electricity consumption and CO_2 emissions. Research focuses on eco-friendly R744 transcritical units for a Greek supermarket, evaluating configurations for energy efficiency and environmental impact, outperforming conventional solutions by up to 20.9% in energy savings.

In this Chapter, a novel approach is introduced, which combines insights on two essential domains: economics and environment. The Engineering Equation Solver (EES) software is employed to construct a robust program for the mathematical model of the DMS-VCR system. This analysis not only facilitates in computing the various parameters of the estimation of critical DMS-VCR system characteristics such as cost, size, energy consumption, and exergetic efficiency under various operating conditions over a broad range, but also undergoes a comprehensive analysis that accounts for a broad range of operating variables. A significant finding in the study is the identification of the optimal degree of subcooling, which is determined to be around 19°C. The optimum degree of subcooling is a secured function of capital recovery factor and yearly operating period, which is economically advantageous because exceeding this limit increases the system's annual cost, which is the work's novelty. In a nutshell, the work's unique feature is that it shows a DMS-VCR system performance analysis based on economics and environment analysis results.

4.2 MATHEMATICAL MODELING

Mathematical modeling supports economic analysis by optimizing capital and operational costs. Furthermore, it aids in environmental analysis and thermoeconomic optimization, evaluating sustainability and cost-effectiveness in energy systems.

4.2.1 Economic analysis

In this Section economic analysis of the system is presented. The economic analysis assists in minimising the area of the heat exchangers used in the system and all the costs i.e. capital, operational and maintenance costs. The heat exchangers employed in this investigation are the evaporator, condenser-1, condenser-2, and subcooler. Bakhtiari et al. [79], designed the VARS components as well as the water chilling application. In the present work, the evaporator and condenser are of the shell and tube type, whereas the subcooler is of the tube in tube type. Table 4.1 shows the additional dimensioning features of different heat exchangers in the current system.

Table 4.1 Parameters for sizing the DMS-VCR system heat exchangers

Description	Tube's inner diameter /mm	Tube's outer diameter /mm	Length of tube /m	Number of turns
Evaporator	13.84	15.87	6.09	4
Condenser-1	13.84	15.87	6.09	2
Condenser-2	13.84	15.87	6.09	2
Subcooler	13.84	15.87	6.09	1

4.2.1.1 Capital and operational costs

This approach ignores the price of pumps, valves, refrigerants, and connecting pipes, but it does account for the overall price of heat exchangers and compressors, Sayyaadi and Nejatolahi [11]. According to Sanaye and Malekmohammadi's [80] estimation, 0.84% of the investment cost is made up of the price of other products, such as pipes, expansion valves, and refrigerant. According to Kizilkan et al. [81] the cost of investment for each heat exchanger is calculated based on the surface area of the heat exchanger. The DMS system's investment cost is determined by the Equations listed below:

$$Z_k = 516.621\, A_k + 268.45 \quad (4.1)$$

DMS, $\forall k \in EoS \cap \{Evap, Cond1, Cond2, Subcooler\}$

The scroll compressor expenditure cost, on the other hand, is given by Eq. (4.2).

$$Z_k = \left(\frac{573 \cdot \dot{m}_{ref}}{0.8996 - \eta_{isen}}\right)\left(\frac{P_{cond}}{P_{evap}}\right)\ln\left(\frac{P_{cond}}{P_{evap}}\right) \quad (4.2)$$

$\text{DMS}, \forall k \in EoS \cap \{Compressor\}$

Further, the capital recovery factor can be demoed as in Eq. (4.3).

$$a^c = \frac{i_{rate}(1+i_{rate})^{N_y}}{(1+i_{rate})^{N_y} - 1} \quad (4.3)$$

Here, interest rate and system lifetime are represented by i_{rate} and N_y.

The isentropic compressor efficiency (η_{isen}), which is dependent on the pressure ratio, is represented by Eq. (4.4).

$$\eta_{isen} = 0.85 - 0.046667\left(\frac{P_{cond}}{P_{evap}}\right) \quad (4.4)$$

Eq. (4.5) calculates the overall cost of the DMS-VCR system and Eq. (4.6), which represents the system's operational cost, yields the quantity of electric power being provided to the compressor.

$$Z_t = \sum_{k \in EoS}(Z_k) \quad (4.5)$$

$\text{DMS} - \text{VCRS}, \forall k \in EoS \cap \{Evap, Cond1, Cond2, Comp1, Comp2, Subcooler\}$

$$C_{oper} = t_{oper} * C_i^{el} * \dot{W} \quad (4.6)$$

The annual operational hours (t_{oper}) and the unit cost of electrical exergy (C_i^{el}) of the DMS-VCR system are assumed as 6000 h and 0.06 USD/kWh respectively. The same is referred from Aminyavari et al. [69].

4.2.2 Environment analysis

Many environmentalists believe that carbon pricing, which acts as a penalty for CO_2 emissions, can be used to address issues related to global warming Aminyavari et al. [69]. Eq. (4.7) can be used to calculate this cost.

$$C_{env} = m_{co_2} * C_{co_2} \quad (4.7)$$

In this context, the cost associated with CO_2 emissions penalty, denoted as, C_{co_2}, is subject to variation across different countries. As stated by Aminyavari et al. [69] the value of this cost ranging from 22 to 117 dollars per tons. However, for the purpose of the current study, the penalty cost (i.e. in 90 USD/ton of CO_2 emission) is assumed accordingly. Additionally, according to Eq. (4.8) mass of CO_2 emission (m_{co_2}) is given by:

$$m_{co_2} = \lambda * \dot{W}_t * t_{oper} \quad (4.8)$$

The conversion factor of emissions is denoted by λ, where CO_2 emissions per kWh of electric energy are determined to be 0.968 kg/kWh. The overall yearly operational cost of the DMS system is calculated by adding the annual electricity cost to the CO_2 penalty cost.

$$C_t = C_{oper} + C_{env} \quad (4.9)$$

4.3 THERMOECONOMIC OPTIMIZATION

The thermoeconomic optimization of the DMS-VCR system involves a comprehensive approach to enhance both the thermodynamic efficiency and the economic feasibility of the system. This process seeks to identify the optimal operating conditions and system configurations that minimize the overall cost while maximizing performance.

In the context of the DMS-VCR system, thermoeconomic optimization involves fine-tuning various system parameters such as temperatures, pressures, degree of overlap, degree of subcooling, and heat exchanger areas. The objective is to strike a balance between achieving the highest energy efficiency and minimizing operational costs, capital investments, and maintenance expenses.

Eq. (4.10) specifies the economic parameters, which incorporate the annual operational costs of the plant.

$$\min C_t(x) = C_{oper} + C_{env} + a^c . \phi . \sum_{k \in EoS} Z_k \quad (4.10)$$

$$\text{DMS} - \text{VCRS}, \forall k \in EoS \cap \{Evap, Cond1, Cond2, Comp1, Comp2, Subcooler\}$$

The calculation described above is divided into three sections. The first portion denotes the expenditure associated with total energy usage, the second part denotes the penalty for CO_2 emissions, and the final part denotes the cost associated with maintenance and capital investment. In the above Eq. (4.10), the maintenance component (ϕ), accounts for about 6% of Z_k, which is fluctuating over time. The thermoeconomic optimization of the DMS-VCR system aims to ensure that the system operates in an economically efficient manner while delivering the desired cooling capacity. By systematically evaluating and adjusting various parameters, engineers and researchers can develop systems that are not only environmentally friendly but also economically viable over their operational lifetimes.

4.4 RESULTS AND DISCUSSION

In this Section the results and discussion are presented for different operating parameters of the DMS-VCR system for refrigerant R134a.

4.4.1 Performance comparison between the equivalent VCR system and DMS-VCR system

A comprehensive comparison is conducted between the DMS-VCR system and an equivalent VCR system designed for industrial water chiller applications. Both systems operate with refrigerant R134a under identical conditions. This assessment encompasses various aspects, including economic and environmental considerations. The operational parameters for implementing water cooling within the DMS-VCR system were obtained through research papers [69], [81] and are detailed in Table 4.2.

Table 4.2 Process data of DMS-VCR system

	Parameters	**Values**
Thermal parameters (Aminyavari et al. [69])	Evaporator cooling capacity ($\dot{Q}_{evap}$, kW)	100
	Evaporator temperature (T_{evap} ^{o}C)	0
	Inlet temperature of evaporator coolant ($T_{in,evap}$ ^{o}C)	10
	Outlet temperature of evaporator coolant ($T_{out,\ evap}$ ^{o}C)	5
	Temperature of Condenser (T_{cond} ^{o}C)	45
	Coolant inlet temperature at condenser ($T_{in,\ cond}$ ^{o}C)	35
	Coolant outlet temperature at condenser ($T_{out,\ cond}$ ^{o}C)	40
	Overlap degree ($T_{overlap}$, ^{o}C)	5
	Degree of subcooling ($T_{subcooling}$ ^{o}C)	5, 19 (optimal)
	Isentropic efficiency of compressors (η_{isen})	0.66, 0.76
	Environment temperature (T_o ^{o}C)	25
	Environment pressure (P_o, kPa)	101.325
	Refrigerants (for both the cycles)	R134a
Economic parameters (Kizilkan et al. [81] and Aminyavari et al. [69])	Interest rate (i_{rate}, %)	10, 2
	Repayment period (N_y, years)	5, 10
	Operation time/year (t_{oper}, hours)	5000, 4000
	Electricity unit cost (C_i^{el} in /$ kWh^{-1})	0.06

4.4.2 Results of economic and environment analysis

Table 4.3 depicts the comparison of results of economic and environmental analysis for DMS-VCR system and equivalent VCR system operating under the same input conditions.

The DMS-VCR system consumes less electricity since the compressor power required in DMS-VCR system is reduced thereby resulting in cost savings in terms of operational costs.

However, it is important to note that DMS-VCR system require a higher initial capital investment due to more number of heat exchangers (resulting in larger heat exchanger area), an additional compressor and expansion valve. Specifically, DMS-VCR system entails a 6.07% increase in the overall heat exchanger area, leading to a corresponding rise in the initial investment cost. However the DMS-VCR system is more economical since it offers a reduction of 6.72% in total annual cost and 10.44% decrease in annual operational costs when compared with an equivalent VCR system. Moreover, when assessing various performance metrics in comparison to an equivalent VCR system, the DMS-VCR system demonstrates superior performance, as shown in Table 4.3. The key environmental metric, which is the emission of CO_2 into the atmosphere, demonstrates that the DMS-VCR system emits 10.43% less CO_2 compared to an equivalent VCR system, even though both systems have the same cooling capacity. This reduction is attributed to the DMS-VCR system's lower electricity consumption. As a result, the DMS-VCR system undoubtedly stands out as a highly reliable and energy-efficient cooling system, offering substantial decarbonization benefits.

Table 4.3 Comparative analysis results of DMS-VCR system with equivalent VCR system for Case-I

Parameters	**VCR system (X)**	**DMS-VCR system (Y)**	**Percentage Change /% [(Y-X)/X*100]**
$\dot{C}_t$ (\$/year)	12444	11608	(-)6.72
$\dot{C}_{oper}$ (\$/year)	7672	6871	(-)10.44
$\dot{m}_{co_2}$ (ton/year)	123.78	110.86	(-)10.43
$A_{cond,1}$ (m^2)	7.73	6.40	(-)17.21
$A_{cond,2}$ (m^2)	-	1.13	-
$A_{cond,\,t}$ (m^2)	7.73	7.53	(-) 2.58
A_{sc} (m^2)	-	0.98	-
A_{evap} (m^2)	5.12	5.12	-
A_t (m^2)	12.85	13.63	(+)6.07

4.4.3 Parametric analysis of DMS-VCR system

In order to make the DMS-VCR system more feasible, it's important to control the cost and size of the system. This can be achieved by choosing appropriate operating parameters such as evaporator and condenser temperatures, degree of subcooling, and degree of overlap,

which can lead to improvements in the system's economics, and environmental analysis. In this Section a parametric study is carried out to examine the effect of these factors.

4.4.3.1 Effect of evaporator temperature (T_{evap})

Figure 4.1 depicts the relationship between the system's evaporator temperature and various expenses connected with system operation, such as the annual cost of the plant (C_t) and overall cost of the system (Z_{total}). The system's overall area rises from 11.28 m^2 to 43.70 m^2 with an increase in evaporator temperature of 8 ^oC owing to a decrease in the overall system's heat transfer coefficient and LMTD.

This causes the system's Z_{total} to increase by 83.82%. However, at an evaporator temperature of 1^oC, the annual plant operation cost (C_t) is found to be at its minimum and begins to increase afterward.

On the other hand, the increase in the evaporator temperature results in a reduction in the system's operational costs (C_{oper}) and environmental damage costs (C_{env}) by about 26%. Since these costs contribute less to the overall plant cost than the initial capital investment, a higher evaporator temperature is financially favorable position from economic view point. A reduced irreversibility rate in a heat exchanger design does not always translate to an optimal outcome, as it leads to an increase in the annual operation cost of the system. Therefore, a refrigeration system with a higher evaporator temperature may not be the best choice.

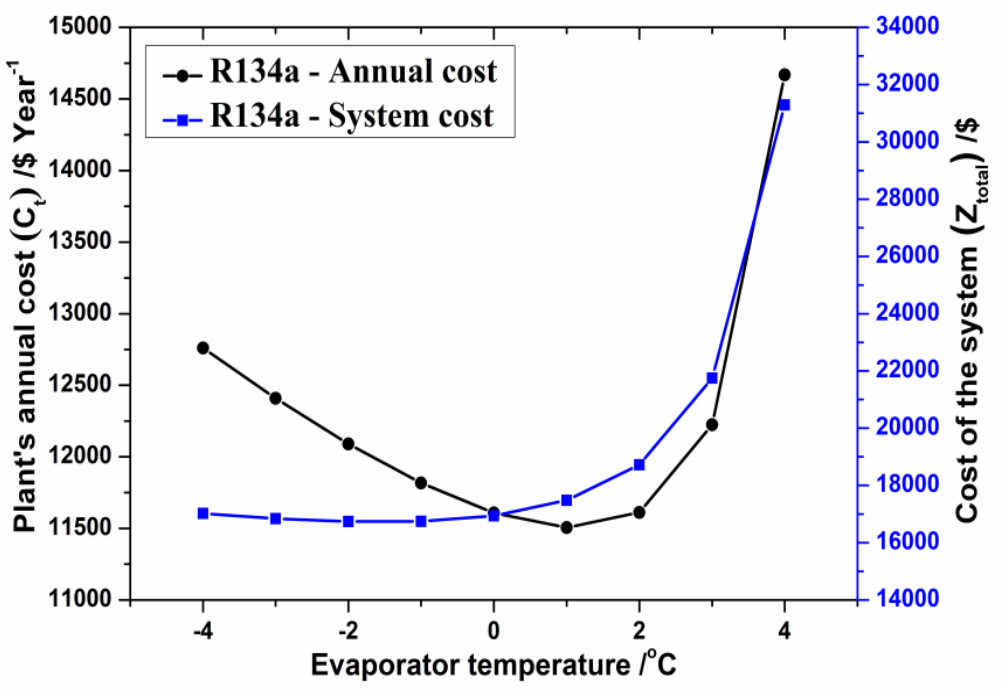

Figure 4.1 Effect of evaporator temperature on plant's annual cost and cost of the DMS-VCR system

4.4.3.2 Effect of condenser temperature (T_{cond})

Figure 4.2 shows how the condenser temperature affect the annual plant costs (C_t) and overall cost of the system (Z_{total}). When the condenser temperature increases, the LMTD is increased from around 3°C to 12°C which results in decrease of the condenser area. Consequently, the total system area and overall cost of the system decrease by 63.72% and 29.74%, respectively. The plant attains its most economical operational cost at a temperature of 44°C, but costs start to increase beyond this optimal point, resulting in an approximately 11.37% increase in annual cost. The system's economic study supports the use of a low condenser temperature, since it results in lower operating costs (C_{oper}) and environmental damage costs (C_{env}). However, the costs associated with environmental damage and system operation increases as the condenser temperature is increased. This leads to around 35% increase in expense of environmental damage and the system operational cost. Therefore, low condenser temperature value is preferable from economic point of view.

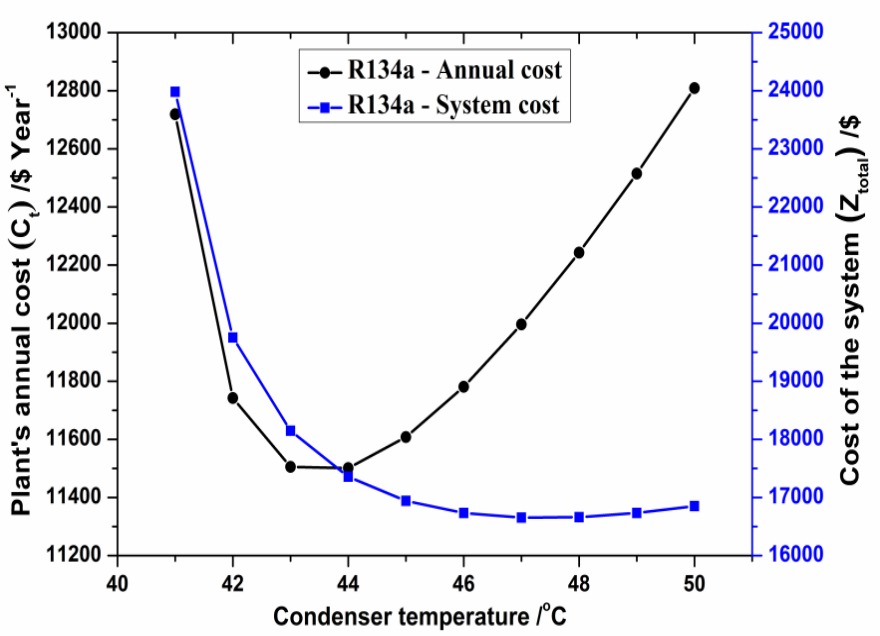

Figure 4.2 Effect of condenser temperature on plant's annual cost and cost of the DMS-VCR system

4.4.3.3 Effect of degree of overlap

The relationship between the degree of overlap and various costs associated with system operation, such as the overall annual cost of the plant (C_t) and overall cost of the system (Z_{total}) is illustrated in the Figure 4.3. The area of the subcooler cycle condenser (condenser-2) increases by 5.6%, but the subcooler area decreases rapidly by 95% with a change in the degree of overlap. Consequently, there is a reduction of 41.21% in the system's overall area which results in a decrease in overall cost of the system (Z_{total}) by 20.68%. As depicted in

Figure 4.3, the optimal point for the objective function concerning the annual cost of the system (C_t) occurs when degree of overlap is 5°C. However, both the system's operating costs (C_{oper}) and environmental damage costs (C_{env}) increase with variations in the degree of overlap by 3.75%. Therefore, from both an economic and environmental perspective, a lower degree of overlap is recommended.

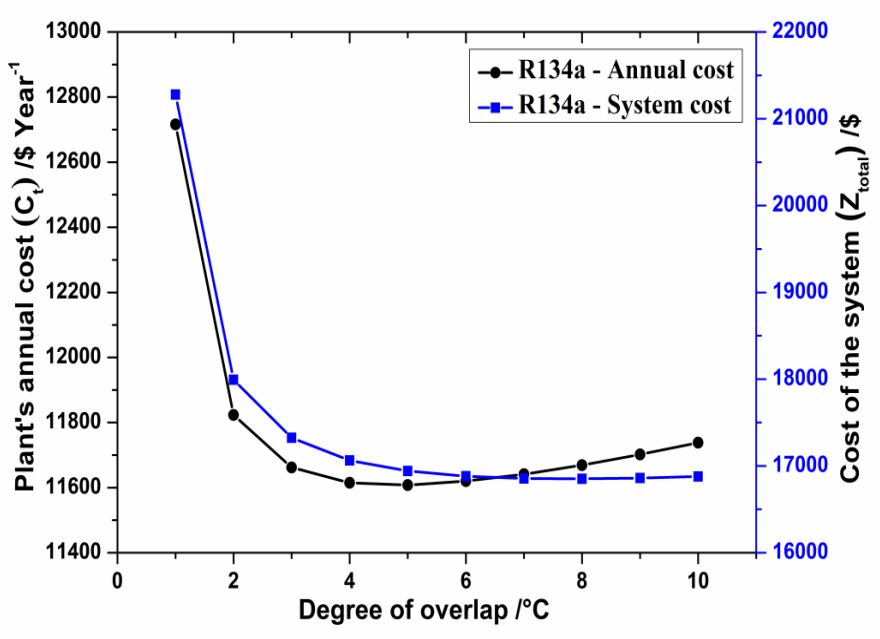

Figure 4.3 Effect of overlap degree on plant's annual cost and cost of the DMS-VCR system

4.4.3.4 Effect of degree of subcooling (DOS)

As depicted in Chapter 3, Figure 3.8, varying the degree of subcooling affects both the COP and the total irreversibility rate of the system. By increase the degree of subcooling from 1°C to 25°C, it reduces the specific cooling effect, leading to a decrease in the refrigerant's mass flow rate. Consequently, the compressor work is reduced by 9.07%, resulting in a lower heat load on condenser-1 but an increased load on condenser-2. As the degree of subcooling increases, the system's COP rises from 3.161 to 3.477. On the other hand, Figure 4.4 shows the changes in the DOS affect the system's annual costs (C_t) and overall cost of the system (Z_{total}). It is observed that there's an 8.06% increase in the total system area due to a decrease in the overall heat transfer coefficient of the DMS system which increases the cost of heat exchangers, however there is a reduction in mass flow rate of refrigerant in compressor bringing a huge reduction in compressor cost of VCR system which acts as a dominating factor in reducing the overall capital cost. Consequently, Z_{total} decreases by 3.33% at degree of subcooling value of 16°C, after which it increases, as the heat exchanger area cost dominates the reduction in compressor cost. At 19°C, the system's annual cost (C_t) reaches its

lowest point and begins to increase beyond that point. A reduced compressor workload leads to a 10% decrease in system operating costs (C_{oper}) and environmental damage costs (C_{env}). Beyond this limit, both operating costs and environmental damage costs increase and therefore, values up to this range of the degree of subcooling are encouraged from an economic and environmental perspective.

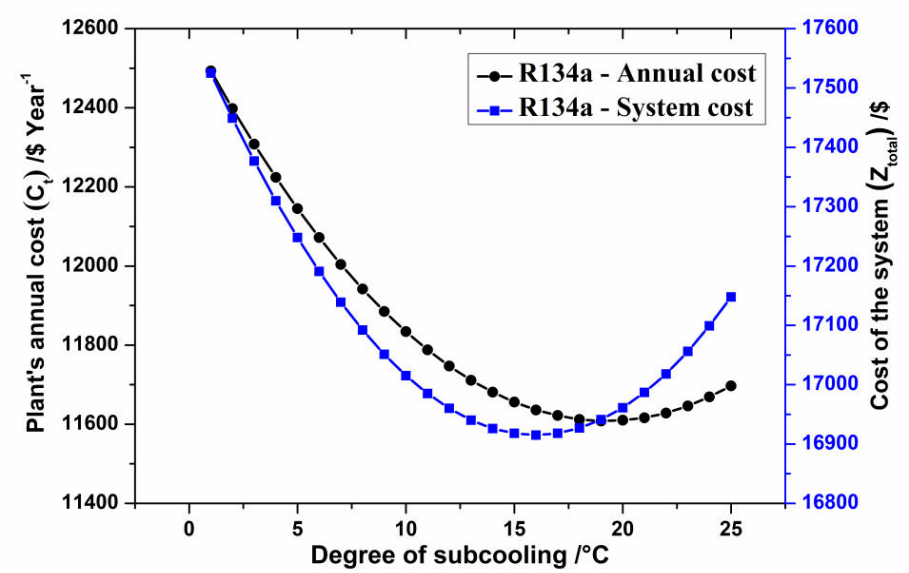

Figure 4.4 Effect of degree of subcooling on plant's annual cost and cost of the DMS-VCR system

4.5 THERMOECONOMIC OPTIMIZATION

In this para, two distinct cases are investigated, each characterized by different ROI values i.e. 10% for Case-I and 2% for Case-II. The results associated with these cases, including performance indicators, are presented in Table 4.4. ROI serves as a critical parameter influenced by a nation's economic context, with different countries offering varying ROI rates, typically ranging from 10% (the highest) to 2% (the lowest). Many nations adopt strategies such as subsidies and lower ROI values to promote system acceptance and, in turn, reduce the payback period. It's important to note that these factors undergo changes over time, reflecting evolving economic conditions and policies.

Table 4.4 Results of thermoeconomic optimization w.r.t. base case

Performance Parameter		**Base Case**	**Thermoeconomic Optimized**	
			Case-I: i_{rate}=10%, N_y=5 yrs and t_{oper}=4000h	**Case-II: i_{rate}=2%, N_y=10 yrs and t_{oper}=5000h**
Low grade	$\dot{Q}_{cond1}$ (kW)	124.95	108.28	106.58

Energy	$\dot{Q}_{cond2}$ (kW)	5.55	17.87	17.14
	$\dot{Q}_{sc}$ (kW)	5.32	16.00	15.48
	$\dot{Q}_{evap}$ (kW)	100	100	100
High Grade Energy	$\dot{W}_{comp1}$ (kW)	30.26	24.28	22.07
	$\dot{W}_{comp2}$ (kW)	0.240	1.87	1.65
	$\dot{W}_{t}$ (kW)	30.50	26.16	23.72
First law Analysis	COP_{VCR}	3.30	4.11	4.531
	COP_{DMS}	22.14	8.54	9.37
	$COP_{overall}$	3.278	3.82	4.21
Second law Analysis	$\dot{I}_{cond1}$ (kW)	3.24	2.28	1.76
	$\dot{I}_{cond2}$ (kW)	0.129	0.34	0.25
	$\dot{I}_{evap}$ (kW)	2.85	2.41	1.95
	$\dot{I}_{comp1}$ (kW)	9.173	7.11	6.24
	$\dot{I}_{comp2}$ (kW)	0.047	0.41	0.36
	$\dot{I}_{sc}$ (kW)	0.121	0.72	0.62
	$\dot{I}_{ev1}$ (kW)	3.44	1.37	1.15
	$\dot{I}_{ev2}$ (kW)	0.015	0.18	0.15
	$\dot{I}_{t}$ (kW)	19.02	14.85	12.50
	η_{II} (%)	37.64	43.23	47.27
Other Parameters	$\dot{m}_{ref1}$ (kg s^{-1})	0.7032	0.6108	0.6023
	$\dot{m}_{ref2}$ (kg s^{-1})	0.0346	0.1078	0.1028
	A_t (m^2)	13.05	17.62	26.23
	Z_t (\$)	17248	18271	20965
	C_t (\$ $year^{-1}$)	**12145**	**11389**	**9708**
Optimized value of operating parameters	Evaporator Temperature		Te=1.084	Te=2.261
	Condenser Temperature		Tc_1=43.52	Tc_1=42.13
	Degree of Overlap		DOO=4.791	DOO=3.376
	Degree of Subcooling		DOS=17.87	DOS=17.61

Selecting an optimal point is more important for the system to operate more efficiently both economically and thermodynamically. Finally, by simultaneously modifying the choice

variables, the conjugate directions technique is employed to determine the objective functions' ideal value. To perform an economic analysis, a basic compression refrigeration cycle with a 5°C subcooling is chosen as the base case. For Case-I and Case-II, Table 4.4 outlines the optimal values for the decision variables, including T_{evap}, T_{cond}, $T_{subcooling}$, and $T_{overlap}$.

It underlines that, relative to the base case (i.e., T_{evap}=0°C, T_{cond}=45°C, $T_{subcooling}$=5°C, and $T_{overlap}$=5°C), size (area) increases in Cases-I and II, yet annual cost greatly lowers in both situations. Consequently, in the optimal scenario, the DMS-VCR system's yearly expenses experience a significant decrease of 6.22% and 20.06% for the two situations with the specified design condition (see Table 4.4). Compared to the base case (13.05 m^2), the heat exchanger area is increased in Case-I (17.62 m^2) and Case-II (26.23 m^2). Cases-I and II both show a sizable improvement in the system's total COP. Thus, the total cost of electricity in compressors is reduced by 14.22% in Case-I and 22.22% in Case-II to generate the same cooling effect. The results indicate that for Case-II, there is a lower overall electricity consumption but a higher equipment cost. In Case-II, the DMS-VCR system's payback period is less than 5.1 years compared to equivalent VCR system ($20965 - $17067 = $3898) due to increased investment costs. It's worth noting that this would result in a payback period for excess expenses that is less than half the system's lifespan.

4.6 CONCLUSIONS

In this Chapter the emphasis is laid on environment and economic analysis of DMS-VCR system and its comparison with VCR system for 100 kW water chiller applications. The following conclusions can be drawn from the present study:

1) The optimum value of degree of subcooling for DMS-VCR system is 19^{o}C. The power consumption of compressors is also reduced by 10.45%, which indicates huge cost savings in terms of electricity consumption cost and simultaneously there is reduction in CO_2 production which also means lower carbon capture cost. Annual CO_2 emissions decrease from 124 tons/year to 110 tons/year with the adoption of the DMS-VCR system. The DMS-VCR system contributes to an 11.30% reduction in the cost of environmental damage.
2) Environment and economic analysis shows that the area required for heat exchangers in DMS-VCR system is 6.07% more than that required for VCR system. However, this increase in area translates into three positive outcomes, i.e. reduction in total cost by 6.72%, reduction in operation cost by 10.44 %, and 10.43% reduction in mass of

CO_2 produced.

The DMS-VCR system emerges as a promising solution, offering substantial energy and environmental benefits in comparison to VCR system.

3) The parametric analysis further shows that the degree of overlap and degree of subcooling significantly influence the performance and cost of the DMS-VCR system. A modest degree of overlap, around 5°C and for the degree of subcooling, a value of 19°C are crucial to achieve optimal performance and cost-effectiveness while minimizing environmental impact.
4) The overall annual cost of operating the DMS-VCR system is 6.72% more cost-effective compared to an equivalent VCR system, with potential for further cost reductions by 1.88% in Case-I and a substantial 16.36% in Case-II.

In summary, this research highlights the significance of considering thermodynamic, economic and environmental aspects when designing efficient and cost-effective cooling systems. It is worth noting that while striving for a high evaporator temperature or low condenser temperature can reduce irreversibility however, it may lead to higher overall system costs. Similarly, raising the subcooler's (evaporator of DMS system) temperature can improve the COP but may not align with economic and environment considerations. In order to have a feasible and optimum system, it is important to combine thermal, economic and environmental aspects. This can be achieved through meticulous parametric optimization, i.e. the system can be made economically viable, environmentally sustainable and energy efficient.

CHAPTER 5

THERMODYNAMIC AND COEFFICIENT OF STRUCTURAL BOND ANALYSIS OF ACTUAL DEDICATED MECHANICAL SUBCOOLED VAPOR COMPRESSION REFRIGERATION SYSTEM

This chapter conducts a thermodynamic analysis along with an examination of the coefficient of structural bond for an actual dedicated mechanical subcooled vapor compression refrigeration system. The goal is to analyze how these factors influence the performance of the actual system.

5.1 INTRODUCTION

The vapor compression refrigeration (VCR) system is widely used technology for heating and cooling purposes in residential, commercial and industrial applications. However, due to the high energy consumption of these systems and rising costs of energy, energy efficiency and energy conservation have become a growing concern. The researchers are therefore exploring methods to enhance the performance of these systems so as to address the above issues. One of the methods to enhance the performance of a VCR system is to subcool the liquid refrigerant leaving the condenser. This can be achieved by incorporating a dedicated mechanical subcooled (DMS) system (which is basically a VCR system only) used in conjunction with the existing VCR system. The sole purpose of DMS system is to subcool the liquid refrigerant leaving the condenser-1 of the VCR system used for cooling or heating application. A number of studies have been conducted on the topic of mechanical and dedicated subcooling of VCR systems as discussed in following paras. Qureshi and Zubair [23], [25] investigated the mechanical subcooling of VCR systems and explored the most efficient methods of operation and management. They analysed the system at 0°C of evaporator temperature and 45°C of condenser temperature. According to Agaro et. al. [28], DMS-VCR system is the most thoroughly studied system and is effectively used to improve the efficiency of the transcritical VCR system. Yang and Yeh [21] examined VCR system that uses various refrigerants (R22, R134a, R410A and R717) to identify ways to enhance their performance and minimize exergy destruction. Wang and Zhang [16] optimised and compared a single-stage transcritical CO_2 VCR cycle with different subcooling methods for district heating and cooling and investigated it on the basis of energy, exergy and economic view point. Agarwal et al. [14] examined the mechanical subcooled VCR system's energy and exergy aspects in order to improve its efficiency. However, they did not take into account the coefficient of structural bonds (CSB) factors, which are crucial in making accurate decisions regarding energy resource utilization. Boer et al. [61] conducted an energy, exergy, and

structural analysis of a single effect vapor absorption cooling cycle that utilized ammonia and water. Through exergy analysis, they were able to assess the level of irreversibility within each component of the cycle as well as the overall system. The CSB analysis is also performed to access the impact that how any change in irreversibility within one component of the system would affect the rest of the components and the system as a whole. To assess the actual thermodynamic efficiency of chemical processes and the distribution of irreversibility in a plant, Tekin and Bayramoglu [62] carried out an exergy and CSB analysis. They reported the decrease in total exergy loss is equal to 4.21%in sugar manufacturing plants. Nikolaidis and Probert [63] analyzed a refrigeration plant that uses a two stage VCR system and demonstrated that the exergy method is effective for studying its behaviour. Misra et al. [60] analyzed an absorption chiller system that is used for air-conditioning purposes and used the CSB technique to assess the economic cost of the product. Their study revealed that the capital cost of the optimal system configuration increased by approximately 33.3% compared to the base case, but this additional cost is offset by the reduced fuel cost, making it a cost-effective option in the long run.

It is thus observed that sustainable and efficient VCR systems should be developed in light of increasing energy costs and energy conservation. The DMS-VCR system is capable of enhancing the energetic and exergetic performance of the system as is evident from the investigations performed by various researchers. Studies have been carried out to evaluate efficacy of DMS-VCR systems. Further, the CSB approach has been observed as a useful tool for assessing the impact of change in irreversibility of a component on the other components and the system. It can thus help the designers to wisely make decisions for changing the design of the component which affects the performance of other components critically.

Previous studies have attempted to improve the performance of mechanical subcooled systems through energy and exergy analysis, but they have overlooked the importance of analyzing the CSB in a system. Most studies on DMS-VCR systems have focused on introductory energy and exergy analysis using typical refrigerants for low cooling capacity systems. In addition to this, the performance analysis studies of DMS-VCR system using specific refrigerants such as R134a for high cooling capacity are observed to be scant in literature. To operate a system efficiently and to reduce energy consumption, it is essential to conduct a CSB analysis so as to find appropriate thermodynamic parameters and improve the design of the component so as to reduce the irreversibility rate. However, the CSB studies of DMS-VCR system are also lacking in literature. In this Chapter the DMS system is incorporated in a commercial water chiller of 100 kW capacities (which is based on actual

vapor compression cycle) and a comprehensive energy, exergy and CSB analysis of the combined DMS-VCR system is carried out under different operating conditions. The novelty of this analysis is that it takes a more practical approach, analyzing an actual DMS-VCR system, providing a comprehensive and applicable perspective of refrigeration systems. The system simulation is carried out for a wide range of various operating parameters using the code developed for the DMS-VCR system using Engineering Equation Solver (EES) software. In this Chapter, the aim is to develop a distinctive model that sets itself apart from earlier studies. This can be achieved by incorporating key factors essential for system analysis, such as subcooling within the condenser and a dedicated subcooler, evaluating pressure drops in the evaporator, suction line, condenser, and liquid line, examining superheating within the evaporator and suction line, and conducting a thorough assessment of desuperheating within the discharge line. It is noteworthy that the impact of these crucial parameters was not analyzed in preceding works. This unique approach aims to determine the optimal subcooling degree for maximizing Coefficient of Performance (COP) and exergetic efficiency. The model also investigates the impact of subcooling on the overall irreversibility rate, providing a comprehensive understanding of its impact on system performance. The inclusion of varying evaporator temperatures (0°C, 5°C, and 10°C) in the analysis significantly enhances its value. By exploring different evaporator temperature scenarios, the research provides a valuable and comprehensive perspective, allowing us to gain deeper insights into the system's behaviour under diverse thermal conditions. This research contributes significant insights into enhancing system performance, making it an essential advancement in the practical field.

5.2 SYSTEM DESCRIPTION OF DMS-VCR SYSTEM

Figure 5.1 shows the schematic diagram of the DMS-VCR system which comprises of two compressors, two condensers, two expansion valves, one evaporator and one sub-cooler. The VCR sub system, of DMS-VCR system, is used for cooling or heating for which DMS sub system is used to subcool the liquid refrigerant leaving the condenser-1 of VCR sub system. The heat exchange between the two sub systems occurs by using the evaporator of DMS sub system as a subcooler heat ex-changer in which the liquid refrigerant leaving the condenser-1 of VCR sub system loses heat and the same is utilized to evaporate the refrigerant entering in the evaporator (used as sub-cooler) of VCR sub system.

Figure 5.2 displays the pressure-enthalpy (P-h) diagram for DMS-VCR cycle. The P-h diagram is drawn considering that the refrigerant in both cycles is same. Hence the condenser

pressure and temperature will be same in both VCR sub system and DMS sub system. However, the evaporator temperature of VCR cycle is lower than that of DMS cycle. The DMS cycle is shown by state points 8-9-10-11-8 and VCR cycle is depicted by state points 1-2-2'-3-3'-4-5-6-6'-7-1.In VCR cycle, a high-temperature, high-pressure superheated refrigerant vapor at state 1 leaves the compressor and loses heat to surroundings in the desuperheating process 1-2 in the discharge line. Further, desuperheating of the superheated refrigerant occurs in the condenser-1 during the process 2-2' followed by conversion of saturated refrigerant vapor into saturated liquid refrigerant during the process 2'-3 in the condenser due to heat transfer to the surroundings. The process 3-3' shows the subcooling of the refrigerant in the condenser and remaining subcooling takes place in the dedicated subcooler in the process 3'-4. The subcooler section is essentially evaporator of the DMS sub system which operates at a temperature below the condenser outlet temperature (T3'). The corresponding process in the evaporator of DMS sub system is process 10-11 during which the refrigerant in DMS evaporator becomes saturated vapor at state point 11. The refrigerant which leaves the subcooler at state point 4 is expanded to state 5 in the expansion valve-1 to evaporator pressure and temperature of the VCR sub system. The desired cooling goal of the DMS-VCR system is achieved by absorbing heat from the space that needs to be chilled during the process 5-6' in the evaporator. The refrigerant at state point 6 (within the evaporator) is saturated and at state point 6' the refrigerant leaves the evaporator in superheated state. Further superheating takes place in the suction line till state point 7 is achieved just before entry to compressor. The superheated refrigerant is then compressed in the compressor-1 (process 7-1). The VCR sub system cycle includes both subcooling in condenser-1, subcooler, superheating in evaporator and suction line and desuperheating in discharge line. Simultaneously pressure drops in condenser and evaporator are also considered as depicted in Fig. 2 i.e. P-h diagram representing various processes of both the cycles taking place in VCR sub system and DMS sub system of DMS-VCR system. Thus the present work is focused on the analysis of an actual VCR sub system subcooled by DMS sub system. The DMS sub system cycle is assumed to be ideal except compression process which is not assumed reversible adiabatic. Thus the considered DMS-VCR system reasonably follows a real system.

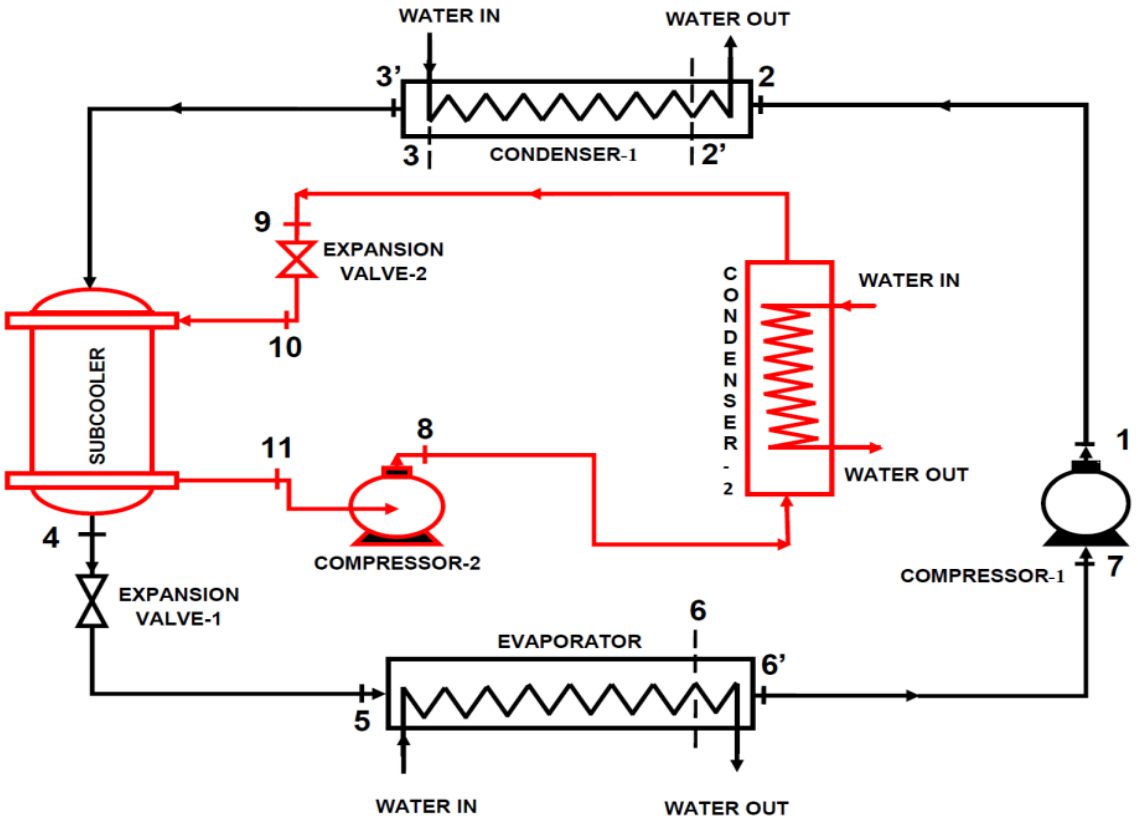

Figure 5.1 Schematic diagram of DMS-VCR system

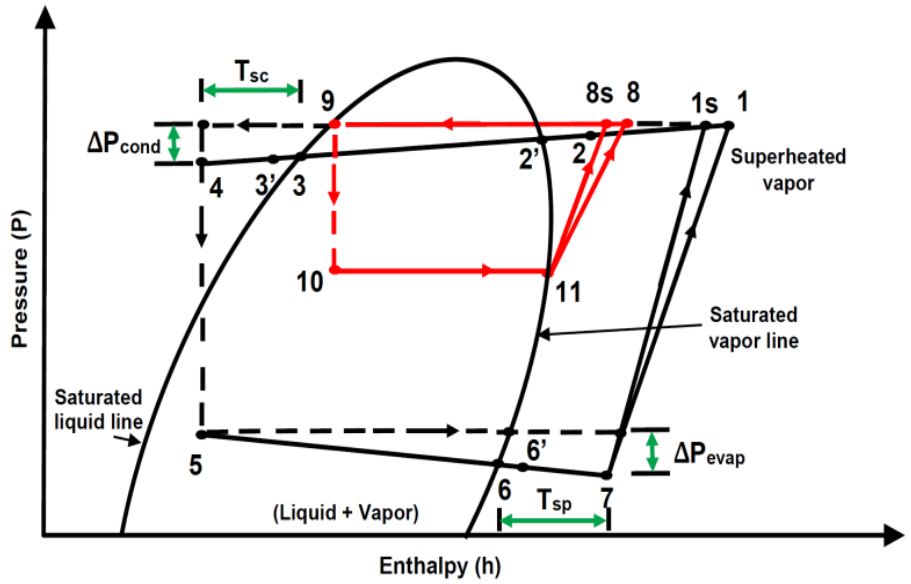

Figure 5.2 Pressure – enthalpy diagram of DMS-VCR cycle

5.3 MATHEMATICAL MODELING OF DMS-VCR SYSTEM

The current system model in the EES software is created while taking into consideration the thermophysical properties of the refrigerant R134a. Table 5.1 shows the governing equations

for the DMS-VCR system's parts.

The following assumptions apply to the system's thermodynamic modeling:

i) The components of the system are operating at a steady-state condition.

ii) The subcooling is assumed to take place in condenser-1 and dedicated subcooler.

iii) The superheating takes place in evaporator as well as in suction line.

iv) The desuperheating takes place in discharge line.

v) The compression processes in compressors are assumed to be irreversible adiabatic.

vi) Water is used as heat exchange fluid in evaporator and condensers.

The components of the DMS-VCR system are analysed by using principles of conservation of mass and energy, and entropy generation [68] and Table 5.1 displays the governing equations for the DMS-VCR System (refer Figure 5.1 for state points).

Table 5.1 Governing equations for various components of the DMS-VCR system

S. No.	Component	Energy analysis equations	Exergy analysis equations
1	Evaporator	$\dot{Q}_{evap} = (\epsilon C)_{evap}(T_{in,\,evap}-T_{evap}) = (\dot{m}_{ef}c_p)_{evap}(T_{in,evap}-T_{out,evap}) = \dot{m}_{ref1}(h_{6'}-h_5)$ $T_{evap}= T_5$ $\dot{Q}_{gain,\,sl}=\dot{m}_{ref1}(h_7-h_{6'})$	$\dot{I}_{evap} = T_o(\dot{m}_{ref1}(S_{6'}-S_5)+ (\dot{m}_{ef} \cdot c_p)_{evap} \cdot \ln((T_{out,evap}+ 273)/(T_{in,evap}+273)))$
2	Condenser-1	$\dot{Q}_{cond1}=(\epsilon C)_{cond1}(T_{cond1}-T_{in,\,cond1}) = \dot{m}_{ref1}(h_2-h_{3'})$ $= (\dot{m}_{ef}c_p)_{cond1}(T_{out,\,cond1}-T_{in,cond1})$ $T_{cond1}= T_3$ $\dot{Q}_{loss,\,dl}=\dot{m}_{ref1}(h_2-h_1)$	$\dot{I}_{cond1} = T_o(\dot{m}_{ref1}(S_{3'}-S_2)+ (\dot{m}_{ef} \cdot c_p)_{cond1} \cdot \ln((T_{out,\,cond1}+ 273)/(T_{in,cond1}+273)))$
3	Condenser -2	$\dot{Q}_{cond2}=(\epsilon C)_{cond2}(T_{cond2}-T_{in,\,cond2}) = \dot{m}_{ref2}(h_8-h_9)$ $= (\dot{m}_{ef}c_p)_{cond2}(T_{out,\,cond2}-T_{in,cond2})$ $T_{cond2}= T_9$	$\dot{I}_{cond2} = T_o(\dot{m}_{ref2}(S_9-S_8)+ (\dot{m}_{ef} \cdot c_p)_{cond2} \cdot \ln((T_{out,\,cond2}+273)/ (T_{in,cond2}+273)))$
4	Compressor-1 [11], [82]	$\dot{W}_{comp1}=(\dot{W}_{comp,isen})/\eta_{isen1}$ $\dot{W}_{comp,isen}=\dot{m}_{ref1}(h_1-h_7)$ $\eta_{isen1}=0.85-0.046667*(\frac{P_{cond1}}{P_{evap}})$	$\dot{I}_{comp1} = T_o(\dot{m}_{ref1}(S_1-S_7))$

5	Compressor-2 [11], [82]	$\dot{W}_{comp2}=(\dot{W}_{sc,isen})/\eta_{isen2}$ $\dot{W}_{sc,isen}=\dot{m}_{ref2}(h_8-h_{11})$ $\eta_{isen2}=0.85-0.046667*(\frac{P_{cond2}}{P_{sc}})$	$\dot{I}_{comp2} = T_o(\dot{m}_{ref2}(S_8-S_{11}))$
6	Subcooler	$\dot{Q}_{SC}=\in_{sc} .\dot{Q}_{SC,\ max}$ $\dot{m}_{ref2}(h_{11}-h_{10})=\dot{m}_{ref1}(h_{3'}-h_4)$ $T_{11}=T_4-\Delta T_{overlap}$	$\dot{I}_{sc}=T_o(\dot{m}_{ref2}(S_{11}-S_{10})$ $+ \dot{m}_{ref1}(S_4-S_{3'}))$
7	Expansion valve-1	$h_4=h_5$	$\dot{I}_{ev1} = T_o(\dot{m}_{ref1}(S_5-S_4))$
8	Expansion valve-2	$h_9=h_{10}$	$\dot{I}_{ev2} = T_o(\dot{m}_{ref2}(S_{10}-S_9))$

The following Equations (5.1) & (5.2) indicate the overall COP of actual VCR system and the DMS-VCR system:

$$COP_{VCRS} = \frac{\dot{Q}_{evap}}{\dot{W}_{comp1}} \tag{5.1}$$

$$COP_{DMS\text{-}VCRS} = \frac{\dot{Q}_{evap}}{\dot{W}_{comp1}+\dot{W}_{comp2}} \tag{5.2}$$

A key point for evaluating the cooling impact and energy intake needed in a system is the coefficient of performance (COP). It does not, however, offer information regarding the efficiency of the energy conversion method or point out the elements that are responsible for irreversibility in a process occurring in a particular component and system. In order to assess the exergetic efficiency of the DMS-VCR system and identify the factors that lead to inefficiency, exergetic analysis is crucial. Exergy analysis can be used to assess the system's exergetic efficiency and encourage energy saving to overcome above restriction. It also pinpoints system's component responsible for irreversibility. The equations are provided in Table 5.1 for calculating the irreversibility in various components of DMS-VCR system. It is calculated by using the Gouy-Stodola theorem as shown in the Equation (5.3).

$$\dot{I}= T_o . \dot{S}_{gen} \tag{5.3}$$

where, T_o is the ambient temperature.

The exergetic efficiency (η_{ex}) of DMS-VCR system is given by [3]:

For DMS-VCR system $\dot{I}_t=\dot{I}_{evap}+\dot{I}_{cond1}+\dot{I}_{cond2}+\dot{I}_{comp1}+\dot{I}_{comp2}+\dot{I}_{sc}+\dot{I}_{ev1}+\dot{I}_{ev2}$ (5.4)

$$\eta_{ex}= \left(\dot{Q}_{evap}\left|1-\frac{T_0}{T_e}\right|\right)/\dot{W}_t \tag{5.5}$$

where, $\dot{W}_t = \dot{W}_{comp1} + \dot{W}_{comp2}$

The CSB approach has now been used after determining the irreversibility rate of each system component [60], [83].

$$CSB_n = \left[\frac{\delta \dot{I}_t}{\delta z_i}\right] / \left[\frac{\delta \dot{I}_n}{\delta z_i}\right] \quad (5.6)$$

DMS, $\forall \in EoS \cap \{evap, cond1, cond2, comp1, comp2, subcooler\}$ $\forall Z_i \in$ system parameter

According to the CSB principle, lowering the irreversibility rate of one component gradually (by changing the system efficiency parameter Z_i) lowers the irreversibility rate of the entire system. Zi (the system efficiency parameter) in this context may be associated with the system temperature (i.e., evaporator or condenser temperature) or the degree of subcooling or the degree of overlap or the isentropic efficiency of the compressor.

Following are the effects of various CSB values:

In **Case-1**, when **CSBn > 1**, the system input decreases faster than the irreversibility rate of the nth element. The nth element has a favorable effect on the system's exergetic efficiency, so strengthening it, will increase the system's exergetic efficiency.

In **Case-2**, when **CSBn < 1**, the system input decreases slower than the nth element's irreversibility rate. In this instance, lowering the irreversibility rate of the nth element has a detrimental effect on the operation of other system components, which in turn has an adverse effect on the performance of the entire system.

In **Case-3**, when **CSBn = 1**, the performance of the entire system remains unchanged. This is because any enhancement in the nth element's performance is balanced by a decrease in the performance of other components, resulting in a rigid system structure that offers no scope for overall performance enhancement.

Therefore, it is important to consider the value of CSBn when designing the DMS-VCR system to ensure the overall performance enhancement of the system.

5.4 MODEL VALIDATION

In this Chapter, a more comprehensive approach by employing a dual validation strategy is taken. This approach combines the comparison of theoretical data of present work with experimental data, significantly enhancing the realism of this analysis. Consequently, the findings are aligned with both theoretical expectations and real-world observations, resulting in a more robust and reliable investigation. The current model is utilized for computation of results corresponding to the input data ($\dot{Q}_{evap}$ = 3.5167kW, T_{evap}, = -10°C, DOS = 5°C, T_{cond1},

T_{cond2} = 50°C, η_{comp1}, η_{comp2} = 80%, $\in_{sc}$ = 0.8, T_o = 25°C, P_o = 101.325 kPa) of Agarwal et al. [70]. The results obtained from the EES programme are compared with the results of Agarwal et al. [70] and it is observed that the results obtained from the present model lie within 3.45% of Agarwal et al. [70], but most of the errors are less than 2% (see Figure 5.3).

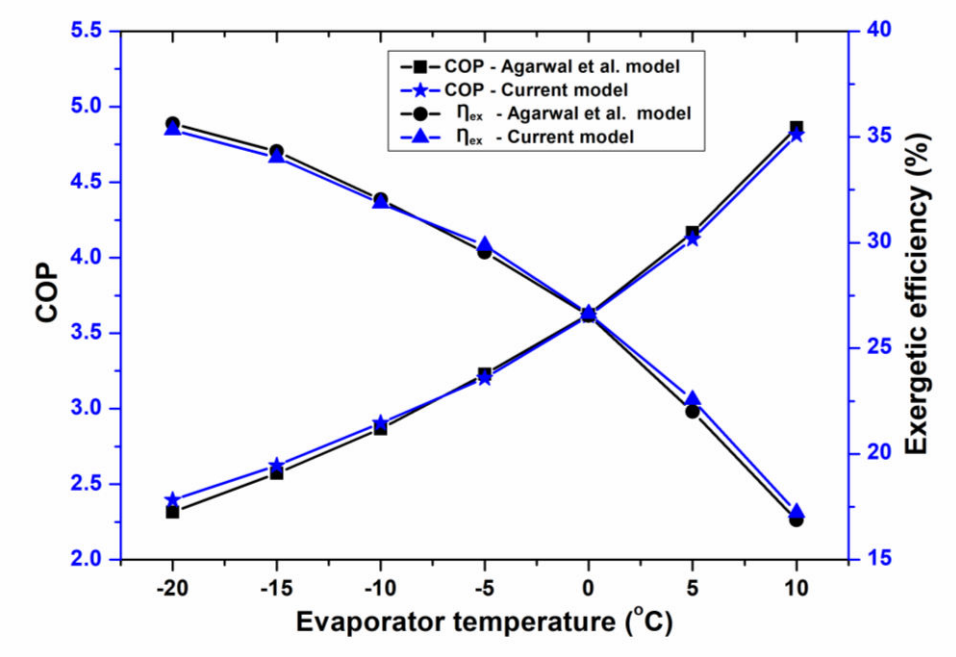

Figure 5.3 Performance comparison for effect of evaporator temperature with refrigerant R134a (T_{cond1} = 50°C)

The numerical simulation data is also compared with the experimental data from Han et al. [84] in order to assess the accuracy of the existing model and to determine the effect of evaporation temperature on COP for R410A. Figure 5.4 compares the coefficient of performance (COP) utilizing fixed superheating (T_{sup} = 8.3°C) and subcooling (T_{sc} = 11.1°C) degrees at varied condenser temperatures. The COP value provided by this study is marginally higher than that provided by Han et al. [84] experimental calculations. The experimental results and the theoretical results obtained from the present model corresponding to the data of Han et al. [84] are consistent and they lie between +1.5% to +5% of the experimental data reported by Han et al. [84] for coefficient of performance (COP).This level of consistency and accuracy in COP reaffirms the robustness and reliability of the model.

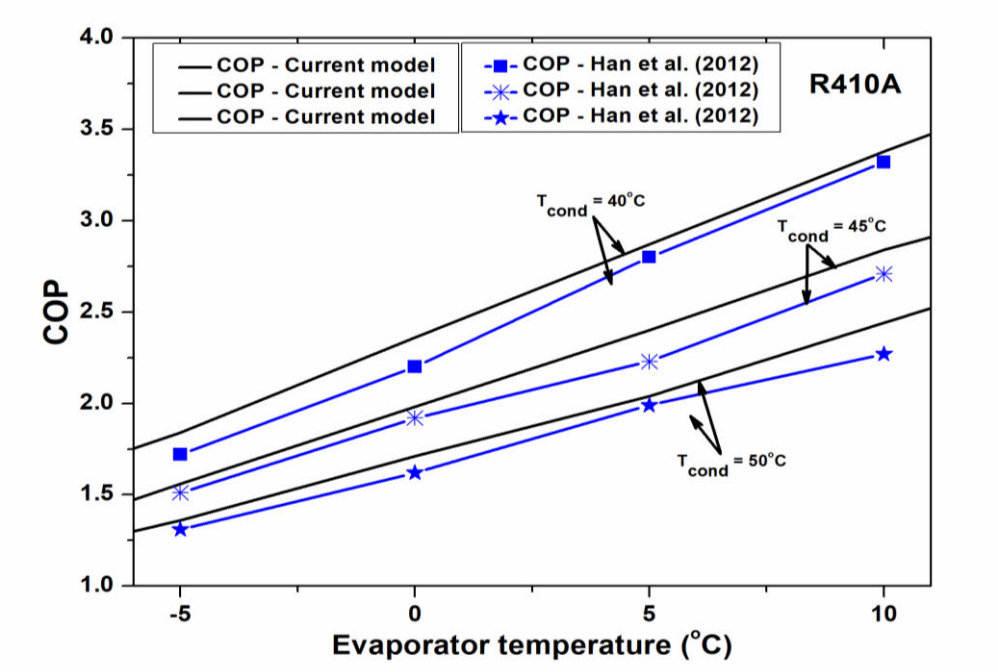

Figure 5.4 COP comparison of current model with the experimental data of Han et al. [84] under different condenser temperature

5.5 RESULTS AND DISCUSSION

This Section presents the results and their discussion based on the process data presented in Table 5.2 of the DMS-VCR system for water cooling application. A comparison of the DMS-VCR system with actual VCR system is carried out using the process data values listed in Table 5.2.

Table 5.2 Process data of DMS–VCR system

	Parameters	**Values**
Thermal parameters [21]	Evaporator cooling capacity (Qevap, kW)	100
	Evaporator temperature (Tevap, °C)	5(range 0 to 10)
	Condenser temperature (Tcond, °C)	40(range 35 to 45)
	Evaporator coolant Inlet temperature (Tevap,in, °C)	15
	Evaporator coolant outlet temperature (Tevap,out, °C)	10
	Condenser coolant inlet temperature (Tcond,in, °C)	30
	Condenser coolant outlet temperature (Tcond,out, °C)	35
	Overlap degree (Toverlap, °C)	5
	Degree of subcooling in condenser (Tsc, °C)	5
	Degree of subcooling in subcooler (Tsc, °C)	10
	Degree of superheating in evaporator (Tsup, °C)	5

	Degree of superheating in suction line (Tsup, °C)	10
	Desuperheating in discharge line (Tdsup, °C)	10
	Environment temperature (To, °C)	25
	Environment pressure (Po, kPa)	101.325
	Refrigerants (for both cycles)	R134a
	Pressure drop in the evaporator (kPa)	10
	Pressure drop in the suction line (kPa)	20
	Pressure drop in the condenser (kPa)	5
	Pressure drop in the liquid line and subcooler (kPa)	10

As shown in Table 5.3, the DMS-VCR system's thermodynamic parameters (pressure, temperature, mass flow rate, entropy, and enthalpy) are calculated at the entry and exit of each component. The values of the performance parameters for the DMS-VCR system and actual VCR system are shown in Tables 5.4 and 5.5 respectively. For the same cooling capacity of 100 kW at T_{evap} = 5°C, refrigerant (R134a) has mass flow rates of 0.59 kg/s (VCR sub cycle), 0.08 kg/s (DMS sub cycle), and 0.66 kg/s (actual VCR system). Additionally, the mass flow rates for external fluid (i. e. cooling water) for condensers-1, 2, and evaporator of the DMS-VCR system are 5.33 kg/s, 0.69 kg/s, and 4.77 kg/s, respectively, as compared with 5.84 kg/s in condenser-1and 4.77 kg/s in evaporator of the actual VCR system. The DMS-VCR system performs better than an actual VCR system.

Table 5.3 Simulation condition data of thermodynamic properties of the DMS-VCR system

State point	**ṁ (kg/s)**	**x**	**T (^{o}C)**	**P (kPa)**	**h (kJ/kg)**	**s (kJ/kg.K)**
1	0.599	1	70.67	1024	304.3	1.016
2	0.599	1	60.67	1024	293.8	0.985
2’	0.599	1	39.82	1021	271.3	0.915
3	0.599	0	39.82	1016	108	0.395
3’	0.599	0	34.82	1012	100.6	0.394
4	0.599	0	24.82	1002	86.15	0.323
5	0.599	0.14	5	349.9	86.15	0.328
6	0.599	1	4.17	339.9	253.3	0.929
6’	0.599	1	9.17	329.9	252.9	0.946
7	0.599	1	19.17	309.9	266.9	0.983

8	0.085	1	45.22	1017	277.1	0.934
9	0.085	0	40	1017	108.3	0.395
10	0.085	0.16	19.82	568.8	108.3	0.399
11	0.085	1	19.82	568.8	261.5	0.922

5.5.1 Energy analysis results

The results of the energy analysis comparing the use of the refrigerant HFC134a in a DMS-VCR system versus an actual VCR system are shown in Table 5.4. The primary goal of analysis is to demonstrate how the DMS-VCR system concept improved the COP and decreased compressor power. According to the results in Table 5.4, with variable evaporator temperatures (T_{evap} = 0°C, 5°C, and 10°C) and constant condenser temperature of 40°C, the DMS-VCR system reduces compressor-1 power usages by 8.65%, 8.49% and 8.31% respectively, while maintaining the same cooling capacity. This decrease is also helpful in reducing heat load on the condenser-1 by 8.75%, 8.68%, and 8.53% respectively. As a result, the COP of the DMS-VCR system increases by 4.60%, 3.18% and 1.75% respectively. Further, heat exchangers play crucial role in ensuring the overall performance and energy efficiency of the system by effectively transporting heat. It is essential to understand how well the evaporator, condensers, and subcooler work in order to maximize the DMS-VCR system's thermal performance and determine whether it is appropriate for use in real-world situations. The calculated effectiveness values for the evaporator, condenser, and subcooler are 0.80, 0.83, and 0.75 respectively.

Table 5.4 Energy analysis results of actual VCR system and DMS-VCR system

Performance Parameters		**Actual VCR system**			**DMS-VCR system**		
		Tevap = 0°C	**Tevap = 5°C**	**Tevap = 10°C**	**Tevap = 0°C**	**Tevap = 5°C**	**Tevap = 10°C**
First law parameters	COP_{VCRS}	3.26	4.08	5.13	-	-	-
	$COP_{DMS-VCRS}$	-	-	-	3.41	4.21	5.22
	$\dot{Q}_{cond1}$ (kW)	127.9	122	117.2	116.7	111.4	107.2
	$\dot{Q}_{cond2}$ (kW)	-	-	-	14.70	14.44	14.19
	$\dot{Q}_{evap}$(kW)	100	100	100	100	100	100
	$\dot{Q}_{sc}$(kW)	-	-	-	13.34	13.10	12.88
	$\dot{W}_{comp1}$ (kW)	30.64	24.49	19.48	27.99	22.41	17.86
	$\dot{W}_{comp2}$ (kW)	-	-	-	1.36	1.33	1.31

	$\dot{m}_{ref1}$ (kg/s)	0.67	0.66	0.64	0.61	0.59	0.58
	$\dot{m}_{ref2}$ (kg/s)	-	-	-	0.08	0.08	0.08
	$\dot{m}_{ef,ev}$(kg/s)	4.77	4.77	4.77	4.77	4.77	4.77
	$\dot{m}_{ef,cond1}$ (kg/s)	6.12	5.84	5.61	5.58	5.33	5.13
	$\dot{m}_{ef,cond2}$ (kg/s)	-	-	-	0.70	0.69	0.68

5.5.2 Exergy analysis results

Table 5.5, displays the outcomes of the exergy analysis performed on the actual VCR system and the DMS-VCR system. The findings show that due to decrease in compressor work, cooling load, and refrigerant mass flow rate, the irreversibility rate in the DMS-VCR system is reduced by 4.68%, 3.17% and 0.87% respectively. In addition, the DMS-VCR system exhibits an increase in exergetic efficiency by 4.38%, 3.09% and 1.61% respectively (at Tevap = 0°C, 5°C, and 10°C), which presents the significance of incorporating DMS sub system. This work introduced the energy and exergy analysis focused on broader spectrum of evaporator temperatures, encompassing 0°C, 5°C, and 10°C, coupled with varying condenser temperatures ranging from 35°C to 40°C. This expansive range of evaporator temperatures facilitates a comprehensive analysis across diverse operational conditions, providing deeper insights into the behaviour of the system.

Table 5.5 Exergy analysis results of actual VCR system and DMS-VCR system

Performance parameters		**Actual VCR system**			**DMS-VCR system**		
		Tevap = 0°C	**Tevap = 5°C**	**Tevap = 10°C**	**Tevap = 0°C**	**Tevap = 5°C**	**Tevap = 10°C**
Second law parameters	$\dot{I}_{cond1}$	3.74	3.36	3.10	3.41	3.07	2.83
	$\dot{I}_{cond2}$	-	-	-	0.36	0.35	0.34
	$\dot{I}_{comp1}$	8.84	6.44	4.72	8.08	5.89	4.33
	$\dot{I}_{comp2}$	-	-	-	0.30	0.29	0.29
	$\dot{I}_{evap}$	5.23	3.17	1.20	5.18	3.13	1.17
	$\dot{I}_{ev1}$	2.49	1.83	1.30	1.35	0.93	0.61
	$\dot{I}_{ev2}$	-	-	-	0.12	0.12	0.11
	$\dot{I}_{sc}$	-	-	-	0.55	0.55	0.54
	$\dot{I}_{t}$	20.30	14.80	10.32	19.35	14.33	10.23
	η_{II}(%)	29.87	29.36	27.19	31.18	30.27	27.63

5.5.3 Results of structural analysis

To enhance the DMS-VCR system's performance, it is necessary to minimize the

irreversibility rate of each system component. The VCR cycle compressor-1 has the greatest irreversibility rate, making up 41.10% of the system's overall irreversibility rate. The DMS-VCR system's components are put in sequence of increasing irreversibility rate at Tevap = 5°C, and the outcomes are: expansion valve-2 (0.12 kW i.e. 0.84%), compressor-2 (0.29 kW i.e. 2.02%), condenser-2 (0.35 kW i.e. 2.44%), subcooler (0.55 kW i.e. 3.84%), expansion valve-1 (0.93 kW i.e. 6.49%), condenser-1 (3.07 kW i.e. 21.42%), evaporator (3.13 kW i.e. 21.84%), and compressor-1 (5.89 kW i.e. 41.10%). Several researchers have proposed the idea of CSB, and in this study, CSB values are calculated for various components of the DSM-VCR system, as presented in Figures 5.5(a-c). The selected components for the CSB analysis include the subcooler, evaporator, condenser-1, condenser-2, compressor-1, and compressor-2, for which the CSB values are computed. The efficiency parameters (zi) of the condenser temperature, evaporator temperature, isentropic efficiency, degree of subcooling and degree of overlap are considered for the purpose of CSB analysis.

Figure 5.5(a) shows that increase in the evaporator's temperature from 0°C to 10°C causes a reduction in the irreversibility rate of evaporator by 77.41% (from 5.18 kW to 1.17 kW), which reduces the system's overall irreversibility rate by 47.13% (from 19.35 kW to 10.23 kW). Accordingly, it is appropriate to maintain the evaporator temperature high and the condenser temperature low for optimum performance of DMS-VCR system, depending on the needs of the particular application. However the condenser temperature depends on the surrounding temperature. As shown in Figure 5.5(a), by decreasing the degree of overlap from 10°C to 0°C leads to a significant decrease of 57.69% (from 0.78 kW to 0.33 kW) in the subcooler's irreversibility rate, which causes the DMS-VCR system's overall irreversibility rate to decline by 5.35% (from 14.75 kW to 13.96 kW). Therefore, it is suggested to use a lower degree of overlap, although this would require a larger area of subcooler for effective heat transfer. In addition, if the temperature of the condenser-1 reduces by 10°C (from 45°C to 35°C), it leads to a significant reduction in its irreversibility rate by 70.83%, (from 5.76 kW to 1.68 kW) and condenser-2 by 79.31% (from 0.58 kW to 0.12 kW), as illustrated in Figure 5.5(b). The total irreversibility rate of the DMS-VCR system also reduces by 43% (from 18.58 kW to 10.59 kW) when condenser-1 temperature is reduced by 10°C and similar reduction in the irreversibility rate of DMS-VCR system is 5.23% (from 14.73 kW to 13.96 kW) for condenser-2.

Additionally, the study reveals that achieving 100% isentropic efficiency in compressor-1 and 2 can lead to a reduction of their irreversibility rates by 100%, indicating an ideal condition.

This would result in a significant decrease in the DMS-VCR system's overall irreversibility rate, with a reduction of 50.24% in compressor-1 (from 16.02 kW to 7.97 kW) and compressor-2 seeing a reduction of 3.64% (from 14.56 kW to 14.03 kW), as shown in Figure 5.5(c). Compressor-1 has the greatest influence on the DMS-VCR system's total irreversibility rate.

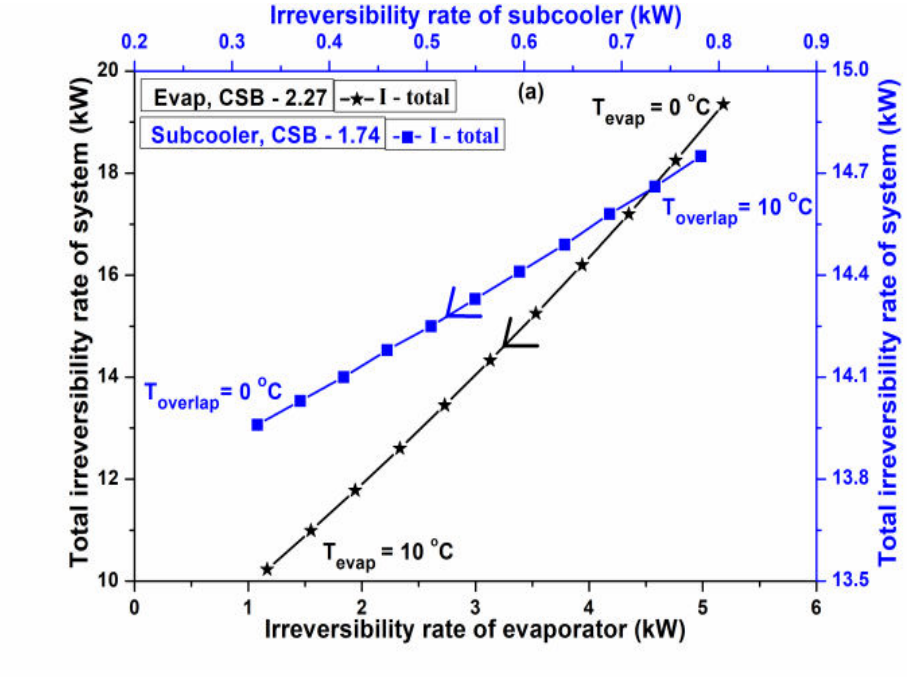

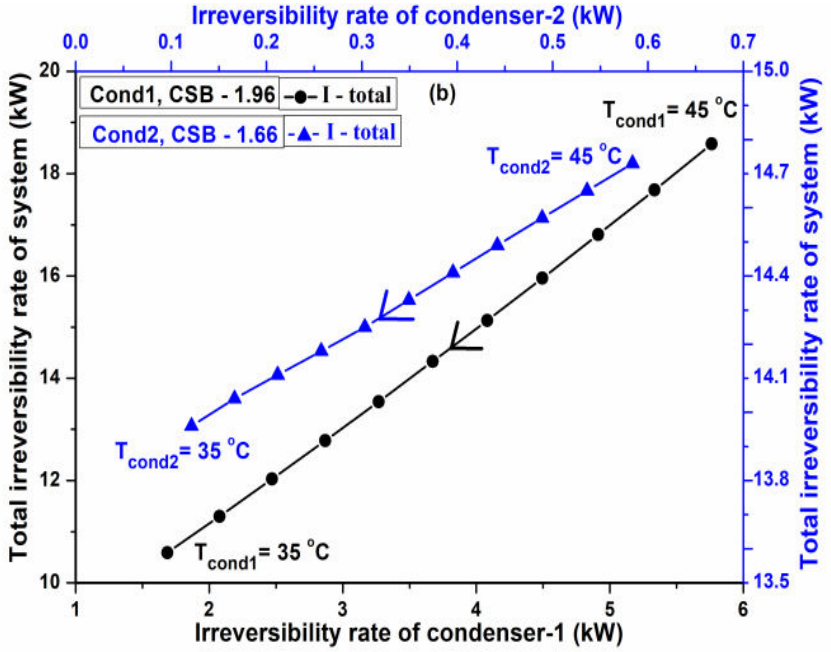

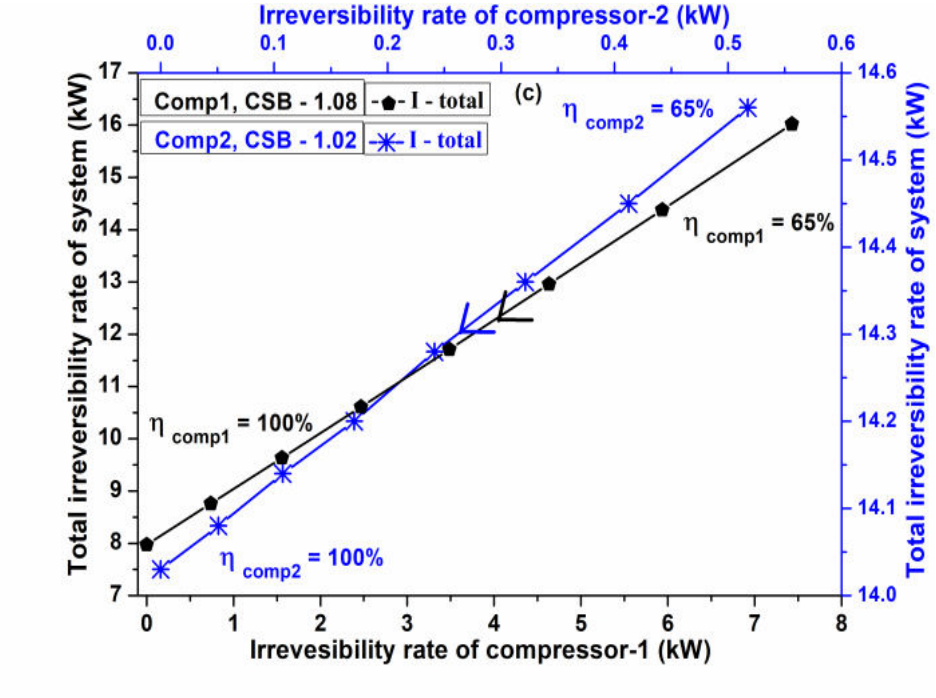

Figure 5.5 shows how the system's overall irreversibility rate has changed in relation to its various components, including (a) evaporator and subcooler, (b) condenser-1 and condenser-2, (c) compressor-1 and compressor-2.

Further, the study shows that, when compared to the other components, compressor-1 adds the most to the overall irreversibility of the DMS-VCR system, accounting for 5.89 kW, or 41.10%. Therefore, improving the efficiency of compressor-1 is crucial for enhancing the DMS-VCR system's performance. The efficiency of the compressors depends on the pressure ratio as mentioned in equations shown under serial number 4 and 5 of the Table 5.1. The pressure ratio across compressors depends on the evaporator and condenser pressures and decides the efficiency of compressors. However, the evaporator pressure depends on the evaporator temperature which is dependent on application temperature for which the system is used for and can be varied only in a narrow range whereas condenser temperature depends on the ambient or surrounding conditions and hence it is not feasible to change it at will. Thus DMS-VCR system pressure ratio across compressor-1 can be changed only in a narrow range depending on the small range of the application for which it is being used.

The computed CSB values for the components of DMS-VCR system are shown in Figure 5.6. The components can be ranked in ascending order of their CSB values, as follows: Compressor-2 (1.02), Compressor-1 (1.08), Condenser-2 (1.66), Subcooler (1.74), Condenser-1 (1.96), and Evaporator (2.27). All the components have CSB values greater than one which means reducing its value will reduce the component irreversibility rate as well as the system irreversibility rate.

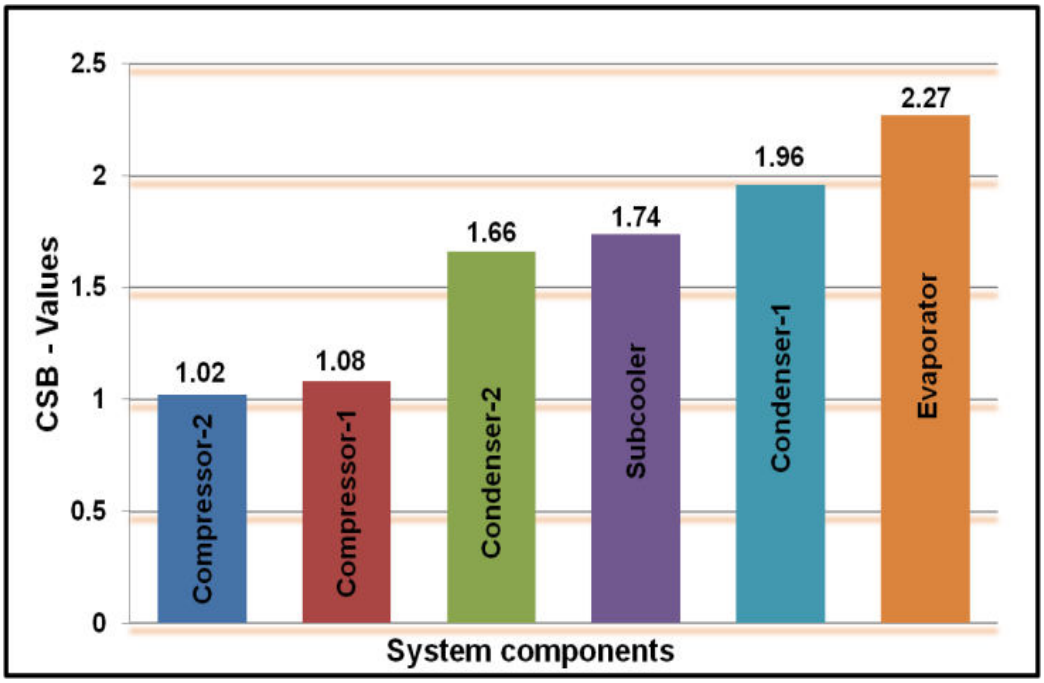

Figure 5.6 Comparison of CSB values of DMS-VCR system components

Therefore, modifying these components' efficiency factors would enhance both the performance of the individual component as well as the performance of the entire system. Therefore, even a minor adjustment to the component's operating parameters with a high CSB number could have a big impact on how well the system performs. The component with the highest CSB value is evaporator (2.27), and its contribution to the total irreversibility rate is 21.84%, followed by the condenser-1 (CSB-1.96) with a contribution of 21.42%. Compressor-1 has the highest overall contribution to the total irreversibility rate, which is 41.10%, but it is less sensitive to improvement in exergetic efficiency as its CSB is low i.e.1.08 compared to other components of the DMS-VCR system. The CSB analysis emphasizes the significance of raising the system's overall efficiency, particularly by focusing on components with higher CSB values, such as the evaporator and condenser-1. The overall performance of the DMS-VCR system can be significantly enhanced by increasing the efficiency of these components.

5.5.4 Effect of evaporator and condenser temperatures

Figure 5.7 illustrates the effect of evaporator temperature on both the coefficient of performance and the total irreversibility rate on DMS-VCR system. Although the working range of the external fluid for the condenser and evaporator is only 5°C (for example, the evaporator's external fluid intake temperature is 15°C and its outlet temperature is 10°C). The DMS-VCR system’s evaporator temperature varies between 0°C and 10°C while maintaining

a constant intake and output temperature for the external fluid and other design parameters. Consequently, the system's overall COP improves from 3.41 to 5.22 on increasing evaporator temperature. The system's total irreversibility rate reduces from 19.35 kW to 10.23 kW, and the exergetic efficiency decreases from 31.18% to 27.63%. This decline in irreversibility rate is exclusively because of the reduction in the temperature difference between the evaporator and external fluid, which is caused by an increase in the evaporator temperature. Hence, high evaporator temperature is necessary from an energy point of view and however from exergetic viewpoint, the evaporator temperature should be lower.

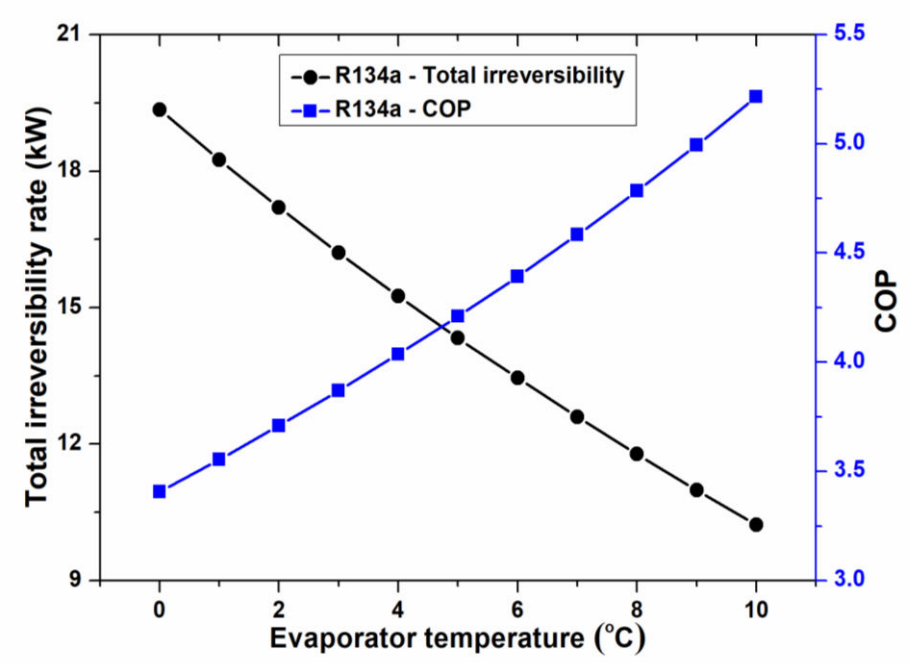

Figure 5.7 Effect of evaporator temperature on total irreversibility rate and COP

Figure 5.8 displays the effect of condenser temperature on the DMS-VCR system's total irreversibility rate and coefficient of performance. The DMS-VCR system's condenser temperature is changed from 35°C to 45°C while maintaining the same temperatures for the external fluid's inlet and exit as well as other design parameters. It causes the system's overall coefficient of performance to drop from 5.07 to 3.53, while the system's exergetic efficiency declines from 36.48% to 25.37% and its total irreversibility rate increases from 10.59 kW to 18.58 kW.

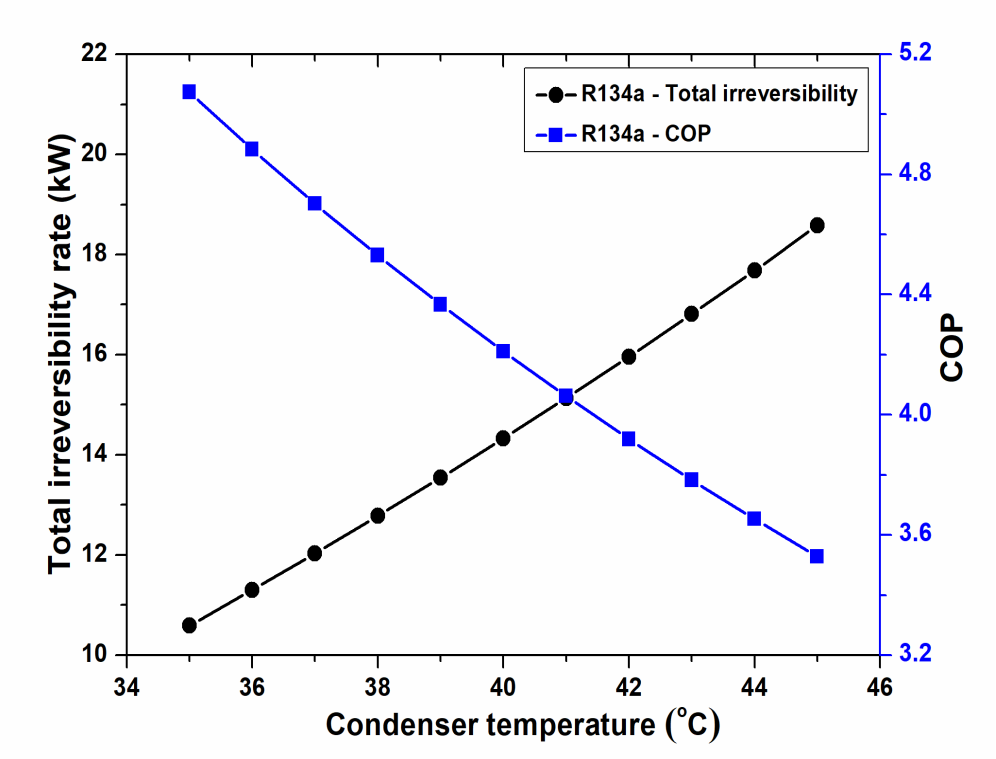

Figure 5.8 Effect of condenser temperature on total irreversibility rate and COP

Figure 5.9 displays the effect of pressure ratio of compressor-1 on total compressor work of the DMS-VCR system. The pressure ratio across compressor increases at lower evaporator and higher condenser temperatures. The compressor power is dependent on pressure ratio and inlet temperature to compressor. Hence the compressor power is observed to be higher for higher pressure ratio. It further explores the effect of compressor pressure ratio on total work at different evaporator temperatures. The effect of temperature at inlet to compressor is not substantial. In nutshell both the evaporator and condenser temperatures affect pressure ratio and the total compressor work. The higher condenser temperature results in higher total compressor work due to higher pressure ratios. On the other hand, higher evaporator temperatures result in a drop in total compressor work due to reduction in pressure ratio.

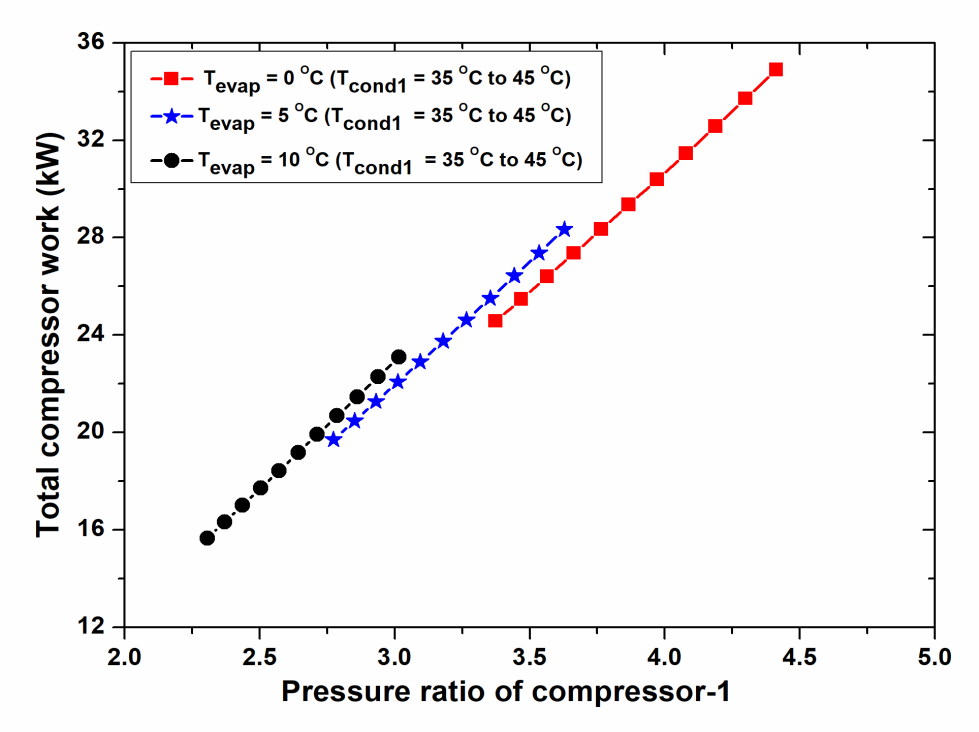

Figure 5.9 Effect of pressure ratio of compressor-1 on total compressor work

5.5.5 Effect of degree of subcooling and superheating

The degree of subcooling has a significant effect on the effectiveness, efficiency, and overall cooling capacity of the system. Engineers and technicians can increase the cooling efficiency of the system and guarantee its optimal performance by optimizing the degree of subcooling. The DMS sub system of DMS-VCR system is made to further cool the refrigerant liquid leaving the condenser below its saturation temperature. This additional cooling is accomplished by transferring heat from the refrigerant in VCR section of DMS-VCR system to another secondary refrigerant in DMS section of DMS-VCR system. The degree of subcooling is varied from 1°C to 20°C keeping the other design parameters constant (see Table 5.2). Through various simulations, it has been concluded that the ideal degree of subcooling is 12°C. According to Figures 5.10 and 5.11, at this subcooling level, the system's overall COP and exergetic efficiency increase, while its total irreversibility rate and total compressor work decreases. Below or above the optimal value of subcooling, the reverse patterns are observed.

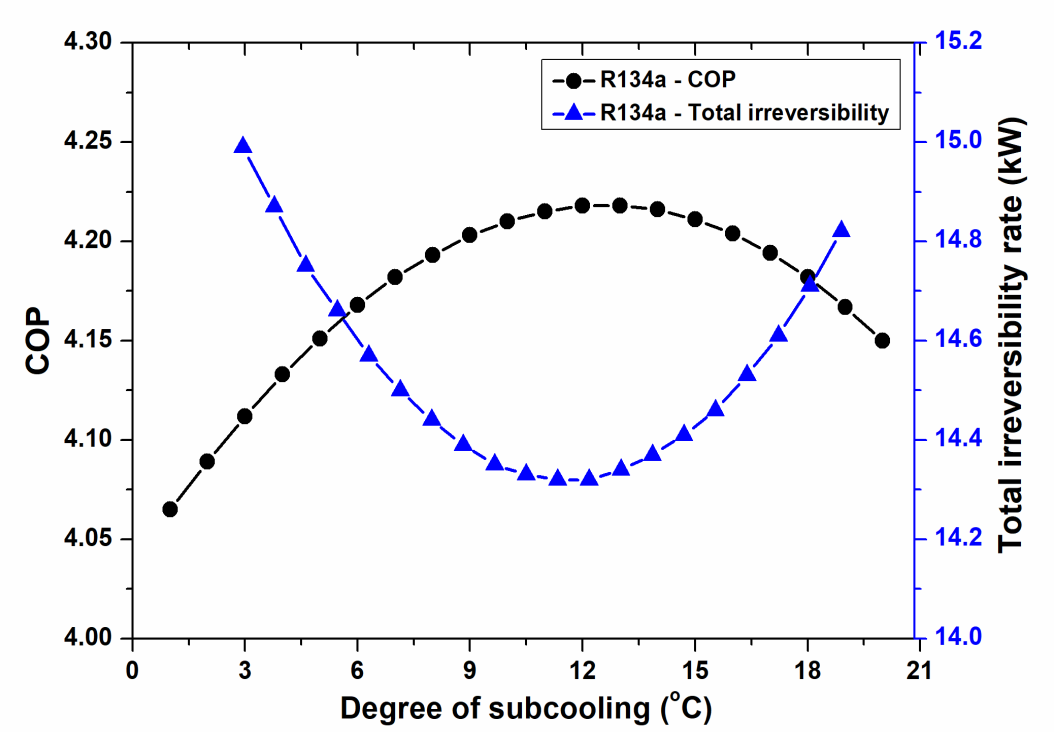

Figure 5.10 Variation of COP and total irreversibility rate with respect to degree of subcooling in dedicated subcooler

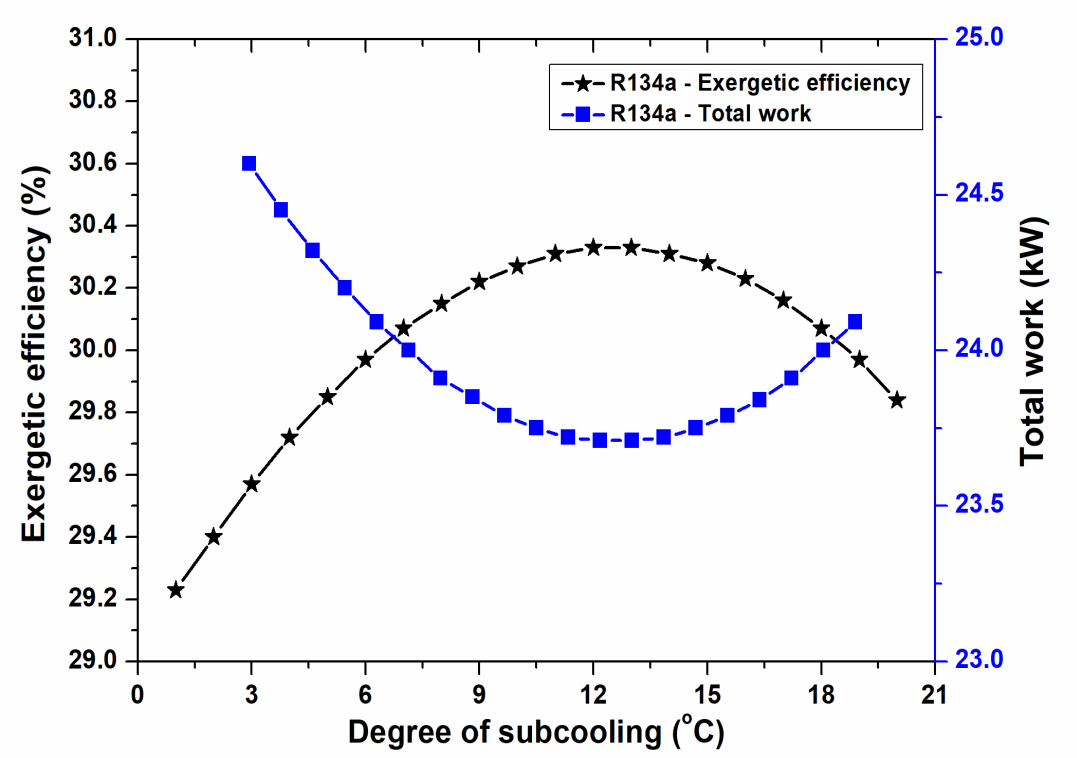

Figure 5.11 Variation of exergetic efficiency and total work with respect to degree of subcooling

Upto ideal degree of subcooling the VCR cycle compressor-1 work decreases from 24.3 kW to 22.04 kW, whereas the DMS cycle compressor work increases from 0.30 kW to 1.67 kW,

resulting in a decrease in the total compressor work from 24.60 kW to 23.71 kW. It increases the system's overall COP from 4.06 to 4.22 (an improvement of 4%). As a result, the system's entire irreversibility drops by 4.5%.

The superheating is also an important parameter to improve the overall performance of the system, as it increases the temperature of the refrigerant leaving the evaporator by gaining heat from the products to be cooled or surrounding. This indirectly contributes to the protection and longevity of the compressor.

In this analysis, the degree of superheat is varied from 1°C to 20°C in the evaporator and suction line of the system, keeping other design parameters constant (see Table 5.2). Figures 5.12 and 5.13, shows the effect of degree of superheating on the performance parameters of the DMS-VCR system. The EES simulation results show that the system's overall COP decreases from 4.40 to 4.04 and the system's entire irreversibility rate increases by 8.83%. Further, the exergetic efficiency decreases from 31.62% to 29.06%, while, the total compressor work increases from 22.74 kW to 24.74 kW. Therefore, it is essential to note that superheating in the present case is not beneficial from the performance view point. In order to maximize performance and ensure safe operation, engineering systems must carefully assess the degree of subcooling and superheating.

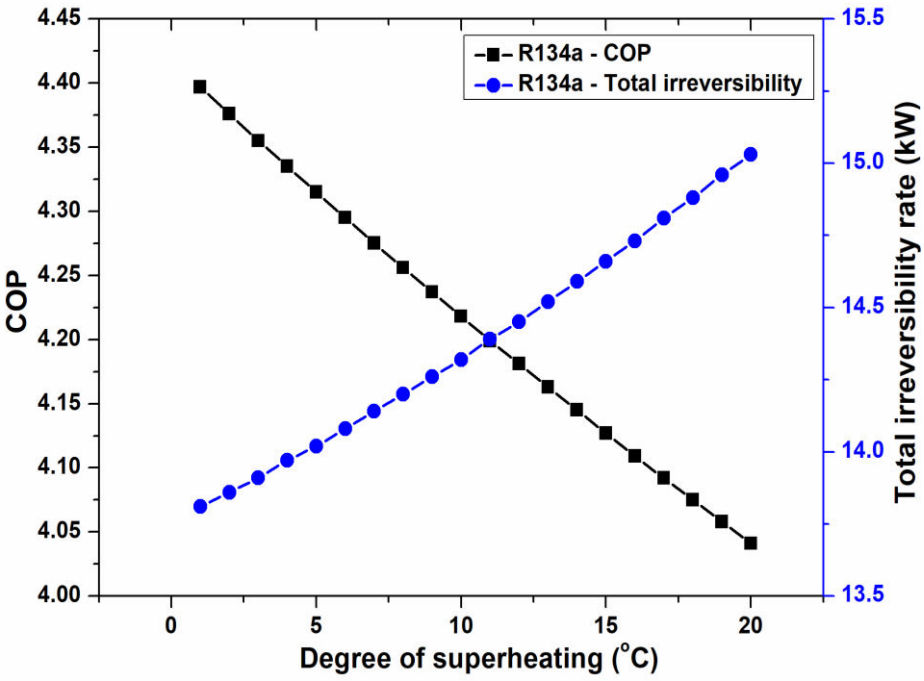

Figure 5.12 Variation of COP and total irreversibility rate with respect to degree of superheating

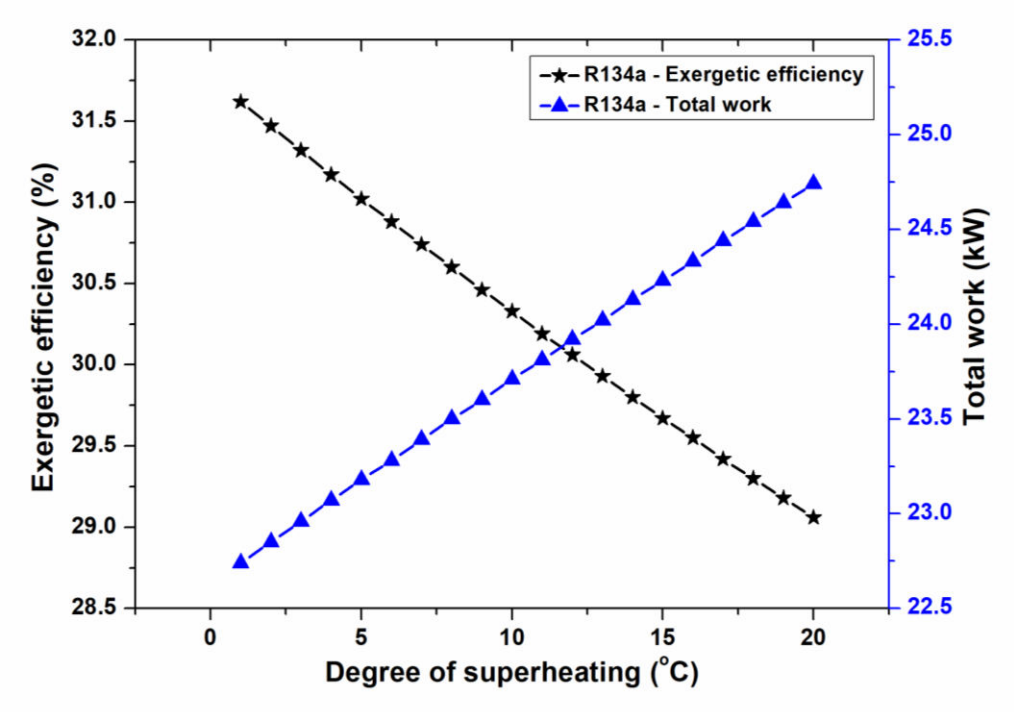

Figure 5.13 Variation of exergetic efficiency and total work with respect to degree of superheating

5.5.6 Effect of pressure drop in evaporator and condenser

The overall pressure drop in an evaporator is influenced by both the momentum pressure drop and the friction pressure drop. As the vapor flows through the evaporator tubes, it experiences frictional resistance with the interior surfaces, leading to a decrease in pressure. Further, as the vapor velocity increases, the momentum pressure increases in the evaporator. But in a condenser, the vapor condenses into a liquid form, resulting in a decrease in vapor velocity and a decrease in momentum pressure drop. However, friction pressure drop continues to be positive, just like in the evaporator, because the fluid faces resistance as it passes through the evaporator and condenser's interior surfaces. The condenser experiences a marginal overall reduction in pressure as a result of the combination of these pressure drops. The pressure ratio across the compressor rises as the evaporator pressure drop increases, increasing the work required by the compressor; nevertheless, the pressure ratio across the condenser does not vary significantly as discussed above. The COP and exergetic efficiency of the DMS-VCR system decreases as a result of the increased compressor work.

Figures 5.14 and 5.15 depicts how a pressure drop in an evaporator affects the COP, total irreversibility rate, exergetic efficiency and total compressor work with variation of pressure drop in evaporator from 0 kPa to 50 kPa. Due to a decrease in the specific refrigerating effect, the cooling capacity decreases as the pressure drop in the evaporator increases, and

compressor work increases as the pressure ratio across the compressor rises. Both of these impacts contribute to decrease the COP from 4.36 to 3.65 and an increase in total compressor work by 19.37%. The total irreversibility rate of the system increases by 29.22% with a decrease in exergetic efficiency from 31.37% to 26.28%.

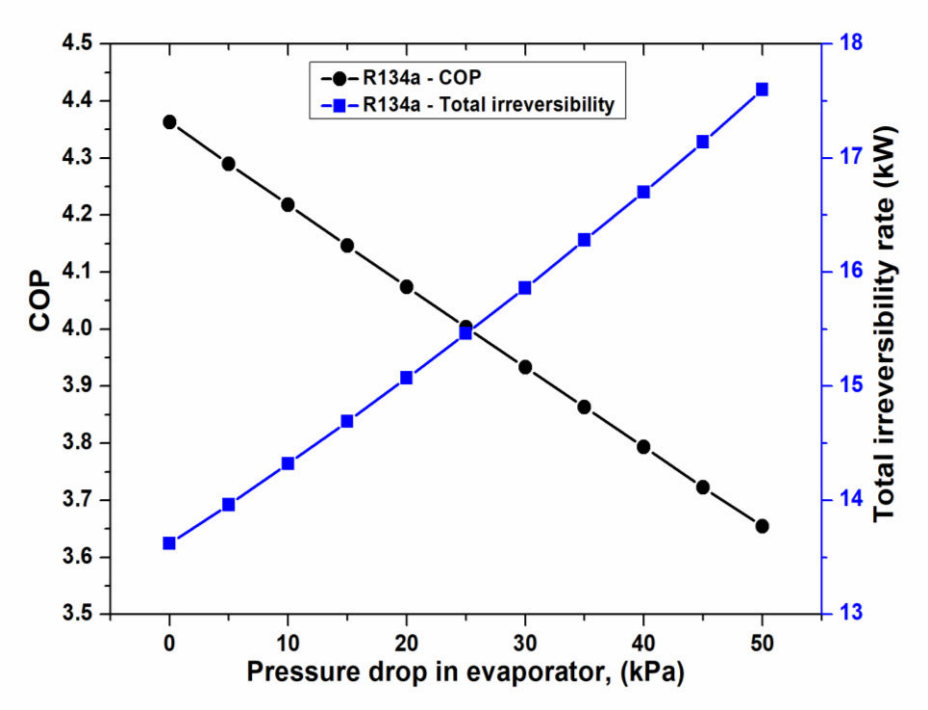

Figure 5.14 Variation of COP and total irreversibility rate with respect to pressure drop in evaporator

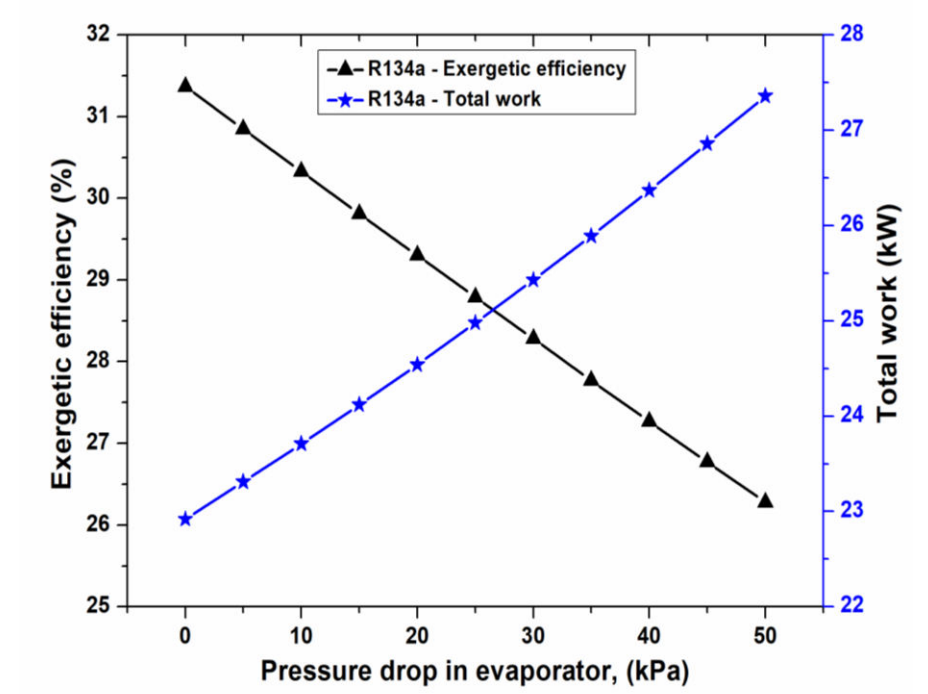

Figure 5.15 Variation of exergetic efficiency and total work with respect to pressure drop in evaporator

Contrary to the above the condenser pressure drop exhibits very marginal changes in the values of performance parameters i.e. COP and exergetic efficiency increases from 4.21 to 4.25 and from 30.30% to 30.60% respectively, while total irreversibility rate and total compressor work decreases from 14.34 kW to 14.14 kW, and from 23.73 kW to 23.53 kW respectively with variation of pressure drop from 0 kPa to 50 kPa (see Figures 5.16 and 5.17). This therefore implies that the evaporator pressure drop has a more significant effect on the overall performance of the DMS-VCR system.

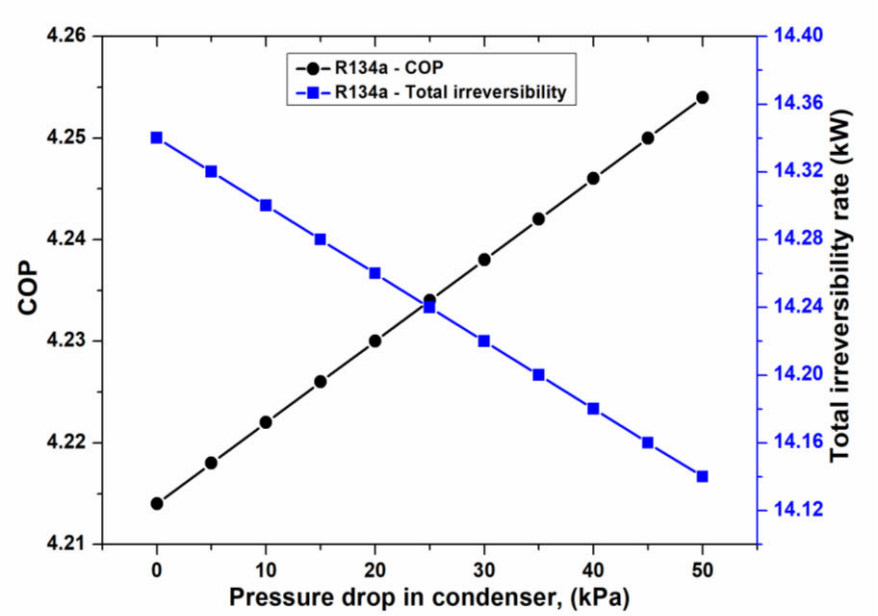

Figure 5.16 Variation of COP and total irreversibility rate with respect to pressure drop in condenser

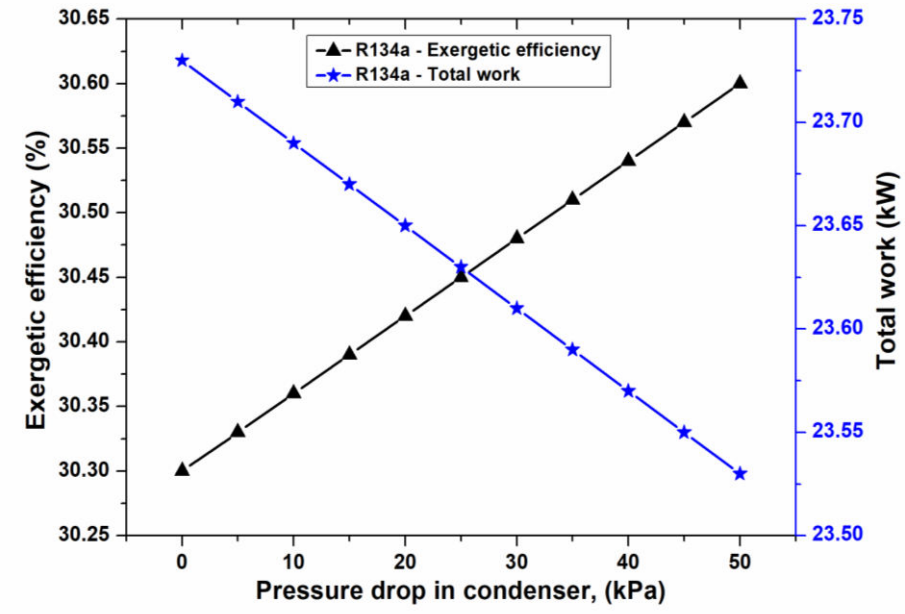

Figure 5.17 Variation of exergetic efficiency and total work with respect to pressure drop in condenser

5.6 CONCLUSION

This Chapter focuses on energy, exergy and CSB analysis of DMS-VCR system. At constant condenser temperature (T_{cond} = 40°C) and variable evaporator temperatures (T_{evap} = 0°C, 5°C, and 10°C), the results show that the actual DMS-VCR system works better than an simple VCR system. At 0°C, the work input for the compressor-1 of the DMS-VCR system is reduced by 8.65%. The COP and exergetic efficiency of DMS-VCR system both increase by 4.60% and 4.38%, respectively. Due to less work being required to provide the same cooling capacity, the DMS-VCR system's operating cost is also reduced. The irreversibility rate of each component is also calculated by exergy analysis, as well as the total irreversibility rate of the DMS-VCR system, which is revealed to be 4.68% lower than the actual VCR system.

The CSB analysis is then employed to investigate how changes in irreversibility rate of individual components affect the system's overall performance. The values of CSB of evaporator and condenser-1 are most suitable for reducing the irreversibility rate of the overall system and increasing the exergetic efficiency.

CHAPTER 6

ADVANCE EXERGY AND COEFFICIENT OF STRUCTURAL BOND ANALYSIS OF DEDICATED MECHANICAL SUBCOOLED VAPOR COMPRESSION REFRIGERATION SYSTEM

This chapter focuses on an advanced analysis of exergy and the coefficient of structural bond in the dedicated mechanical subcooled vapor compression refrigeration system. The aim of this chapter is to provide a deeper understanding of how these factors contribute to the system's performance and efficiency.

6.1 INTRODUCTION

The vapor-compression refrigeration system is an established technology which is nearly two century old and most of the current systems work on the vapor compression refrigeration cycle (VCR cycle). It is utilised for different applications of “heating and cooling” like water heating, space cooling, refrigeration, and air-conditioning with temperature ranging from 4K – 300K Chakravarthy et al. [8]. Effective refrigeration systems are needed to supply the demand for high-grade energy (electricity) during peak load considering VCR system's widespread use despite using a sizeable amount of the world's electricity production. Due to the rising cost of high-grade energy, people are calling for creating of efficient and sustainable VCR system.

To reduce the electricity consumption in VCR system, researchers are continuously working upon to find out new technology or alternative to it. The best suitable technology is dedicated mechanical subcooled vapor-compression refrigeration system. Agarwal et al. [14] examined the effects of varying the sub-cooler's efficacy (0.3–1.0) and the compressors' isentropic efficiency (0.1–1.0) and found that the dedicated mechanically subcooled VCR cycle is an enhanced version of the simple VCR cycle. Mohammadi and Ameri [85] investigated various cooling strategies for the cascade air conditioning system with energy and exergy methodologies. They calculated the systems' exergetic efficacy and performance parameters under various operating situations, and their findings showed that the system with water-cooled chillers has the highest second-law efficiency. Refer to the literature survey on advanced exergy and coefficient of structural bond (CSB) analysis of Section 2.5 in Chapter 2, which shedding light on their significance in evaluating the performance of refrigeration systems. This Section highlights the need to incorporate advanced exergy and CSB analysis for a more holistic assessment.

The literature review compiled from various reputable data sources, such as science direct, google scholar, and research gate, etc., reveals that the researchers are still concentrating on advanced exergy analysis and structural bond analysis of the various configurations of the refrigerating machines. Each machine has its own advantage and disadvantage. This study is peculiar since, as far as the authors are aware, there is no existing literature on a dedicated mechanical subcooled system based on advanced exergy analysis and CSB analysis. This analysis was motivated by the fact that the majority of DMS-VCR system studies are introductory in nature and only focus on the system's energy and exergy analysis. In conclusion, the study stands out since it illustrates a DMS-VCR system performance based on advanced exergy analysis and CSB analysis. To better understand the design and operation of energy conversion systems, this investigation extends beyond the applicable standard approaches. In this Chapter, based on the results of CSB and AEA method, suggestion are provided for getting better performance of present system. The system mathematical model is constructed in Engineering Equation Solver (EES) software and the proposed model predicts the system energy and exergy performance. This study focuses on the DMS system's applicability in industrial water chillers. After developing a model, a system analysis for a variety of operating factors is put into practice. In order to select the optimal amount of subcooling, consideration must be given to the systems overall COP, exergetic efficiency, and total irreversibility rate. Many EES simulations have revealed that 15^{o}C is the optimum level of subcooling, as shown in Figure 6.1. Beyond this, the opposite trends are observed, so it is regarded as the ideal degree of subcooling in this work. Up to this level, the overall COP increases and the total irreversibility of the system decreases.

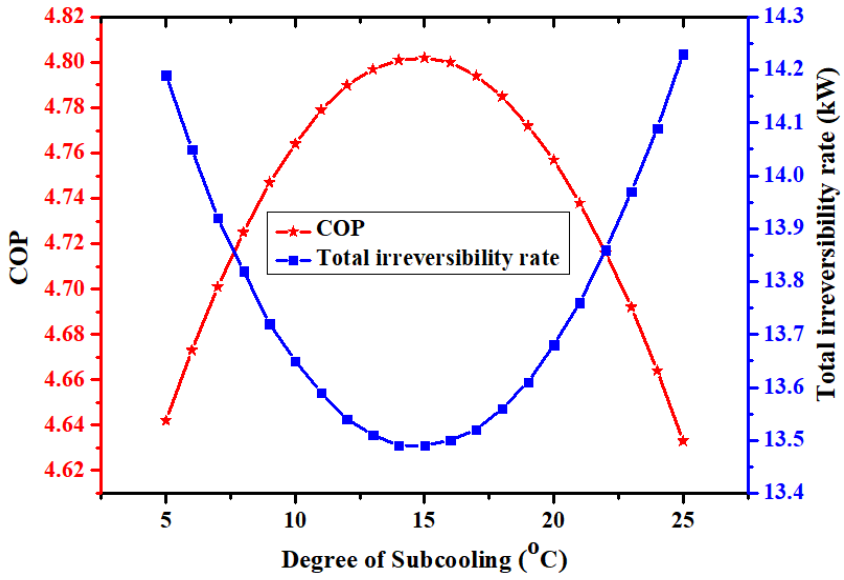

Figure 6.1 Optimal degrees of subcooling v/s COP and total irreversibility rate

6.2 SYSTEM DESCRIPTION AND MODELING

The DMS-VCR system is used to achieve efficient cooling through refrigerant subcooling before entering the evaporator section. Description of the system, alongside the theoretical formulation of the DMS-VCR system, involves modeling its components, treating all components of the DMS-VCR system as control volumes and developing governing equations specific to the system's state points.

6.2.1 Description of the DMS-VCR system

Listed below are the primary elements of a dedicated subcooled vapor compression refrigeration system. Figure 6.2 illustrates the various components of the system, including (i) two compressors, (ii) two condensers, (iii) two expansion valves, (iv) one evaporator, and (v) one sub-cooler. The schematic layout of the dedicated subcooled system is shown in Figure 6.2, and the pressure-enthalpy (P-h) diagram for the main cycle and auxiliary cycle is shown in Figure 6.3, whereas Figure 6.4 represents the temperature-entropy (T-s) diagram of the same. The cycle operates at the corresponding temperatures of the condenser and evaporator.

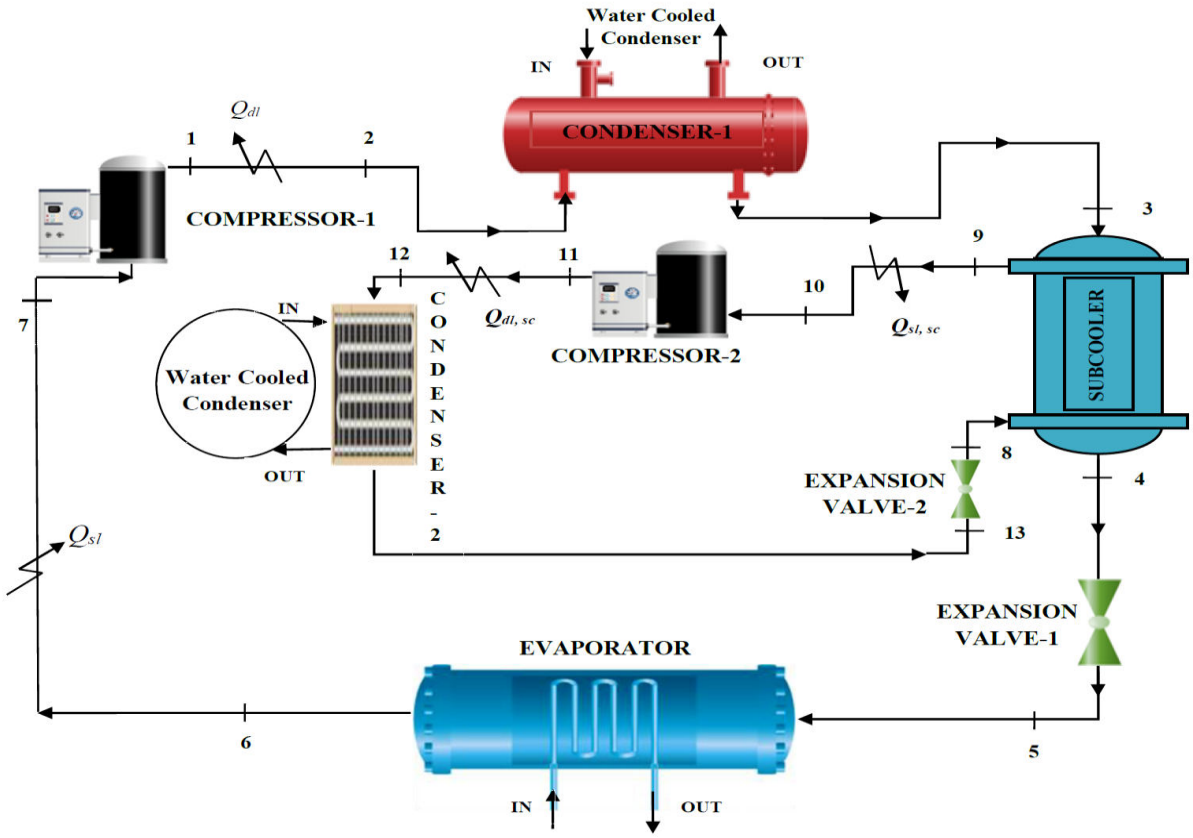

Figure 6.2 Schematic diagram of a DMS-VCR system

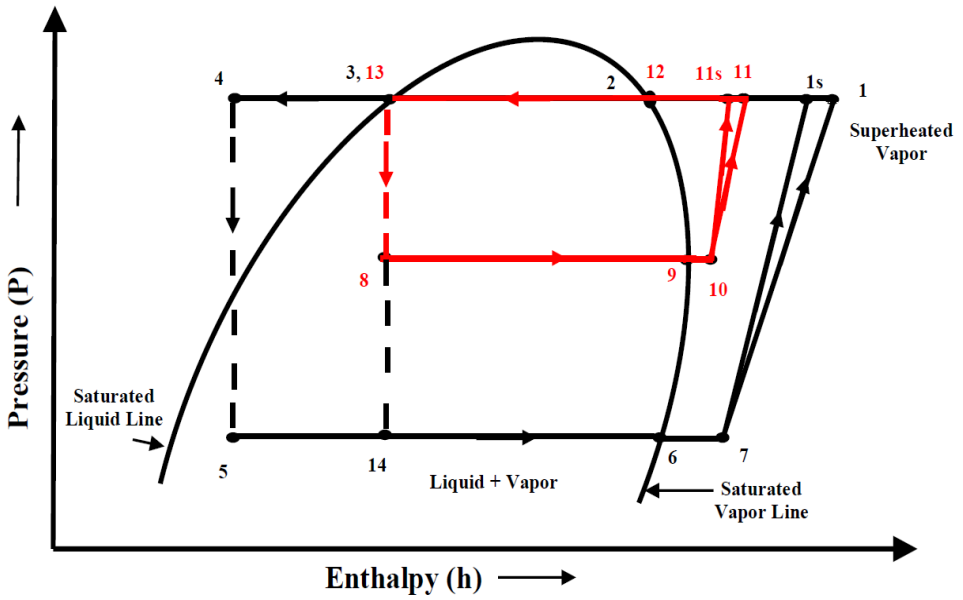

Figure 6.3 Pressure-enthalpy diagram

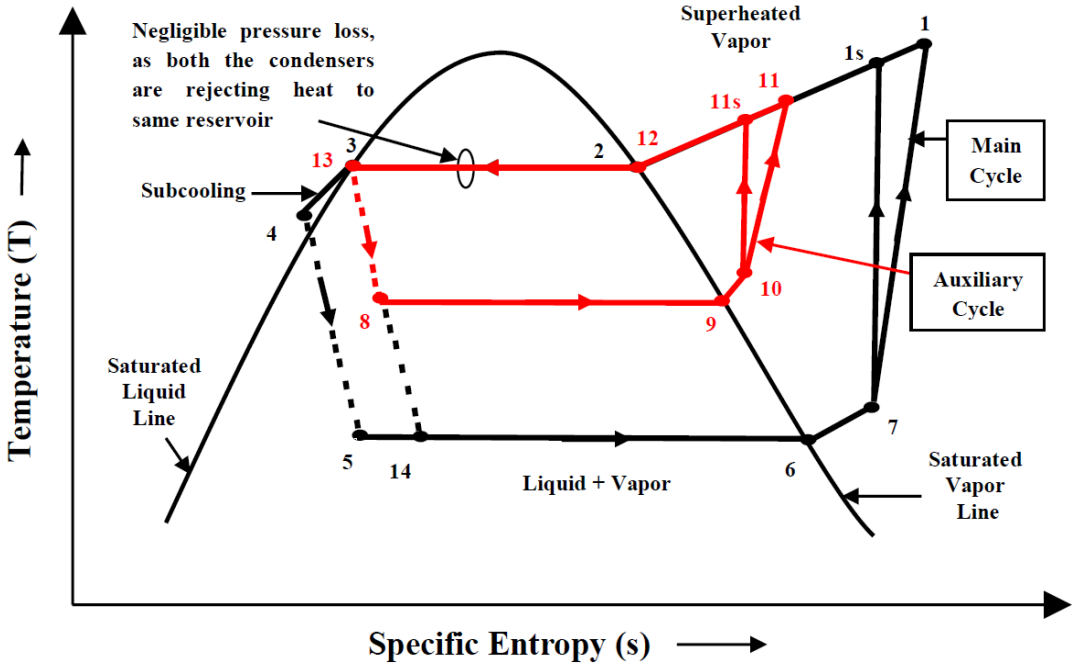

Figure 6.4 Temperature-entropy diagram

The minor cycle (8-9-10-11-12-13) is associated with the auxiliary cycle, which connects to the main cycle at the main cycle condenser-1's exit, while the main cycle (1-2-3-4-5-6-7) is related to a dedicated subcooled system. The components of the main and auxiliary cycles are linked through a piping system in a folded loop with a provision for heat transmission to the

surrounding fluid. The system can run two cycles with the same refrigerant or with different refrigerants. The cycle processes are listed below:

i) Although compression is never isentropic, processes 7-1s and 10-11s reflect the compression of vapor under isentropic conditions. As a result, the compressor's exit states in the actual processes (i.e. 7-1 and 10-11), are 1 and 11, respectively.

ii) Processes 1-2 and 11–12 depict the heat rejection from the discharge lines to the surroundings at constant pressure.

iii) The condenser's heat rejection is seen in processes 2-3 and 12–13 when the pressure is constant.

iv) The processes 4-5 and 13-8 stand in for an irreversible adiabatic expansion of vapor through the expansion valves. The liquid experiences a decrease in temperature and pressure. A small amount of liquid partially evaporates throughout the expansion process. As the expansion process is irreversible, it is depicted by a dotted line.

v) The heat absorption in the evaporator at constant pressure is shown by processes 5–6, and 8–9. The last states 6 and 9 represent the refrigerant (as it exits the evaporator) in its dry saturated form.

vi) Since the temperature at the exit is lower than the ambient temperature, processes 6-7 and 9–10 demonstrate that heat is transferred from the environment to the refrigerant in the suction line under constant pressure.

A high-temperature high pressure superheated vapor (refrigerant state-1) in the main cycle at the exit condition of compressor-1 passes through main cycle condenser-1 (2–3) for releasing heat to the surrounding. Then refrigerant enters into the subcooler section, where it is cooled below the saturated liquid state at a fixed pressure and enters the main cycle expansion valve-1. The subcooling of the refrigerant from state 3 to state 4 takes place here. Then refrigerant passes through the expansion valve-1 of main cycle to evaporator pressure for gaining the required objective of cooling by taking up the heat from the space to be cooled before moving into compressor-1 and hence completing the cycle.

Similarly, auxiliary (acting as a heat exchanger) cycle also functions like a main vapor compression cycle, at approx same pressure and temperature condition at condenser section, and at high pressure and temperature condition at evaporator section as it is clear from the Figures 6.3 and 6.4. Thus the working is same in auxiliary cycle as it is in main cycle.

Interestingly, if condenser-2 of auxiliary cycle is combined with condenser-1 of main cycle to save the condenser cost, it will become an integrated subcooled system. Which have been the

focus study for many researchers [25], [86] in past. However, this conversion in layout is not possible when different pairs of refrigerants are used in auxiliary and main cycle of DMS-VCR system.

In the present analysis R410A is selected as a refrigerant in both the cycles of DMS-VCR system as it has zero ODP & low GWP and widely used in commercial chillers [87]. The process data chosen for the operation of present DMS-VCR system is close to the design conditions of commercial water chillers and is given in Table 6.4.

6.2.2 DMS-VCR system theoretical formulation.

The thermophysical characteristics of the refrigerant R410A are taken into account while developing the current DMS-VCR system model in the EES software. The Equations for the various DMS-VCR system components are displayed in Table 6.1.

The assumptions for the thermodynamic modelling of present DMS-VCR system are as follows:

i) The system component is operating at a steady-state level.
ii) The evaporator and condenser's refrigerants are in a constant state at the exit.
iii) Expansion valves are where the isenthalpic process occurs.
iv) Ignore pressure losses in a system's other components and associated pipelines.
v) Ignore the heat gains or losses in various components.
vi) When analyzing exergies, disregard changes in kinetic, potential, and chemical exergies in favor of physical exergy.
vii) Cooling and chilling processes utilize water.

The governing equations for DMS-VCR system according to the state points shown in Figure 6.2 are shown in Table 6.1.

Table 6.1 The equations of operation for various DMS-VCR system components

S. No.	System components	1st Law Equations	2nd Law Equations
1.	Evaporator	$\dot{Q}_{evap}=(\epsilon C)_{evap}(T_{in,\,evap}-T_{evap})$ $=(\dot{m}_{ef}.c_p)_{evap}(T_{in,evap}-T_{out,evap})$ $=\dot{m}_{ref1}(h_6-h_5)$ $T_{evap}=T_5$ $Q_{loss,\,sl}=\dot{m}_{ref1}(h_7-h_6)$	$\dot{I}_{evap}=T_o\,(\dot{m}_1(S_6-S_5)$ $+(\dot{m}_{ef}.c_p)_{evap}\cdot$ $\ln((T_{out,evap}+273)/(T_{in,evap}+273)))$
2.	Condenser-1	$\dot{Q}_{cond1}=(\epsilon C)_{cond1}(T_{cond1}-T_{in,\,cond1})$ $=\dot{m}_{ref1}(h_2-h_3)$ $=(\dot{m}_{ef}.c_p)_{cond1}(T_{out,\,cond1}-T_{in,cond1})$ $T_{cond1}=T_3$	$\dot{I}_{cond1}=T_o\,(\dot{m}_{ref1}(S_3-S_1)$ $+(\dot{m}_{ef}\cdot c_p)_{cond1}\cdot$ $\ln((T_{out,\,cond1}+273)/(T_{in,cond1}+273)))$

		$\dot{Q}_{loss,\,dl}=\dot{m}_{ref1}(h_2-h_1)$	
3.	Condenser-2	$\dot{Q}_{cond2}=(\epsilon C)_{cond2}(T_{cond2}-T_{in,\,cond2})$ $=\dot{m}_{ref2}(h_{12}-h_{13})$ $=(\dot{m}_{ef}.c_p)_{cond2}.(T_{out,\,cond2}-T_{in,cond2})$ $T_{cond2}=T_{13}$ $\dot{Q}_{scloss,\,dl}=\dot{m}_{ref2}(h_{12}-h_{11})$	$\dot{I}_{cond2}=T_o\,(\dot{m}_{ref2}(S_{13}-S_{11})+$ $(\dot{m}_{ef}\,.\,c_p)_{cond2}\,.$ $.\ln((T_{out,\,cond1}+273)/(T_{in,cond1}+273)$
4.	Compressor-1	$\dot{W}_{comp1}=(\dot{W}_{comp,isen})/\eta_{isen1}$ $\dot{W}_{comp,isen}=\dot{m}_{ref1}(h_1-h_6)$ $\eta_{isen1}=0.85-0.046667\cdot(PR)$	$\dot{I}_{comp1}=T_o\,(\dot{m}_{ref1}(S_1-S_6))$
5.	Compressor-2	$\dot{W}_{comp2}=(\dot{W}_{sc,isen})/\eta_{isen2}$ $\dot{W}_{sc,isen}=\dot{m}_{ref2}(h_{11}-h_9)$ $\eta_{isen2}=0.85-0.046667\cdot(PR)$	$\dot{I}_{comp2}=T_o\,(\dot{m}_{ref2}(S_{11}-S_9))$
6.	Subcooler	$\dot{Q}_{sc}=\epsilon_{sc}\cdot\dot{Q}_{sc,\,max}$ $\dot{Q}_{sc}=\epsilon_{sc}\cdot\dot{m}_{ref1}\cdot C_P\cdot(T_3-T_8)$ $\dot{m}_{ref2}(h_9-h_8)=\dot{m}_{ref1}(h_3-h_4)$ $T_9=T_4-\Delta T_{ol}$	$\dot{I}_{sc}=T_o(\dot{m}_{ref2}(S_9-S_8)+\dot{m}_{ref1}(S_4-S_3))$
7.	Expansion valve-1	$h_4=h_5$	$\dot{I}_{ev1}=T_o\,(\dot{m}_{ref1}(S_5-S_4))$
8.	Expansion valve-2	$h_{13}=h_8$	$\dot{I}_{ev2}=T_o\,(\dot{m}_{ref2}(S_8-S_{13}))$

The following equations defined the COP of VCR system and DMS-VCR system:

$$COP_{VCR\ system}=\frac{\dot{Q}_{evap}}{\dot{W}_{comp1}} \tag{6.1}$$

$$COP_{DMS\text{-}VCR\ system}=\frac{\dot{Q}_{evap}}{\dot{W}_{comp1}+\dot{W}_{comp2}} \tag{6.2}$$

The COP is an important measure to compare the cooling effect and the energy input needed for the cooling effect, but it cannot be used to assess the quality of the process for converting energy. Exergetic analysis can be used to address this issue because it offers details on the efficiency of the energy conversion process and the conservation of available energy. Additionally, it pinpoints the system parts to reduce irreversible losses. Table 6.1 lists the equations for calculating the irreversible loss in the various DMS-VCR system components. The components that need to have their designs improved in order to reduce irreversibility loss are identified via exergetic analysis. Here, the Gouy-Stodola theorem is applied to the equation below to determine the irreversibility loss of the DMS system's component parts Nag [68].

$$\dot{I}=T_o\,\dot{s}_{gen} \tag{6.3}$$

Where, T_o is the ambient temperature

The overall DMS irreversibility rate is stated as,

$$\dot{I}_t = \sum \dot{I}_n \quad (6.4)$$

DMS,$\forall$ n $\in$ EoE $\cap$ {Evap, Cond1, Cond2, Compressor-1, Compressor-2, Subcooler}

6.3 COEFFICIENT OF STRUCTURAL BONDS ANALYSIS

Beyer created the structural bond analysis as a technique for exergy analysis component optimization. In the present study, the system structure is investigated and system component optimization is carried out using structural coefficients. After establishing the irreversibility of each system component, the CSB concept has now been implemented.

$$CSB_n = \left[\frac{\delta \dot{I}_t}{\delta z_i}\right] / \left[\frac{\delta \dot{I}_n}{\delta z_i}\right] \quad (6.5)$$

DMS,$\forall$ n $\in$ EoE $\cap$ {Evap, Cond1, Cond2, Compressor-1, Compressor-2, Subcooler}

According to the CSB principle, a gradual decrease in the irreversibility rate of one component (by changing the system efficiency parameter z_i) results in a decrease in the irreversibility rate of the entire system. Here z_i, (system efficiency parameter) may be the degree of overlap, degree of subcooling or system temperature [60].

The implication of different CSB values is as follows:

If $\mathbf{CSB_n > 1}$, the system's input (exergy saving) falls off faster than the n^{th} element's irreversibility rate (under consideration). The changes to z_i, strengthen the other parts including the n^{th} element. The n^{th} element should therefore receive more design attention in order to increase the system's overall efficiency because it has a positive effect on the performance.

If $\mathbf{CSB_n < 1}$, the system's input (exergy saving) falls off gradually than the n^{th} element's irreversibility rate (under consideration). In this case, it is evident that a decrease in the irreversibility rate in the n^{th} element is accompanied by a rise in the irreversibility rates in other system components. As a result, the structure of the system becomes unfavourable.

If $\mathbf{CSB_n = 0}$, There are no effects on the overall system performance due to a balance between the n^{th} element's performance enhancement and the other components' performance loss. As a result, the system structure is rigid and leaves no room for overall system performance improvement.

The DMS- VCR system's exergetic efficiency (η_{II}) is listed below Nag [68].

$$\eta_{II} = \left(1 - \frac{\dot{I}_t}{\dot{W}_t}\right) \quad (6.6)$$

Where, $\dot{I}_t = \dot{I}_{evap} + \dot{I}_{cond1} + \dot{I}_{cond2} + \dot{I}_{comp1} + \dot{I}_{comp2} + \dot{I}_{sc} + \dot{I}_{ev1} + \dot{I}_{ev2}$ and $\dot{W}_t = \dot{W}_{comp1} + \dot{W}_{comp2}$

6.4 ADVANCED EXERGY ANALYSIS

Exergy analysis is a useful method for assessing how energy is used to carry out the thermodynamic process Gong and Boulama [56]. By increasing the effectiveness of a system component, the high irreversibility rate stated by the traditional approach of exergy analysis can be lowered Misra et al. [60]. In circumstances, where it is technically impossible to increase the performance of a component with a large irreversibility loss, it is nevertheless advantageous to do so for the remaining components of the system.

The advanced exergy analysis approach can be used to overcome the aforementioned issue. According to Morosuk and Tsatsaronis [52], the technique employed in the current study is primarily based on two posits:

i) Calculating the endogenous and exogenous contributions to irreversibility loss.

ii) Calculating the irreversible loss of components that are both avoidable and unavoidable.

In the first posit, endogenous irreversibility loss is completely based on the component itself, whereas, in case of exogenous irreversibility loss, the other system components are also operational. Thus, the first posit in an equation form can be written as given below Gong and Boulama [56].

$$\dot{I}_n = \dot{I}_n^{END} + \dot{I}_n^{EXO} \quad (6.7)$$

In the second posit, the irreversible loss of the system's components is divided into avoidable and unavoidable parts. Consequently, the second assertion could be expressed as follows:

$$\dot{I}_n = \dot{I}_n^{AVO} + \dot{I}_n^{UNA} \quad (6.8)$$

The avoidable component can be avoided by offering technical development to boost system performance, which will undoubtedly present a superior option for design engineers. The unavoidable fraction governs the fragment of irreversibility loss that cannot be averted. The overall irreversibility loss of each component is therefore divided into four primary categories: endogenous avoidable, exogenous avoidable, endogenous unavoidable and exogenous unavoidable losses. These categories are reflected in the equation below.

$$\dot{I}_n = \dot{I}_n^{END,\,AVO} + \dot{I}_n^{END,\,UNA} + \dot{I}_n^{EXO,\,AVO} + \dot{I}_n^{EXO,\;UNA} \quad (6.9)$$

DMS, $\forall$ n $\in$ EoE $\cap$ {Evap, Cond1, Cond2, Compressor-1, Compressor-2, Subcooler}

The procedure of Morosuk and Tsatsaronis [52] and Jain et al. [88] has been followed to quantify the terms of the Equation (6.19). Mainly three systems analysed concurrently for the calculation of the same are given below:

- **Real system:** It is a system in which the compressor's isentropic efficiency is considered as a function of the pressure ratio between high pressure and low pressure side, as shown in Table 6.1, and the terminal temperature variance between all heat exchangers is assumed to be 5^{o}C. Furthermore, the degree of overlap, which is set at 5^{o}C, determines the effectiveness of the subcooler. The expansion process is assumed to be isenthalpic at both expansion valves.
- **Ideal system:** This fictional system has extremely fictitious design features. The terminal temperature difference in each heat exchanger is assumed to be 0^{o}C by assuming that the subcooler is 100% effective and that both compressors are 100% isentropically efficient. Each expansion valves' irreversibility is zero because it is assumed that the expansion process at both of them is isentropic.
- **Unavoidable system:** This intermediary system's design features fall between real and ideal systems. The degree of overlap, in this case is considered to be 0.5^{o}C, and the isentropic efficiency of both compressors are assumed to be 90% to determine the effectiveness of the subcooler. It is assumed that there is a 0.5^{o}C terminal temperature differential between the two heat exchangers. At both expansion valves, it is presumed that the expansion process is isenthalpic.

Here, initially the irreversible loss of all the DMS-VCR system components, $\dot{I}_n$ (real) and $\dot{I}_n^{UNA}$ (unavoidable) is calculated by using real and unavoidable system settings. The endogenous exergy destruction (real) $\dot{I}_n^{END}$ is then calculated using ideal system settings, in which real system setting is used for computation of $\dot{I}_n^{END}$ for each component of the system. Furthermore, under ideal system conditions, endogenous unavoidable exergy destruction ($\dot{I}_n^{END,UNA}$) is calculated for each system components. It should be noted that any system component's $\dot{I}_n^{UNA}$ is calculated using the unavoidable system setting. Below procedural equations are followed to determine all the four terms described in Equation (6.19).

$$\dot{I}_n^{END,\ AVO} = \dot{I}_n^{END} - \dot{I}_n^{END,\ UNA} \quad (6.10)$$

$$\dot{I}_n^{EXO} = \dot{I}_n - \dot{I}_n^{END} \quad (6.11)$$

$$\dot{I}_n^{EXO,\ UNA} = \dot{I}_n^{UNA} - \dot{I}_n^{END,\ UNA} \quad (6.12)$$

$$\dot{I}_n^{EXO,\ AVO} = \dot{I}_n^{EXO} - \dot{I}_n^{EXO,\ UNA} \quad (6.13)$$

The flow chart depicting the solution procedure of the present system is shown in Figure 6.5.

6.5 ENVIRONMENT ANALYSIS

Many environmentalists suggest that issues related to global warming can be solved by assigning carbon pricing as the penalty for CO_2 emissions Aminyavari et al. [69]. The "yearly penalty cost" is the CO_2 emissions into the atmosphere caused by the production of power from fossil fuels. Equation (6.14) can be used to calculate this cost.

$$C_{env} = m_{co_2} \cdot C_{co_2} \quad (6.14)$$

Here, C_{co_2} which varies among nations, is used to represent the cost of the CO_2 emissions penalty. According to Aminyavari et al. [69], the penalty cost of CO_2 emissions in the current work is assumed to be US \$90 per tonne. Additionally, mass of CO_2 emission (m_{co_2}) is given by Equation (6.15):

$$m_{co_2} = \lambda \cdot \dot{W}_t \cdot t_{oper} \quad (6.15)$$

where, the DMS refrigeration system's annual operational hours (t_{op}) and the conversion factor of emissions (λ) are assumed to be 5000 h and 0.968 kg/kWh, respectively.

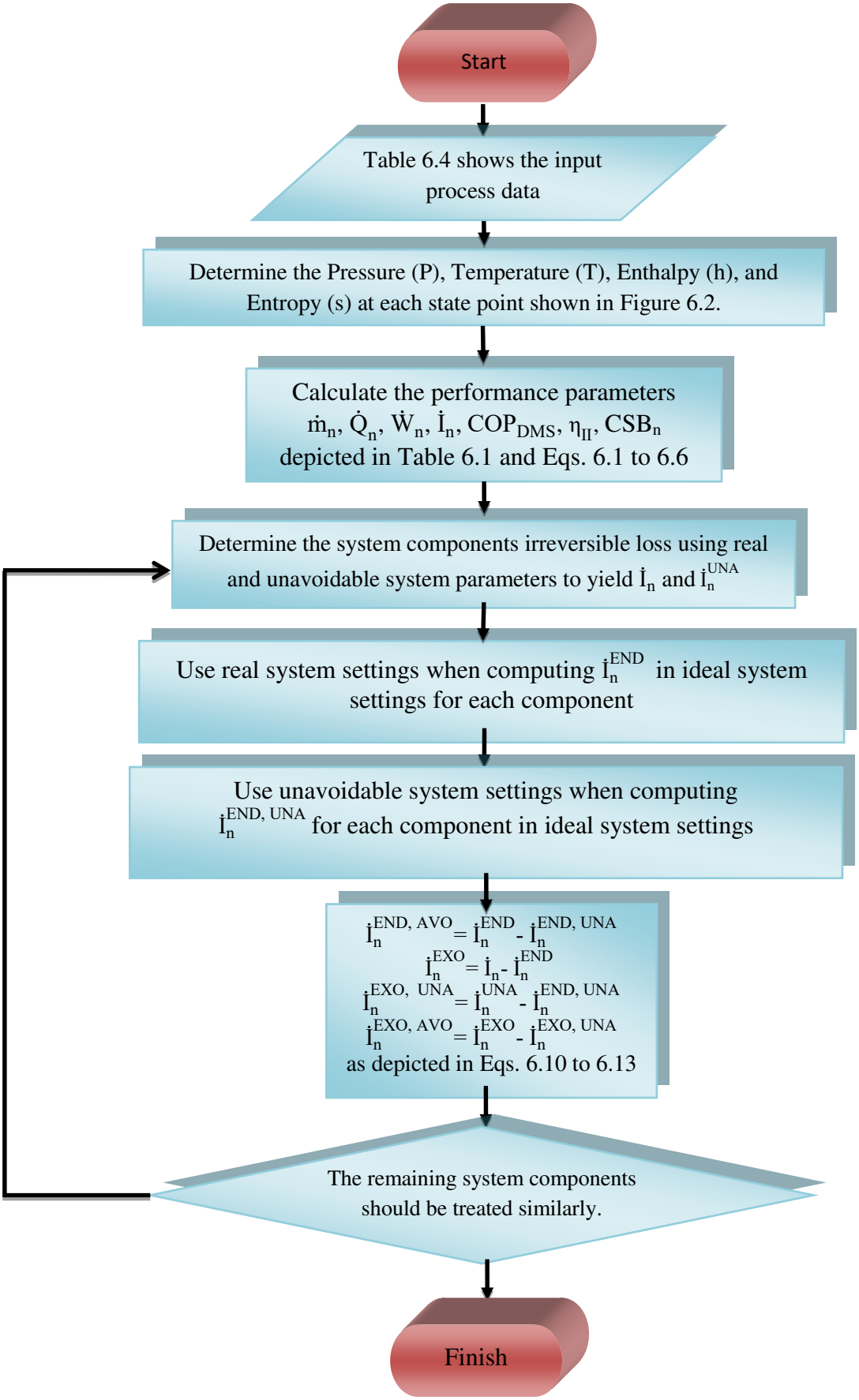

Figure 6.5 Flowchart for CSB and AEA solution procedure

6.6 MODEL VALIDATION

The initial work on the DMS-VCR system was based on numerical analysis. The current model is validated using the work of Agarwal et al. [70]. When the ambient temperature (T_o) and pressure (P_o) are 25 °C and 101.325 kPa respectively, the net refrigerating effect ($\dot{Q}e$) is 3.5167 kW, the evaporator-1 temperature ($T_{evap,\ DMS}$) is -10 ^oC, the degree of subcooling is up to 5 ^oC, the condenser-1 and condenser-2 temperatures are 50 ^oC, the isentropic efficiency of the compressors (η_{comp1}, η_{comp2}) is 80% and the effectiveness of the subcooler ($\in_{sc}$) is 0.8.

The simulation program is subsequently updated for model validation in order to make the simulation results consistent with the findings of Agarwal et al. [70] theoretical analysis. Here, model validation is performed for the evaluation of a dedicated subcooled vapor compression system on the EES program. The results depict that all relevant quantities (compressor power, exergetic efficiency, and COP) are anticipated by the EES model effectively with a maximum encountered error of 3.57%, but most of the errors were less than 2% (see Table 6.2 and Table 6.3).

Table 6.2 Comparison of performance data from Agarwal et al. [70] for effect of evaporator temperature with refrigerant R134a (T_{cond} = 50^oC)

$T_{in,evap}$ (^oC)	$\dot{W}^*_{comp}$ (kW)	$\dot{W}_{comp,mod}$ (kW)	error (%)	η_{II}^*	$\eta_{II,,mod}$	error (%)	COP^*	COP_{mod}	error (%)
-20	1.52	**1.52**	**0.00**	0.3562	**0.3533**	**0.81**	2.315	**2.395**	**3.45**
-15	1.36	**1.32**	**2.94**	0.3432	**0.3402**	**0.87**	2.572	**2.623**	**1.98**
-10	1.22	**1.20**	**1.63**	0.3204	**0.3186**	**0.56**	2.867	**2.905**	**1.32**
-5	1.10	**1.12**	**1.81**	0.2955	**0.2987**	**1.08**	3.229	**3.202**	**0.83**
0	0.96	**0.98**	**2.08**	0.2655	**0.2665**	**0.37**	3.625	**3.615**	**0.27**
5	0.84	**0.87**	**3.57**	0.2201	**0.2257**	**2.54**	4.166	**4.123**	**1.03**
10	0.72	**0.74**	**2.77**	0.1688	**0.1723**	**2.07**	4.863	**4.813**	**1.02**

*****From the performance data of Agarwal et al. [70]

Table 6.3 Comparison of present model with work of Agarwal et al. [70] for effect of condenser temperature with refrigerant R134a (Te = -10^oC)

$T_{in,cond}$ (^oC)	W^*_{cp} (kW)	$W_{cp,mod}$ (kW)	error (%)	η_{II}^*	$\eta_{II,,mod}$	error (%)	COP^* (kW)	COP_{mod} (kW)	error (%)
30	0.780	**0.780**	**0.00**	0.5069	**0.5003**	**1.30**	4.505	**4.505**	**0.00**
35	0.905	**0.905**	**0.00**	0.4370	**0.4357**	**0.29**	3.885	**3.886**	**0.02**
40	1.039	**1.039**	**0.00**	0.3803	**0.3833**	**0.78**	3.383	**3.383**	**0.00**
45	1.186	**1.185**	**0.08**	0.3333	**0.3399**	**1.98**	2.965	**2.965**	**0.00**
50	1.347	**1.347**	**0.00**	0.2933	**0.3030**	**3.30**	2.610	**2.611**	**0.03**

*From the performance data of Agarwal et al. [70]

6.7 RESULTS AND DISCUSSION

The thermodynamic analysis of the DMS-VCR system using variables from the first and second laws, with known thermophysical properties of the working substance and environmental conditions, is compared with the equivalent VCR system for similar input conditions as shown in Table 6.4. Following that, the reliability of DMS-VCR system is examined using parametric analysis, CSB and AEA techniques along with environmental benefits.

Table 6.4 Process data of dedicated mechanical subcooled refrigeration system

Parameters	Values
Cooling capacity of evaporator (Q_{evap}, kW)	100
Temperature of evaporator ($T_{evap,}$ ^{o}C)	5
Inlet temperature of evaporator coolant ($T_{evap,in,}$ ^{o}C)	15
Outlet temperature of evaporator coolant ($T_{evap,out,}$ ^{o}C)	10
Temperature of condenser ($T_{cond,}$ ^{o}C)	40
Coolant inlet temperature of condenser ($T_{cond,in,}$ ^{o}C)	30
Coolant outlet temperature of condenser ($T_{cond,out,}$ ^{o}C)	35
Overlap degree (T_{ol}, ^{o}C)	5
Degree of subcooling ($T_{sc,}$ ^{o}C)	15 (optimized)
Isentropic efficiency of compressors (η_{isen})	0.72, 0.77
Environment temperature ($T_{o,}$ ^{o}C)	25
Environment pressure (P_o, kPa)	101.325
Refrigerants (for both the cycles)	R410A

6.7.1 Comparative study of DMS-VCR system with equivalent VCR system

Using the process data values mentioned in Table 6.4, comparative study of DMS-VCR system is performed with simple VCR system. The thermodynamic parameters of DMS-VCR system (pressure, temperature, mass flow rate, entropy and enthalpy) are calculated at the inlet and outlet of each component, as shown in Table 6.5.

For the identical input settings as shown in Table 6.4, Table 6.6 shows the values of performance parameter for DMS-VCR system and its equivalent VCR system. R410A has a mass flow rate of 0.5454 kg/s (main cycle), 0.09136 kg/s (auxiliary cycle), and 0.6386 kg/s (equivalent VCR system) for same cooling capacity of 100 kW. Furthermore, in the DMS-VCR system, the condensers-1, 2, and evaporator's mass flow rates for the cooling water

(external fluid) are 5.008 kg/s, 0.7735 kg/s, and 4.772 kg/s, respectively, as contrasted to 5.863 kg/s and 4.772 kg/s in the equivalent VCR system. The DMS system's COP is 8.2% higher when compared to an equivalent VCR system.

Table 6.5 Thermodynamic properties at the DMS-VCR system design stage

State point	$\dot{m}$ (kg/s)	x (%)	T(^{o}C)	P(kPa)	h(kJ/kg)	s (kJ/kg.K)
1	0.545	-	62.21	2.426	458.1	1.83
2	0.545	-	-	-	-	-
3	0.545	0	40	2.462	266.2	1.221
4	0.545	-	25	-	239.5	1.133
5	0.545	0.149	4.91	-	239.5	1.142
6	0.545	1	5	9.332	422.8	1.801
7	0.545	-	-	-	-	-
8	0.091	0.179	20	-	266.2	1.228
9	0.091	1	20	1.443	425.8	1.772
10	0.091	-	-	-	-	-
11	0.091	-	51.14	2.426	443.1	1.784
12	0.091	-	-	-	-	-
13	0.091	0	40	2.426	262.2	1.221

The irreversibility losses for each system component are also displayed in Table 6.6. The DMS system's overall irreversibility rate is 13.49 kW, which is 11% lower than the corresponding VCR system. Furthermore, it can be seen that the DMS system is more exergy efficient than an equivalent VCR system because it has higher exergetic efficiency of 7.6%.

Table 6.6 Comparison analysis of the DMS-VCR system and equivalent VCR system performances

Serial No.	Performance analysis parameters		VCR system	DMS-VCR system
1	First law parameters	COP_{VCRS}	4.439	-
		$COP_{DMS\text{-}VCRS}$	-	4.802
		$\dot{Q}_{cond1}$ (kW)	122.50	104.70
		$\dot{Q}_{cond2}$ (kW)	-	16.16
		$\dot{Q}_{evap}$ (kW)	100	100

		$\dot{Q}_{sc}$ (kW)	-	14.58
		$\dot{W}_{comp1}$ (kW)	22.53	19.24
		$\dot{W}_{comp2}$ (kW)	-	1.58
2	Second law parameters	$\dot{I}_{cond1}$	3.59	3.06
		$\dot{I}_{cond2}$	-	0.42
		$\dot{I}_{comp1}$	5.49	4.69
		$\dot{I}_{comp2}$	-	0.33
		$\dot{I}_{evap}$	2.77	2.78
		$\dot{I}_{ev1}$	3.30	1.41
		$\dot{I}_{ev2}$	-	0.19
		$\dot{I}_{sc}$	-	0.61
		$\dot{I}_{t}$	15.15	13.49
		η_{II} (%)	32.75	35.24

It will be hostile to compare the performance of present DMS system with equivalent VCR system at the mentioned design conditions of Table 6.4. To provide complete insight and benefits of proposed DMS-VCR system, it is suggested to compare the system at off-design operating conditions of evaporator and condenser also. The DMS system's COP improves by 9.78% at 0 ^{o}C and 6.18% at 10 ^{o}C when the evaporator temperature of the VCR system is changed. Additionally, when comparing the DMS system with an equivalent VCR system, it is found that at 0 ^{o}C, there is a significant reduction in total irreversibility of 11.96%, whereas at 10 ^{o}C, only a reduction of 9.47% is seen. Above results indicate that lower temperature refrigerations applications are much favourable in case of DMS system.

Similar to this, on varying condenser temperature from 35 ^{o}C to 45 ^{o}C, the DMS system's COP increased by 5.75% at 35 °C and 10.68% at 45 °C when compared to an equivalent VCR system. At 45 °C, the overall irreversibility rate decreases by a maximum of 12.90%, but at 35°C, it decreases by just 8.88%. Therefore, in hot climate conditions where the condenser temperature is high, a DMS system is more advantageous than a traditional VCR system.

6.7.2 Parametric analysis of DMS-VCR system

In order to maximise the performance of the system by determining the ideal values for the system parameters, parametric analysis is a crucial technique for researchers working in the

field of thermodynamics. Therefore, the effects of changing parameters like evaporator and condenser temperatures, the degree of subcooling, and the degree of overlap on the energy and exergy analysis of the mechanical subcooled system are examined in this section. Only one variable is changed during the parametric analysis; all other variables, as shown in Table 3, remain constant at their initial values.

6.7.2.1 Effect of evaporator temperature

Figure 6.6 illustrates how the evaporator temperature affects the rate of energy destruction and performance coefficient. The specific volume of both refrigerants decreases when the evaporator temperature rises from 0°C to 10°C, which results in a 32% reduction in compressor power. The fluid that has to be cooled outside is still flowing at a constant mass flow rate and temperature. Additionally, the system's COP increases from 3.98 to 5.85 when the evaporator temperature varies significantly up to 10°C. The resulting decrease in compressor work causes the mass flow rate of external water to decrease, which also lessens the heat load on the condensers of both cycles (i.e., the main and auxiliary cycle). The rise in evaporator temperature causes the irreversibility rate of the evaporator section to drop from 4.73 kW to 0.87 kW (R410A), which lowers the average temperature difference between chilled water and the evaporator.

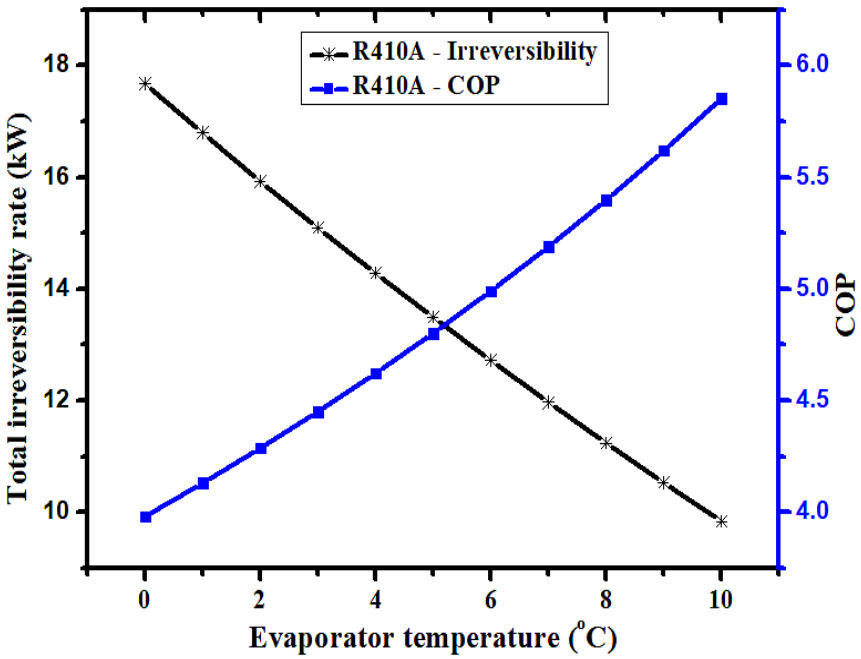

Figure 6.6 Effect of evaporator temperature on COP and overall irreversibility rate of the system

The irreversibility rates for different system components are also seen to be decreasing, resulting in a 44.30% drop in the overall irreversibility rate. The exergetic efficiency thus

rises by around 43.13%. This indicates that from an energy and exergy perspective, a high evaporator temperature is beneficial.

6.7.2.2 Effect of condenser temperature

Figure 6.7, illustrates how condenser temperature affects the irreversibility rate and COP. A change in the condenser temperature and compressor discharge pressure results in a 45.80% increase in compressor work under the same conditions. As a result, their COP decreases by 31.41% and their irreversibility rate increases by 77.55%. The system's exergetic efficiency also decreases, going from 42.28% to 29.76% (R410A). Low condenser temperature is therefore advantageous from an energy and exergy standpoint.

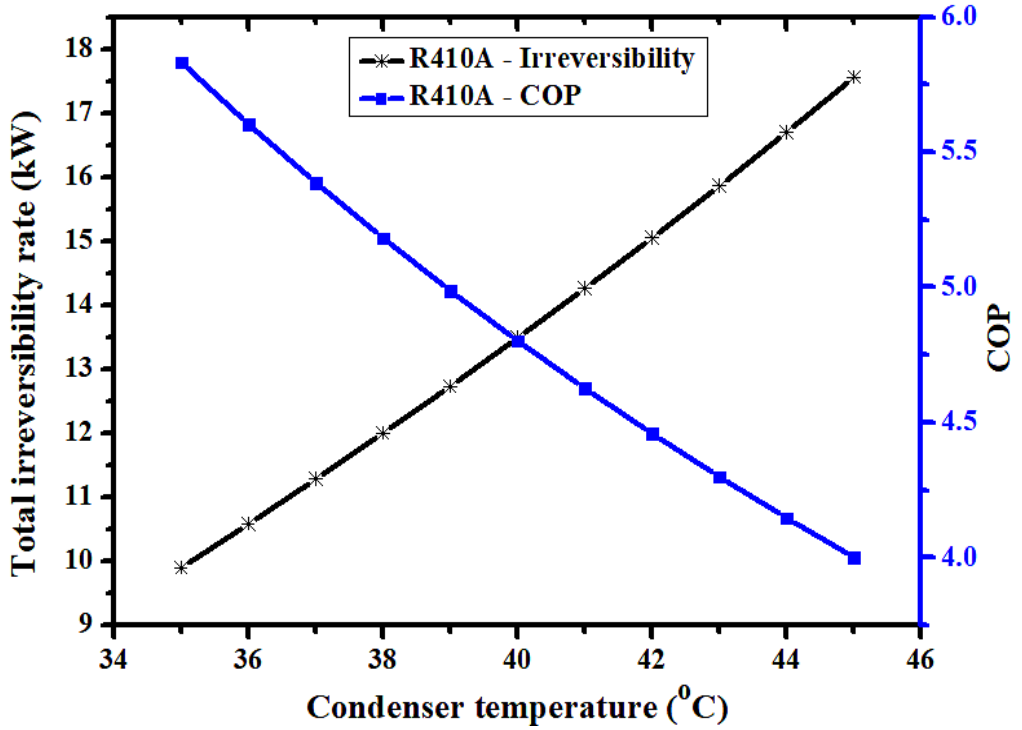

Figure 6.7 Effect of condenser temperature on COP and the irreversibility rate of the system

6.7.2.3 Effect of degree of overlap

The degree of overlap is the difference in temperature between the main cycle exit fluid (state 4) after subcooling and the auxiliary unit exit fluid (state 9) from the subcooler. When the degree of overlap changes from 0°C to 10°C (with a difference in effectiveness from 100% to 60%), the heat load over the auxiliary cycle condenser (i.e., condenser-2) increases by 6.11% while maintaining the subcooler temperature and other design parameters unchanged as indicated in Table 6.4. Figure 6.8 shows how variation in COP and total irreversibility rate are influenced by the degree of overlap. The performance of the main compressor section is unaffected by the fixed evaporator temperature. The auxiliary cycle compressor work,

however, increases by 84.50%, increasing the overall compressor work from 20.37 kW to 21.33 kW.

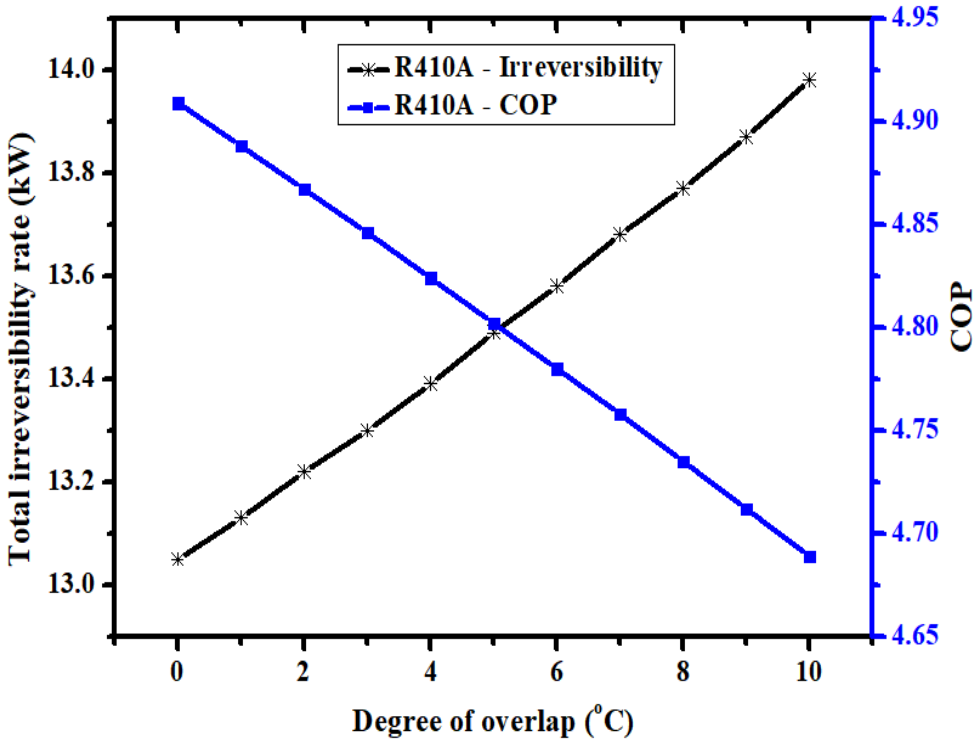

Figure 6.8 Effect of overlap degree on COP and overall irreversibility rate of the system

The overall COP of the system decreases from 4.91 to 4.69, as a result, increasing total irreversibility by 7.12%. Thus, for energy and exergy point of view, low overlap values are recommended.

6.7.3 CSB method: Exergy analysis results of DMS-VCR system

The irreversibility loss of each system component must be kept to a bare minimum to improve the efficiency of the DMS system. The main cycle's compressor-1 experiences the greatest irreversible loss, which is 34.8% of the system's overall irreversibility rate. The DMS system's components can be organized in increasing order of irreversibility as follows: expansion valve-2 (0.1931kW/1.4%), compressor-2 (0.3334kW/2.5%), condenser-2 (0.4155kW/3.1%), subcooler (0.6122kW/4.5%), expansion valve-1 (1.407kW/10.4%), evaporator (2.767kW/20.5%), condenser-1 (3.065kW/22.7%), and compressor-1 (4.693kW/34.8%).

Various researchers have proposed the idea of CSB. According to Figures 6.9(a-f), the CSB values of various DMS-VCR system components are estimated. For the current study, the CSB values for the subcooler, condenser-1, condenser-2, evaporator, compressor-1, and compressor-2 are determined. The efficiency parameters (z_i -mention equation number) for

the CSB analysis are the evaporator temperature, condenser temperature, isentropic effectiveness, and degree of overlap, respectively. Figure 6.9(a) demonstrates that when the degree of overlap gradually fall off (10°C to 0°C) keeping the other parameters of Table 6.4 as constant, the subcooler's irreversibility rate decreases by 58.1% (0.86 kW - 0.36 kW), which in turn lowers the DMS system's overall irreversibility rate by 6.65% (13.98 kW - 13.05 kW). Therefore, a lower degree of overlap is preferred; however it will ultimately result in a larger subcooler.

If the condenser temperature changes by 10 ^{o}C (45 ^{o}C to 35 ^{o}C) while keeping the other process parameters of Table 6.4 as constant, the irreversibility rate of condenser-1 and condenser-2 decreases by 74.4% (4.941 kW - 1.266 kW) and 78.4% (0.6946 kW - 0.1501 kW), respectively. This reduces the total irreversibility rate of the DMS system for condenser-1 and condenser-2 by 43.7% (17.56 kW - 9.895 kW) and, 6.8% (13.99 kW - 13.04 kW) respectively, as shown in Figures 6.9(b, c). As the temperature increases from 0 °C to 10 °C (see Figure 6.9(d)), while maintaining the other design parameters as constant, the irreversibility rate of the evaporator decreases by 81.5% (4.729 kW - 0.8743 kW) and the total irreversibility rate of the DMS system decreases by 44.3% (17.67 kW - 9.841 kW). Therefore, the condenser temperature needs to be low and the evaporator temperature of the DMS system should be high as per application.

Additionally, as the isentropic efficiency of compressors 1 and 2 increases up to 100% (with the constant value of other process parameters), their irreversibility rates decrease by 100%, demonstrating their ideal condition, and eventually, as shown in Figures 6.9(e, f), the overall irreversibility rate of the DMS system decreases by 46.8% (15.76 kW - 8.391 kW) and 4.6% (13.77 kW - 13.13 kW). Compressor-1 has a greater impact on the DMS system's overall irreversibility rate compared to the other components. Additionally, compared to the systems other component, compressor-1's contribution to the overall irreversibility loss is highest (i.e., 4.693kW/34.8%). Therefore, it is crucial that compressor-1's efficiency is improved. Compressor-1's efficiency is a function of the pressure ratio, which is influenced by the main cycle working fluid's evaporation and condensation temperatures. In a DMS system, the pressure ratio over compression-1 might drop off by either lowering the condenser temperature or raising the evaporator temperature.

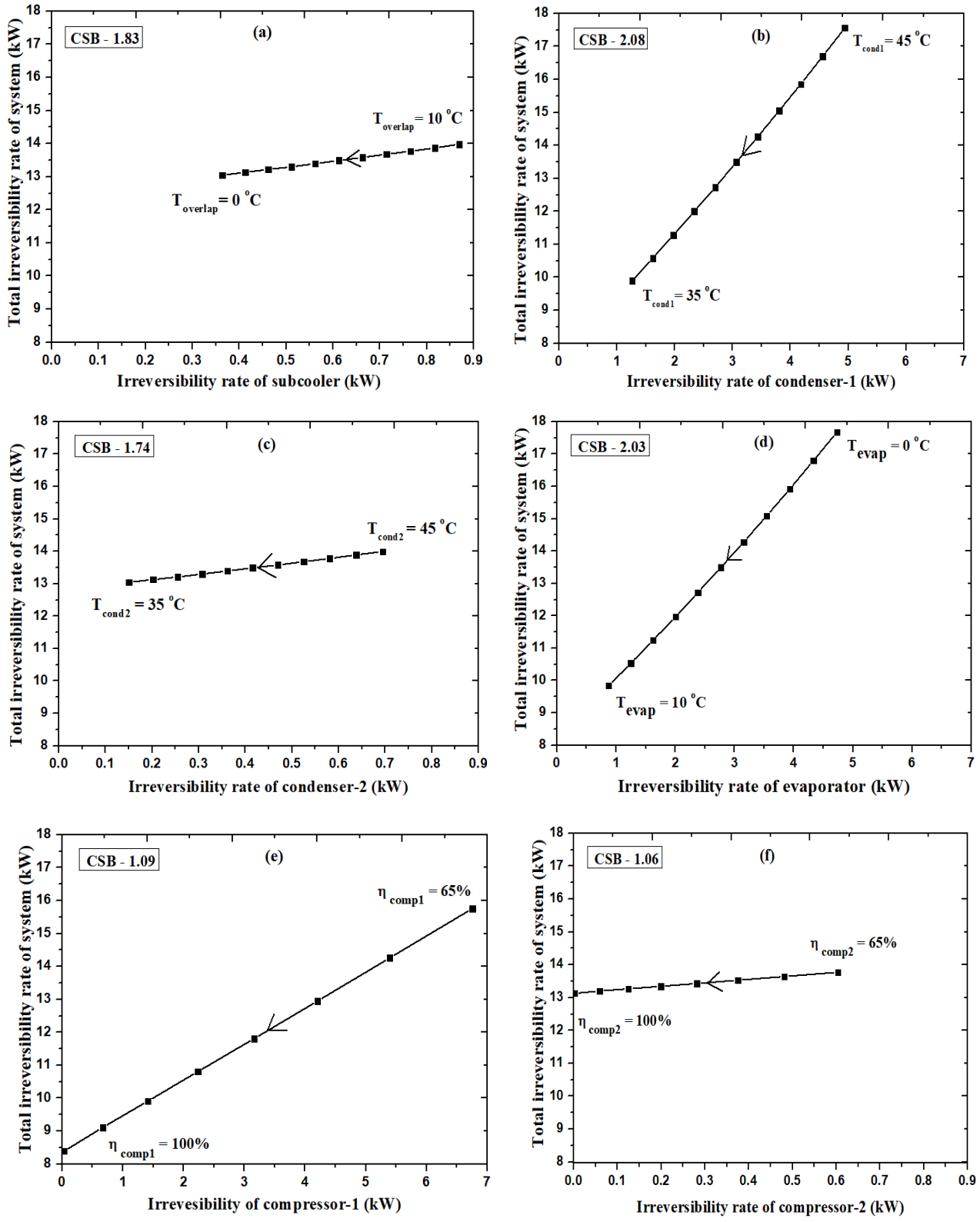

Figure 6.9 Variation in the system's overall irreversibility rate with the (a) subcooler, (b) condenser-1, (c) condenser-2, (d) evaporator, (e) compressor-1, and (f) compressor-2.

As per increasing CSB values, the computed values for the selected DMS-VCR system components are arranged in Figure 6.10 as follows: Compressor-2 (1.06), Compressor-1 (1.09), Condenser-2 (1.74), Subcooler (1.83), Evaporator (2.03), and Condenser-1 (2.08).

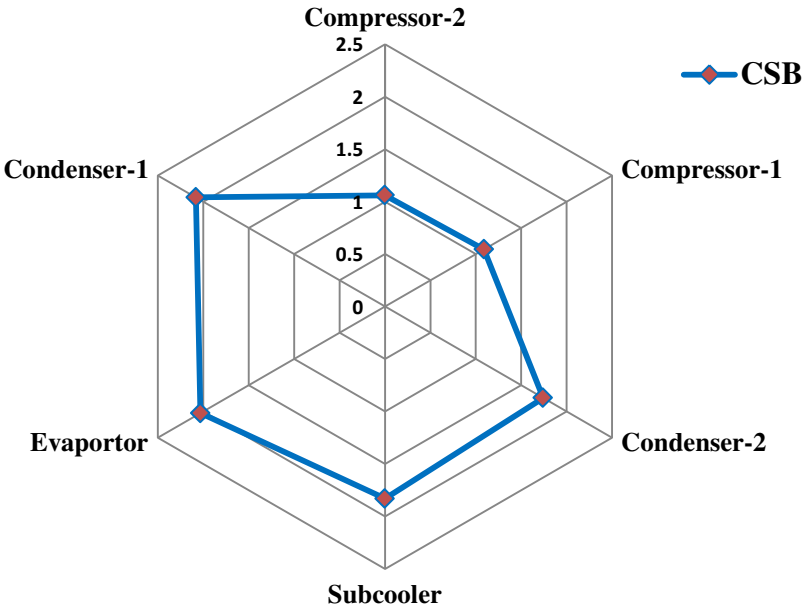

Figure 6.10 Spider diagram showing system's components comparison of CSB value.

The CSB values of all the components are greater than 1, which indicates that the system's irreversibility rate has decreased more than that of its individual components. Therefore, improving the efficiency parameters of these components will improve both their performance and the performance of the other system components, ultimately improving the system as a whole. Hence, a modest adjustment to the component's operating parameter that has a high CSB value will enhance the system's performance. The next sensitive component is the evaporator (CSB-2.03) and its contribution to the irreversibility rate is 20.5%. Condenser-1 has the highest CSB value among the components (2.08) and contributes 22.7% of the total irreversibility rate. Compressor-1's overall contribution to the total irreversibility rate is 34.8%, which is the largest figure, but it is less sensitive (CSB-1.09) when compared to other parts of the DMS system. Therefore, there is a debate over, which part of the system should be the emphasis. The CSB method also has the drawback of only evaluating the performance of one system component at a time, regardless of other components. Consequently, a different analysis technique, such as advanced exergy analysis, is required to determine the system's potential for performance improvement.

6.7.4 AEA method: Exergy analysis results of DMS-VCR system

The values of the set parameters for base/real, unavoidable, and ideal systems are presented in this Section of the advanced exergy analysis method while maintaining the identical processing parameters for each of the three systems (as shown in Table 6.7). In the ideal system, which substitutes isentropic turbines for expansion valves, both expansion valves are considered to be isentropic. As a result, there is a slight reduction in enthalpy (about 1%) at the expansion valves' exit. The modified definition of COP (Equation 6.16) and exergetic efficiency (Equation 6.17) in the context of the ideal system is presented below.

$$COP_{\text{DMS-VCR system, ideal}} = \frac{\dot{Q}_{evap}}{\dot{W}_{comp1} + \dot{W}_{comp2} - (\dot{W}_{ev,1} + \dot{W}_{ev,2})} \tag{6.16}$$

$$\eta_{II,\text{ ideal}} = \left(1 - \frac{\dot{I}_t}{\dot{W}_t - (\dot{W}_{ev,1} + \dot{W}_{ev,2})}\right) \tag{6.17}$$

The outcomes of the first and second law parameters for ideal, real, and unavoidable systems are shown in Table 6.7. The comparison analysis demonstrates that, as would be expected, in the case of the ideal system, the electrical energy delivered to the compressor is lowest. As a result, when compared to the ideal system, the overall COP of the real and unavoidable systems decreased by 29.4% and 11.4%, respectively. Additionally, an ideal system's exergetic efficiency is determined to be the highest at 70.6%, followed by 53.6% and 35.2% in the avoidable and real systems, respectively, due to the lowest irreversibility loss in an ideal system.

Table 6.7 Comparison of performance parameters of three systems (Real, Ideal & Unavoidable)

S.No.	Parameters for performance analysis		Real system	Unavoidable system	Ideal system
1.	First law parameters	COP_{VCRS}	5.197	6.418	7.225
		$COP_{DMS\text{-}VCRS}$	9.224	14.34	16.67
		$COP_{OVERALL}$	4.802	6.025	6.800
		$\dot{Q}_{cond1}$ (kW)	104.70	101	98.16
		$\dot{Q}_{cond2}$ (kW)	16.16	15.60	15.14
		$\dot{Q}_{evap}$ (kW)	100	100	100
		$\dot{Q}_{sc}$ (kW)	14.58	14.58	14.39
		$\dot{W}_{comp1}$ (kW)	19.24	15.58	13.84

		$\dot{W}_{comp2}$ (kW)	1.58	1.02	0.86
		$\dot{W}_{t}$ (kW)	20.82	16.6	14.71
2.	Second law parameters	$\dot{I}_{cond1}$ (kW)	3.06	2.06	1.86
		$\dot{I}_{cond2}$ (kW)	0.42	0.28	0.25
		$\dot{I}_{comp1}$ (kW)	4.69	1.41	0
		$\dot{I}_{comp2}$ (kW)	0.33	0.09	0
		$\dot{I}_{evap}$ (kW)	2.78	1.93	1.85
		$\dot{I}_{ev1}$ (kW)	1.41	1.41	0
		$\dot{I}_{ev2}$ (kW)	0.19	0.13	0
		$\dot{I}_{sc}$ (kW)	0.61	0.39	0.36
		$\dot{I}_{t}$ (kW)	13.49	7.70	4.32
		η_{II} (%)	35.24	53.61	70.64

The effect of the DMS refrigeration system on the environment must be taken into account due to growing concerns about environmental issues, notably those connected to global warming brought on by greenhouse gases. The CO_2 emissions that DMS systems emit are quantified in order to assess this impact. The DMS-VCR system emits 100 tonnes/year (Real), 80 tonnes/year (Unavoidable), and 71 tonnes/year (Ideal) of CO_2. In contrast, a typical VCR system emits about 110 tonnes of CO_2 annually. Additionally, the three alternative DMS systems significantly reduce CO_2 emissions as compared to an equivalent VCR system, with reductions of 9.09% (Real), 27.27% (Unavoidable), and 35.45% (Ideal), respectively. As a result, the compressor uses less energy, significantly reducing CO_2 emissions. The comparable VCR system's annual penalty cost is $9900, whereas for DMS systems, it is $9000 (Real), $7200 (Unavoidable), and $6390 (Ideal), respectively. The DMS system is therefore unquestionably a very consistent decarburizing and energy-efficient cooling system.

According to the bar graph in Figure 6.11, the DMS system's overall irreversibility loss (of the unavoidable type) is 57.1%; this loss cannot be excluded. However, by increasing the efficiency parameters, the system's 42.9% avoidable type irreversibility loss can be reduced.

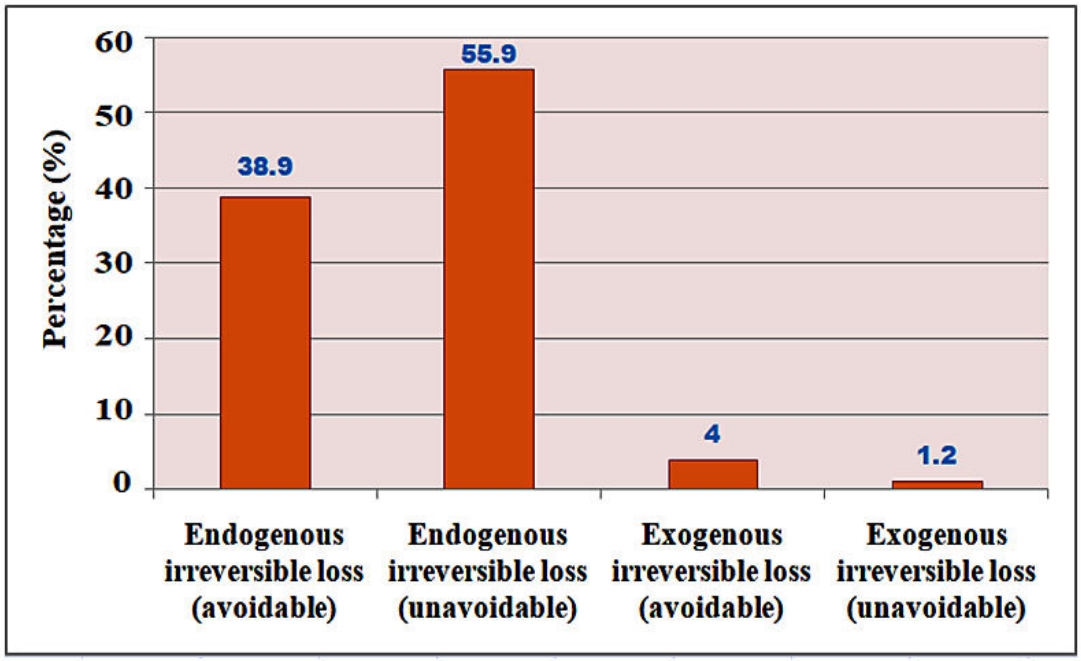

Figure 6.11 Endogenous and exogenous percentage irreversibility loss of DMS system

According to Table 6.8, compressor-1 accounts for a significant 34.76% of the overall rate of irreversibility, and the value of CSB for the same is 1.09. In light of the advanced analysis, just 0.5% of the total 34.8% are of an exogenous character, while the remaining 34.3% are of endogenous nature (which is based on the selection of equipment and their design). Additionally, 24% of compressor-1's irreversibility (which is primarily endogenous) can be avoided by increasing isentropic efficiency.

Evaporator and condenser-1 roughly contribute 20% of the DMS system's overall irreversibility. The evaporator's performance is unaffected by the performance of other parts of the system since its exogenous irreversibility is zero. As a result, by increasing the effectiveness of its parameter, just 6.2% of the overall irreversibility rate may be avoided out of 20.5%. By contrast, raising the efficiency parameter of condenser-1 can only avoid 7.5% of its overall irreversibility rate.

Table 6.8 provides a full breakdown of the components for irreversible loss in terms of endogenous and exogenous. Additionally, the Sankey diagram, which is depicted in Figure 6.12, is used to further describe the situation more systematically using values upto 1 decimal point.

Table 6.8 Results of the DMS-VCR system's advanced exergy analysis

S. No	System components	Endogenous loss of irreversibility (kW)		Exogenous loss of irreversibility (kW)		Overall irreversibility of the components (kW)
		Avoidable	Unavoidable	Avoidable	Unavoidable	
1.	Evaporator	0.84	1.94	0	0	2.78
2.	Condenser-1	0.70	1.93	0.31	0.12	3.06
3.	Condenser-2	0.11	0.27	0.03	0.01	0.42
4.	Compressor-1	3.24	1.39	0.04	0.02	4.69
5.	Compressor-2	0.14	0.09	0.09	0.01	0.33
6.	Expansion valve-1	0	1.41	0	0	1.41
7.	Expansion valve-2	0	0.12	0.06	0.01	0.19
8.	Subcooler	0.22	0.38	0.01	0.00	0.61
Total irreversibility rate of DMS system		5.25	7.53	0.54	0.17	**13.49**

Out of the 2.5% irreversibility in the case of compressor-2, 1.8% is endogenous in nature, and the remaining 0.7% is exogenous. Additionally, by using more effective methods, 1.8% of the overall irreversibility rate can indeed be avoided. The respective percentages of expansion valves-1 and 2's overall irreversibility are 10.4% and 1.4%. The rate of irreversibility for expansion valve-1 is entirely unavoidable since it is endogenous; however, for expansion valve-2, out of 1.4%, 0.4% may be avoided (by enhancing the system component) because it is exogenous.

According to Table 6.8, the subcooler section's 4.5% contribution to the overall irreversibility rate is primarily endogenous in nature. The performance of this component can be enhanced by changing the design, which essentially expands the heat transfer area. 4.5% of the subcooler's irreversibility rate is endogenous in nature, out of which 1.7% can be avoided by enhancing component design.

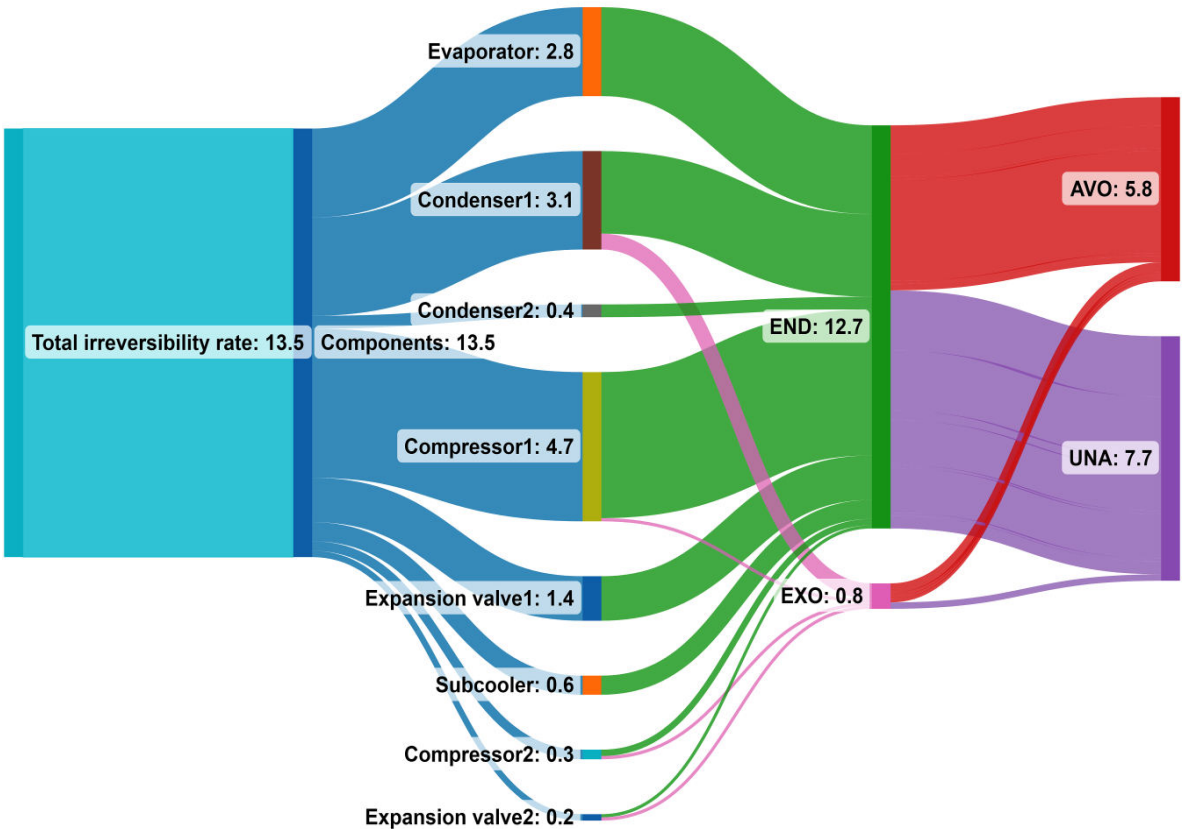

Figure 6.12 Sankey graphic displaying the findings of an advanced exergy study

6.8 CONCLUSIONS

The present work reports improvement in the performance of VCR system with the help of DMS configuration followed by coefficient of structural bond and advanced exergy analysis. When compared to VCR system, the DMS system's compressors require 7.6% less work input, which results in an 8.2% gain in COP. The results of the exergetic analysis also reveal that the DMS system's overall irreversibility rate is 11% lesser than the VCR system. Further, the parametric study of DMS-VCR system recommends low condenser, high evaporator temperature with low degree of overlap for better thermodynamics performance of the system. Additionally, the CSB and AEA methods for system optimization are used to further investigate the performance of DMS-VCR system from an exergy perspective. Compressor-2, compressor-1, condenser-2, subcooler, evaporator and condenser-1 all had CSB values of 1.06, 1.09, 1.74, 1.83, 2.03, and 2.08, respectively. Condenser-1 has the highest CSB value (2.08), but its overall contribution to the irreversibility rate is just 22.7%. In contrast, compressor-1 demonstrated a high irreversibility rate (34.8%), but with a lower CSB value of 1.09. Therefore, the AEA approach is utilized to calculate the system's potential performance. Out of the overall irreversibility of the DMS-VCR system, the AEA technique

reveals that 94.8% is endogenic in nature (Intrinsically) and 5.3% is exogenous in nature (due to other system components), out of which 42.9% of irreversibility can be avoided subject to increase in the system's component's parameter efficiency.

By improving the parameter efficiency of the system's component, the expansion valve-1's avoidable irreversibility rate is zero. The descending order of the avoidable irreversibility rate of other DMS-VCR system's part is as follows: compressor-1, condenser-1, evaporator, compressor-2, subcooler, condenser-2, and expansion valve-2, with respective values of 24.3%, 7.5%, 6.2%, 1.8%, 1.7%, 1%, and 0.5%, respectively. Therefore, by raising these component's performance parameters, it is possible to reduce their irreversibility and thus improve the DMS-VCR system's performance. As a result, DMS-VCR system emerges as a more potential energy-efficient cooling solution that promotes sustainability and energy conservation because of less power consumption. Moreover, the above trends in results will help the designer to design a thermodynamically impeccable VCR system with dedicated subcooling.

CHAPTER 7

DESIGN AND DEVELOPMENT OF EXPERIMENTAL TEST RIG OF DEDICATED MECHANICAL SUBCOOLED VAPOR COMPRESSION REFRIGERATION SYSTEM

This chapter discusses the working of test facility of dedicated mechanical subcooled vapor compression refrigeration setup along with its design, development, fabrication and its trouble shooting during operation.

7.1 INTRODUCTION

The continuous advancement of refrigeration and air conditioning technologies plays a pivotal role in meeting the increasing demand for energy-efficient and environmentally friendly solutions. This exploration focuses on the design and development of an experimental setup modified for a dedicated mechanical subcooled vapor compression refrigeration system. This innovation holds great promise in enhancing overall efficiency, sustainability, and adaptability of refrigeration systems.

Refrigeration systems, particularly vapor compression systems, are integral to various industries, providing crucial services such as food preservation, medical storage, and climate control. The traditional vapor compression systems, while effective, face challenges related to efficiency, capacity modulation, and environmental impact. Subcooling, the process of lowering the refrigerant temperature below its saturation point emerges as a solution to address these challenges and improve system performance. This enhancement is particularly crucial in regions with high ambient temperatures, where conventional systems may struggle to meet the cooling demands. Additionally, subcooling allows for better control over the refrigeration cycle, resulting in a more responsive and adaptable system. The significance of dedicated mechanical subcooled vapor compression refrigeration systems lies in their potential to revolutionize the industry by providing a sustainable and energy-efficient alternative. As global concerns about climate change and energy consumption rise, researchers and engineers are compelled to explore innovative solutions that strike a balance between performance and environmental responsibility.

The primary objectives of designing and developing the experimental setup are rooted in addressing key challenges and advancing the understanding of subcooled vapor compression refrigeration systems. The goals include improving efficiency, exploring enhanced capacity modulation, assessing environmental impact, optimizing system components, and ensuring

long-term reliability. Efficiency improvement is a central focus, aiming to quantify the impact of subcooling on energy consumption and coefficient of performance (COP). Additionally, the setup aims to explore the potential for improved capacity modulation, allowing the system to adapt seamlessly to varying cooling loads. Environmental impact assessment is crucial, aligning with global sustainability goals by examining the reduction in greenhouse gas emissions and overall carbon footprint. Component optimization focuses on refining individual elements within the system to maximize the benefits of subcooling, while reliability and durability assessments ensure the practical feasibility of subcooled vapor compression systems in real-world applications.

Several notable studies have laid the groundwork for experimental investigations in the area of refrigeration systems. These studies provide valuable insights that inform and support the experimental work undertaken in this study, serving as essential references in understanding the underlying principles and potential outcomes. Qureshi et al. [24] conducted experiments to demonstrate the effectiveness of the dedicated subcooling cycle concept and investigated how the efficacy of the DMS-VCR system is affected by considering different combinations of various refrigerants. They also reported that subcooling R22 refrigerant by 5°C-8°C in the VCR cycle led to a 0.5 kW increase in the load-bearing capacity of the evaporator. Andres et al. [89] focused on enhancing the performance of transcritical CO_2 plants through subcooling systems, notably the Dedicated Mechanical Subcooling system (DMS). An experimental study on a transcritical CO_2 plant utilizing an R-152a DMS reveals optimized operational conditions for varying ambient and cold sink temperatures. Measured values indicate increased cooling capacity and COP, with proposed correlations aiding in determining optimal pressure and subcooling degree based on gas-cooler outlet temperature and evaporation level. Sumeru et al. [90] experimentally evaluated that dedicated subcooling (DS) is an effective method for significantly improving air conditioning (A/C) system performance. However, the economic viability of DS depends on the capacity ratio between the subcooler and the main A/C system (RSM). This study experimentally investigates the A/C system's performance with DS at smaller RSM, emphasizing the economic advantages. The experiments were conducted under constant outdoor, evaporation, and condensation temperatures. Results revealed that DS lowered the condenser outlet temperature, increasing the degree of subcooling and subsequently enhancing the cooling capacity of the main system by 1.4 kW. The system's input power decreased, leading to a 7.8% improvement in the coefficient of performance (COP). The economic analysis suggests that the system with DS is economically viable, with a short payback period of just 11.81 months. Domenech et al. [27]

explored the potential enhancement of CO_2 refrigeration systems through zeotropic blends in dedicated mechanical subcooling systems, aligning evaporating temperatures with CO_2 profiles. Theoretical analysis identifies optimal compositions of R-600, R-32, and CO_2 with R-152a, corroborated by experimental testing under varying heat rejection temperatures. Results show a 1.4% increase in COP, emphasizing the role of zeotropic mixtures in reducing cycle irreversibilities and enhancing thermal parameters of the subcooler, aligning with prior theoretical findings. Kilicarslan [91] did experimental and theoretical analysis of a two-stage vapor compression cascade refrigeration system employing R-134a. Performance evaluations of single-stage and cascade systems reveal that water flow rate variations have minimal impact on COP, which is primarily dependent on evaporator temperature and pressure. A comparison between single-stage and cascade systems indicates significant improvements in condensing pressure reduction, compressor power decrease, and COP increase, emphasizing the benefits of cascade configurations under similar refrigeration loads. Ozsipahi et al. [92] explored R290/R600a refrigerant mixtures' impact on variable speed hermetic compressors in household refrigeration. They analyzed four compositions of R290/R600a blends, comparing them to baseline R600a to assess COP, refrigerant mass flow rate, and power consumption. Their findings indicate higher R290 content boosts COP despite increasing power consumption, with an optimal compressor speed around 2100 rpm. The COP of R290/R600a mixtures surpasses R600a by 10–20%, suggesting their potential for enhancing energy efficiency in refrigeration systems. Kim and Kim [93] investigated auto-cascade refrigeration with R744/134a and R744/290 mixtures, noting the system's pressure control advantage. Tests vary secondary fluid temperatures, revealing higher R744 composition enhances cooling capacity but reduces COP while increasing system pressure. Xuan and Chen [94] introduced a ternary near-azeotropic mixture featuring HFC-161 as a potential alternative refrigerant to R502, with similar physical characteristics and environmentally friendly performance. Experimental tests on a vapor compression refrigeration system designed for R404A reveal comparable pressure ratios to R404A and favorable COP under varying conditions. Results suggest this new refrigerant could serve as a promising retrofit option for R502 without requiring modifications to system components. Niu and Zhang [95] presented a new binary mixture of R744 and R290 as a natural refrigerant substitute for R13, with eco-friendly attributes. Experimental tests on a modified cascade refrigeration system show higher COP and refrigeration capacity compared to R13. However, the binary mixture also exhibits increased pressure and temperature parameters. Overall, it is considered a promising alternative for evaporator temperatures above 201 K. Venkataramanamurthy and Kumar [96]

compared the energy and exergy flow, as well as second law efficiency, of R22 and its substitute R436b in vapor compression refrigeration cycles. They aim to identify areas of significant energy and exergy losses and assess the effect of different environmental conditions. Results show comparisons of exergy flow, efficiency, and losses at various points in both cycles. Esbri et al. [97] investigated the energy performance of a vapor compression system using R1234yf as a drop-in replacement for R134a. Experimental tests with vary operating conditions, showing a 9% lower cooling capacity and 19% lower COP with R1234yf compared to R134a. However, the use of an internal heat exchanger helps reduce these differences in energy performance. Chesi et al. [98] explored cycle modifications for R744 refrigeration applications, focusing on the parallel compression cycle in flash tank configuration. Through experiments and thermodynamic analysis, critical parameters influencing performance are identified. While theoretical improvements in refrigerating capacity and coefficient of performance are achievable. Yan et al. [99] introduced an energy-saving cooling system that combines a traditional vapor compression cycle with a pumped liquid two-phase cooling cycle, operating in two modes: compression cycle and pump cycle. Experimental evaluation demonstrates higher Energy Efficiency Ratio (EER) compared to traditional compressor systems, particularly at lower ambient temperatures. Analysis suggests an optimal shift temperature of around -5°C for improved EER and cooling capacity. Gill and Singh [100] investigated using a mixture of R134a and LPG (28:72) as an alternative to R134a in a vapor compression refrigeration system. Experimental comparisons show lower power consumption, discharge temperature, and pull-down time with R134a/LPG (28:72), along with higher refrigeration capacity and COP. Their findings suggest the potential of R134a/LPG (28:72) as a long-term replacement for R134a due to its environmentally friendly properties and improved refrigeration performance. Anand and Tyagi [101] investigated extensive experimental examination of a 2TR vapor compression refrigeration cycle, focusing on varying refrigerant charge percentages through exergy analysis. Using a test rig with R22, the study assesses coefficient of performance, exergy destruction, and exergetic efficiency under different operating conditions. Their findings indicates that a 2TR window air conditioner reveal notable losses in the compressor, while losses in the condenser are comparatively lower than those in the evaporator and expansion device. Exergy destruction is highest at 100% refrigerant charge and lowest at 25%.

The integration of mechanical subcooling loop in simple vapor compression refrigeration systems presents its own set of challenges that cannot be overlooked. Refrigerant selection, heat exchanger design, control strategies, system modeling, and experimental validation

present complex considerations. Addressing these challenges is vital for the successful design and implementation of subcooled systems. Refrigerant selection involves balancing thermodynamic properties, environmental impact, and component compatibility. Heat exchanger design requires careful consideration to facilitate efficient heat transfer while minimizing pressure drops. Control strategies must be intelligent and adaptive, guiding the system through dynamic operating conditions. Accurate system modeling is crucial for predicting performance, and experimental validation ensures real-world applicability.

The contributions of the experimental setup include enhanced efficiency, improved cooling capacity, sustainability, practical insights for industry stakeholders, and academic advancement. The research strives to offer valuable insights that can shape the future of refrigeration technology, providing a foundation for further exploration and innovation. So, the design and development of an experimental setup for a dedicated mechanical subcooled vapor compression refrigeration system represent a commitment to advancing technology for a more sustainable and energy-efficient future.

7.2 SYSTEM DESCRIPTION AND WORKING

Dedicated mechanical subcooling is an established method employed to enhance the coefficient of performance (COP) of a system by integrating a subcooler with conventional vapor compression refrigeration systems. This technique involves the interconnection of two distinct cycles, forming a loop configuration with the aid of a subcooler. The key components essential for dedicated mechanical subcooled vapor compression refrigeration system include two condensers, two compressors, two expansion valves, an evaporator, and a sub-cooler. The selection of refrigerants is conditional depending upon the desired output and performance conditions.

This experimental test setup comprises two cycles: the primary cycle at the bottom, serving as the main cycle, and the secondary cycle at the top, functioning as the dedicated subcooler cycle. Here, the bottom cycle circulates R410A refrigerant, while the top cycle circulates R134a refrigerant. The components of the dedicated mechanical subcooled vapor compression refrigeration system test-rig are illustrated in the Figure 7.1. State points (see Table 7.1), indicating the inlet and outlet condition of system components, these points, depicted in the block diagram of vapor compression refrigeration system with dedicated mechanical subcooling, play a crucial role in calculations. The pressure enthalpy (P-h) diagram of the related system is illustrated in Figure 7.2.

Table 7.1 State points of the DMS-VCR system

State Point	Position
1.	Inlet of compressor of the main cycle
2.	Outlet of compressor of the main cycle
3.	Inlet of condenser of the main cycle
4.	Outlet of condenser of the main cycle
5.	Inlet of sub-cooler in the main cycle
6.	Outlet of sub-cooler in the main cycle
7.	Inlet of evaporator of the main cycle
8.	Outlet of evaporator of the main cycle
9.	Inlet of water for condenser of the main cycle
10.	Outlet of water for condenser of the main cycle
11.	Inlet of water for evaporator of the main cycle
12.	Outlet of water for evaporator of the main cycle
1'.	Inlet of compressor of the sub-cooler cycle
2'.	Outlet of compressor of the sub-cooler cycle
3'.	Inlet of condenser of the sub-cooler cycle
4'.	Outlet of condenser of the sub-cooler cycle
5'.	Inlet of sub-cooler in the sub-cooler cycle
6'.	Outlet of sub-cooler in the sub-cooler cycle
7'.	Inlet of air for condenser of the sub-cooler cycle
8'.	Outlet of air for condenser of the sub-cooler cycle

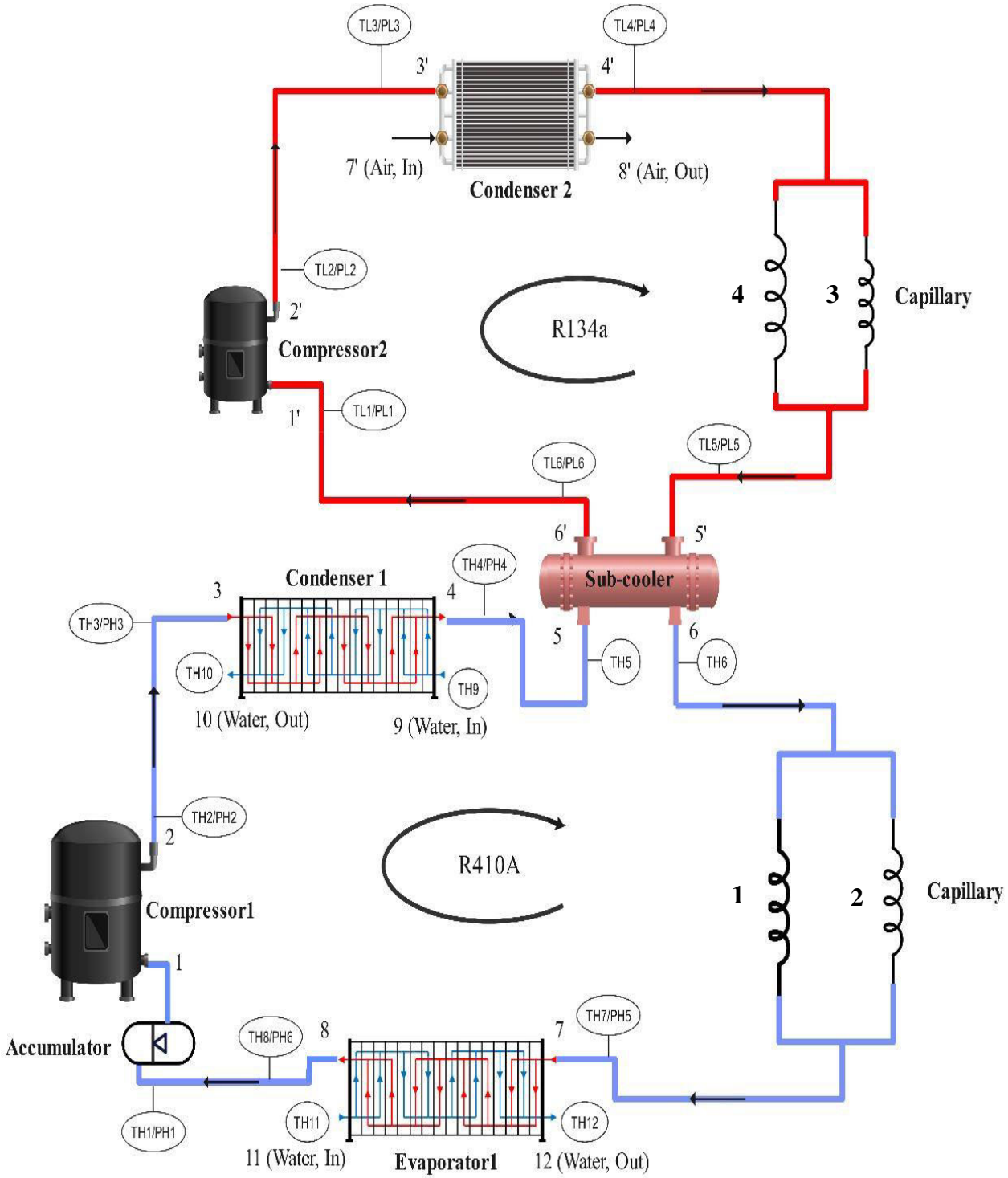

Figure 7.1 Block diagram of VCR system with dedicated mechanical subcooling

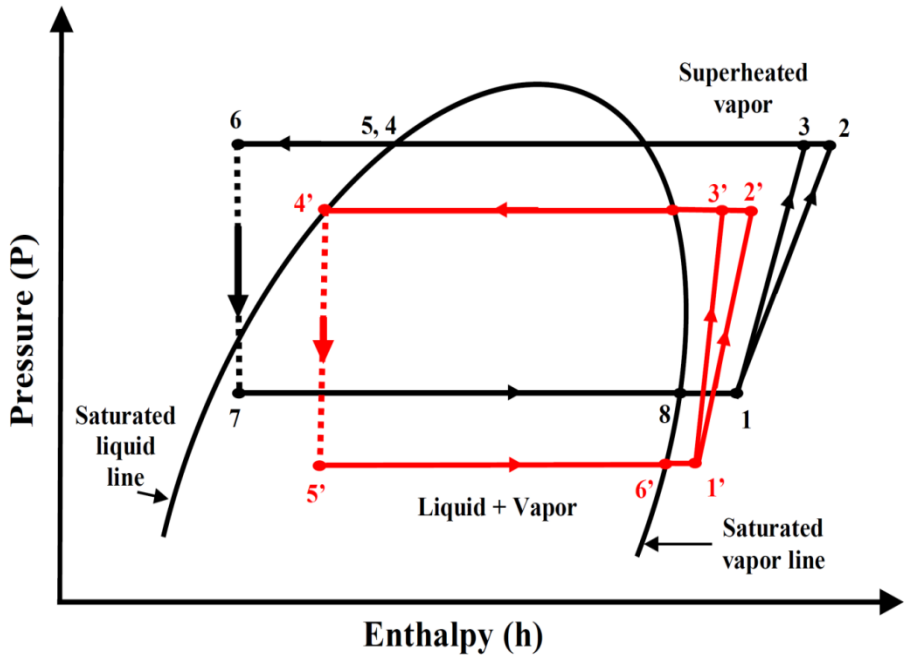

Figure 7.2 Pressure – Enthalpy (P-h) diagram of DMS-VCR cycle

Water is used to release heat to the refrigerant in the evaporator-1, and to facilitate the flow of water through the evaporator, an evaporator pump is used. At the bottom, an evaporator tank is used to store low temperature water. After the evaporator section, refrigerant (R410A) flows into the main cycle compressor which has a capacity of 2TR. The compressor increases the temperature and pressure of the refrigerant which then flows into the water cooled condenser through the discharge line. To circulate water through the condenser for absorbing heat from the refrigerant, a condenser pump is used, and a condenser tank is used to store the water that flows through the main cycle condenser-1.

After rejecting heat in the condenser-1, refrigerant (R410A) passes through a subcooler where it is subcooled 5°C to 7°C below the liquid line. To remove any moisture, the refrigerant flows through a drier, and a sight glass is placed to ensure that the refrigerant is in a liquid state. The refrigerant then flows through an expansion valve in the bottom cycle, where its temperature and pressure are reduced, and then it flows into the evaporator of the main cycle to absorb heat from the water.

The temperature and pressure at the inlet and outlet of different components in the bottom cycle are measured using 12 RTD type PT-100 thermocouples and 6 pressure transducers, respectively. This enables accurate temperature and pressure measurements throughout the bottom cycle. In addition to the bottom cycle, there is a dedicated subcooler in this experimental test rig, which acts as an evaporator for the top cycle. The refrigerant (R134a)

flows through the top cycle and absorbs heat from the refrigerant (R410A) in the bottom cycle, a process known as subcooling. After passing through the subcooler, refrigerant (R134a) flows into the top cycle compressor, which has a capacity of 1/6TR. The compressor increases the temperature and pressure of the refrigerant before it flows into the air-cooled condenser-2, where refrigerant (R134a) rejects heat to the atmosphere. To remove any moisture from the refrigerant, it flows through a drier, and a sight glass is used to ensure that the refrigerant is in a liquid state. The refrigerant then flows through the expansion valve of the top cycle, where its temperature and pressure are reduced, and then it flows through the subcooler to absorb heat from the refrigerant (R410A) in the bottom cycle. Temperature and pressure at the inlet and outlet of different components in the top cycle are measured using 6 RTD type PT-100 thermocouples and 6 pressure transducers, respectively. This enables accurate temperature and pressure measurements throughout the top cycle (see Figure 7.1 and Figure 7.3). Detailed information regarding the components used in the test rig is provided in Table 7.2, while specific details about temperature sensors for 2TR (R410A) and 1/6TR (R134a) are outlined in Tables 7.3 and 7.4, respectively. Additionally, pressure transducer details for both refrigerants are presented in Tables 7.5 and 7.6 for 2TR (R410A) and 1/6TR (R134a), respectively.

Table 7.2 List of components used in DMS-VCR system test-rig

1. Evaporator (PHE)	2. Accumulator	3. Compressor 2TR
4. Condenser (PHE)	5. Sight Glass (R410A)	6. Sub-Cooler
7. Dryer (R410A)	8. Capillary (R410A)	9. Compressor 1/6TR
10. Condenser (Air-cooled)	11. Sight glass (R134a)	12. Dryer (R134a)
13. Capillary (R134a)	14. Evaporator Pump	15. By pass control valve (Evap.)
16. Evaporator Water flow meter	17. Evaporator water tank	18. Condenser Pump
19. By pass control valve (Cond.)	20. Condenser water flow meter	21. Radiator
22. Condenser water tank	23. Refrigerant flow meter (R410)	24. Refrigerant flow meter (R134a)
25. Pressure Gauge 2TR (Low)	26. Pressure Gauge 2TR (High)	27. Pressure Gauge 1/6TR (Low)
28. Pressure Gauge 1/6TR (High)	29. Overload protection switch	

Table 7.3 Temperature sensor details of 2 TR (R410A) system

TH1 - Comp. suction temp.	TH2- Comp. delivery temp.	TH3 - Cond. inlet temp.
TH4 – Cond. Outlet temp.	TH5 – Sub-cooler inlet temp.	TH6 – Sub-cooler outlet temp.
TH7 – Evap. Inlet temp.	TH8 – Evap. Outlet temp.	TH9 – Cond. Water inlet temp.
TH10 – Cond. Water outlet temp.	TH11 – Evap. water inlet temp.	TH12 – Evap. Water outlet temp.

Table 7.4 Temperature sensors details of 1/6 TR (R134a) system

TL1 - Comp. suction temp.	TL2- Comp. delivery temp.	TL3 - Cond. inlet temp.
TL4 – Cond. Outlet temp.	TL5 – Evap./subcooler inlet temp.	TL6 – Evap./subcooler outlet temp.

Table 7.5 Pressure transducer details of 2 TR (R410A) system

PH1 - Comp. suction Pressure	PH2- Comp. delivery Pressure	PH3 - Cond. inlet Pressure
PH4 – Cond. Outlet pressure	PH5 – Evaporator inlet pressure	PH6 – Evaporator outlet pressure

Table 7.6 Pressure transducer details of 1/6 TR (R134a) system

PL1 - Comp. suction Pressure	PL2- Comp. delivery Pressure	PL3 - Cond. inlet Pressure
PL4 - Cond. Outlet pressure	PL5-Evap./subcooler inlet pressure	PL6-Evap./subcooler outlet pressure

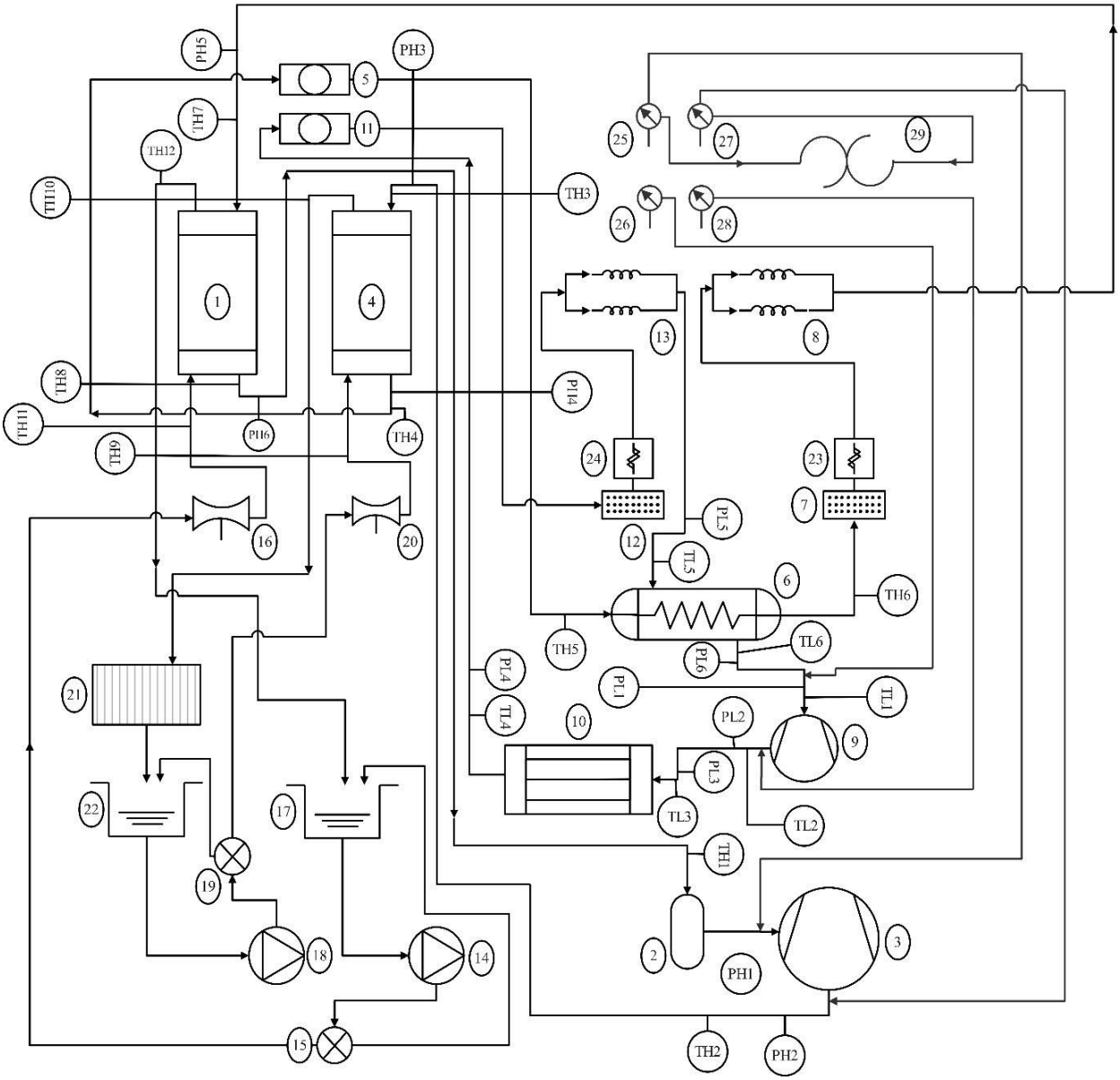

Figure 7.3 Line diagram of experiment test-rig of DMS-VCR system

The Figure 7.4 depicts the actual system of a dedicated mechanical subcooled vapor compression refrigeration system, showcasing the various components involved in its operation. Each component plays a crucial role in the refrigeration process, contributing to the overall performance and functionality of the system.

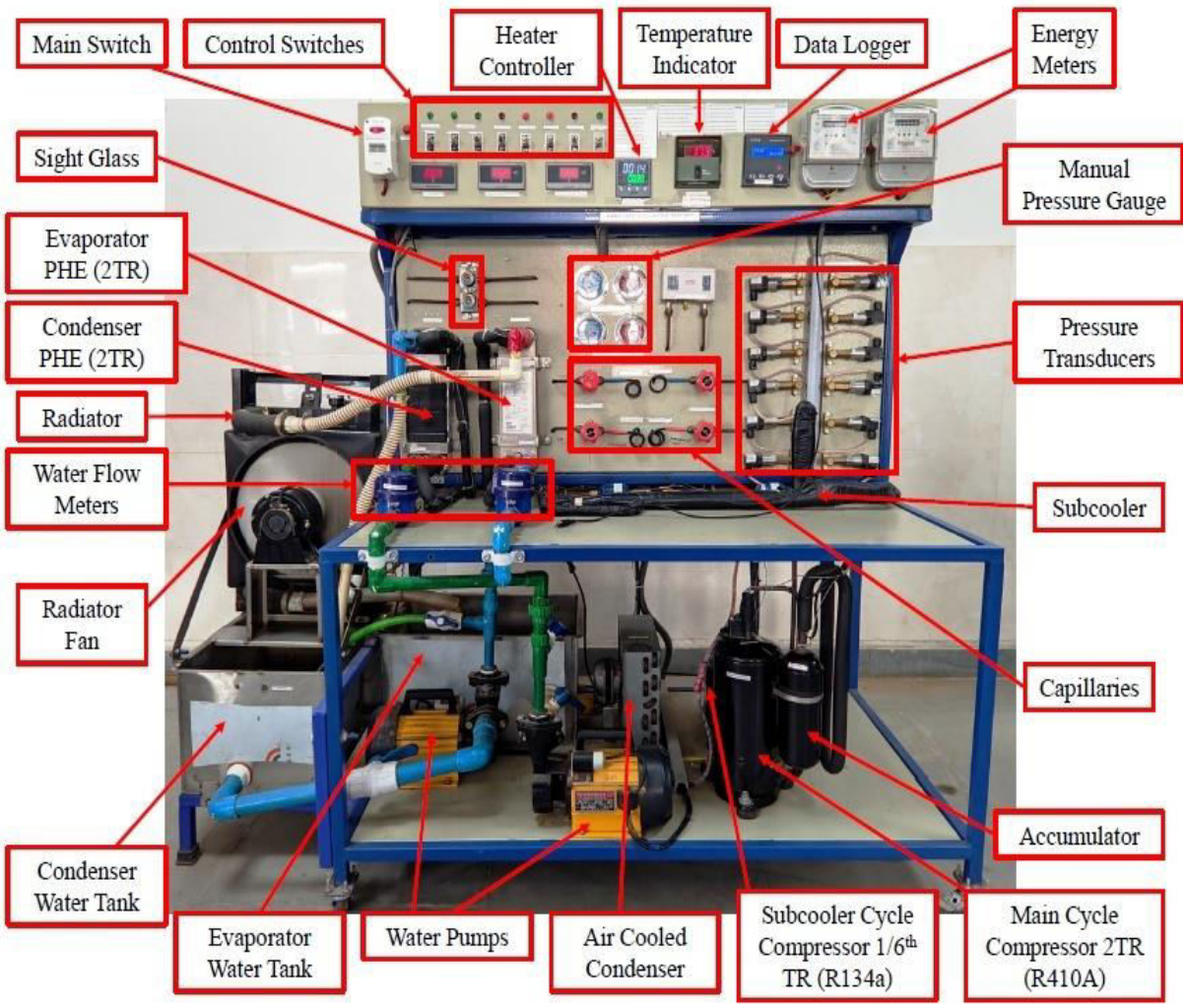

Figure 7.4 Components of DMS-VCR system test rig

The specifications of major and instrumentation components outlined in Table 7.7 provide essential details crucial for understanding the construction and operation of the refrigeration system. These specifications detail the dimensions, materials, and operational characteristics essential for the effective functioning of the refrigeration system.

Table 7.7 Specifications of major and instrumentation components of DMS-VCR system

S. No.	Item Name With Specifications
	MAJOR COMPONENTS
1	**Tank** SS 304 grade 1.2mm thick 350 x 450 x 300 mm size
2	**Electric Heater** Immersion type 32mm OD thread type, 2kW, 230volts AC
3	**Condenser and Fan** Condenser 11" x 10" x 2 row horizontal flow type Tube size 9.6mm OD and 6.9 mm ID Fan size 9 inch diameter Motor : 230volts AC, 0.20 amps, 28watt, foot mount type water cooled 2TR (PHE)/ Air cooled 1/6 TR
4	**Evaporator** PHE, water cooled 2TR
5	**Compressor** 2TR Reciprocating compressor (Main) 1/6TR Reciprocating compressor (Sub-cooler), Least count = 0.01kW
6	**Capillary** For R134a two size, Ø 0.36 x 8 feet and Ø 0.36 x 12 feet length For R410A two size, Ø 0.70 x 510mm and Ø 0.60 x 510mm
7	**Sub cooler** Pipe in pipe type Outer tube diameter Ø 22.4mm OD and Ø 19.6mm ID Inner tube diameter Ø 12.4mm OD and Ø 9.6mm ID Length of subcooler is 630mm
	INSTRUMENTATION COMPONENTS
1	**Pressure sensor** $1/4^{th}$ thread, 24volts DC input, 4-20ma output, range 0- 25bar of 8 numbers and 0- 40 bar of 4 numbers, Least Count = 0.001 bar.
2	**Temperature sensor** 4 x 70 mm tube, RTD TYPE PT-100, 3 Core wire length 3 meter , range -50 to 199.9 Degree Celsius, Least count = 0.1K
3	**Refrigerant mass flow sensor** $1/4^{th}$ BSW thread, 5 volts DC input, 0-5 mv output, ultrasonic base frequency counter type liquid flow sensor, Least count = 0.001 LPM

7.3 PERFORMANCE INDICATOR

The experimental COP is defined as the energy conversion efficiency in the system; the net COP is the ratio of total heat transfer from the evaporator section to the total work consume by the compressors. The Equation (7.1) shows the formula for net COP (COP_{net}) is given as:

$$COP_{net} = \frac{\dot{Q}_{evap}}{\dot{W}_{comp1} + \dot{W}_{comp2}} \quad (7.1)$$

where,

$$\dot{Q}_{evap} = (\dot{m}_{water} * C_p)_{evap}(T_{11} - T_{12}) \quad (7.2)$$

where,$\dot{W}_{comp1}$ and $\dot{W}_{comp2}$, can be directly calculated from the energy meter.

7.4 TROUBLESHOOTING IN SYSTEM OPERATION

The initial steps in troubleshooting the test-rig involved powering up the main supply switch and subsequently starting the system by pressing the 'ON' button of the panel. This triggered the flow of electricity within the system, evident from the illuminated switch and the displayed readings. Furthermore, the data logger switch was also activated, facilitating the initiation of the data acquisition system for recording readings.

To initiate the water flow, the switches were employed to activate the evaporator and condenser pumps. The commencement of the refrigerant flow in the lower cycle involved starting the compressor of the bottom cycle, initiating the cooling process for the water in the evaporator tank. Readings for various parameters of the lower cycle were recorded before initiating the compressor of the upper cycle. This action led to the subcooling of the refrigerant in the sub-cooler, positioned after the water cooled condenser of the lower cycle.

However, an unexpected issue arose over time, with ice formation observed in the evaporator tank and the water in the condenser tank becoming overheated, contrary to expected results. To address this problem, modifications were implemented on the test-rig, including:

1. Installation of a heater inside the evaporator tank to sustain the water temperature above a specified level, preventing the formation of ice. The heater's temperature can be regulated using a heater controller.
2. Swapping the water exit pipes of the evaporator and condenser. This ensures that hot water, having absorbed heat in the condenser, enters the evaporator tank, while cooled water from the evaporator enters the condenser tank. This prevents overheating in the condenser tank and the occurrence of ice formation in the evaporator tank. These modifications were made to resolve the issues observed in the test-rig, ensuring

smooth operation without overcooling or ice formation in the evaporator tank, and overheating of water in the condenser tank.

During the initial experimental testing of the test rig, it was noted that the sub-cooler, measuring 250 mm in length, generated only a subcooling of 3°C. This observation raised concerns as it contributed to a lower coefficient of performance (COP) compared to the simple VCR system. To address this, a troubleshooting process was initiated to pinpoint the underlying cause. After a detailed analysis, it was determined that the sub-cooler's length was insufficient to achieve the desired level of subcooling. To solution this, the sub-cooler's length was increased to 630 mm. Following this adjustment, the test rig was reoperated, yielding promising results. The sub-cooling produced by the sub-cooler significantly rose to 7°C to 8°C, resulting in a notable enhancement in the overall COP of the system. Through the systematic implementation of the troubleshooting process, the issue was successfully identified and resolved. The modification to the sub-cooler's length has notably improved the performance of the test rig.

7.5 RESULTS AND DISCUSSION

Before experimental investigation of vapor compression refrigeration system with dedicated mechanical subcooling, theoretical investigation is done in Chapters 3, 4, 5 and 6, in which it was observed and verified that performance of VCR system improves when dedicated mechanical subcooling is used with VCR system. A parametric study has also been conducted for the system in which it is observed that performance of system increases when evaporator temperature increases, condenser temperature decreases, degree of overlap is reasonable and degree of sub-cooling is as maximum as possible. In theoretical analysis optimization of system is also done based on the process parameters (see Table 3.1, Table 4.2, Table 5.2 and Table 6.4).

In experimental investigation of dedicated mechanical subcooled vapor compression refrigeration system, readings of the experimental setup are taken at different load on the evaporator and condenser of the main cycle by operating the capillaries in multiple combinations. To conduct the experiment, the evaporator and condenser loads are adjusted using varying water flow rates to regulate the cooling and heat extraction respectively. In addition, the load on either the evaporator or condenser is changed while keeping the other's flow rate as constant. This allowed for observing real changes and obtaining a better understanding of the flow rate conditions during the experiment.

The experimental configuration comprises four capillaries, specifically two for R410A (Capillary 1 & 2) and two for R134a (Capillary 3 & 4). These capillaries undergo testing through four distinct configurations, with two arranged in a cross formation and the other two positioned face to face, resulting in four pairs of capillaries (**Set-1:** Capillary 1 & 3, **Set-2:** Capillary 1 & 4, **Set-3:** Capillary 2 & 3, and **Set-4:** Capillary 2 & 4). When the test-rig operates on the first capillary pair, it is denoted as "Set-1," and so onward. Each set commences with the operation of the main cycle compressor for 20-30 minutes. Subsequently, the subcooler cycle is initiated and runs for an additional 20-30 minutes, operating with different capillary settings as specified earlier. Power consumption is monitored throughout the experiment using energy flow meters, and a total of four capillary configurations are tested.

The experimental analysis relies on various readings stored in the system through a data logger. These readings are retrieved using Prolog software, and thermophysical properties of the refrigerant and cooling fluid at different state points.

The main cycle utilizes **Capillary-1** (Diameter: 0.70 mm and Length: 510mm) and **Capillary-2** (Diameter: 0.60 and Length: 510mm), while the subcooler incorporates **Capillary-3** (Diameter: 0.36mm and Length: 2438.4 mm) and **Capillary-4** (Diameter: 0.36mm and Length: 3657.6 mm). Experimental results demonstrated that dedicated mechanical subcooling significantly improved the coefficient of performance (COP) of the vapor compression refrigeration system (VCRS). To achieve a maximum net COP, it was necessary to have high mass flow rates of refrigerant in the main cycle and low mass flow rates in the subcooler cycle. By increasing the subcooler length led to higher subcooling degrees, which enhance the overall performance of the system. Additionally, maintaining a high evaporator temperature and a low condenser temperature proved beneficial for system performance. It was observed that the compressor work of the subcooler cycle should be significantly lower than that of the main cycle to achieve a higher net COP. These findings emphasize the importance of effectively managing mass flow rates, optimizing subcooling levels, controlling temperature differentials, and selecting appropriate capillary combinations to attain superior refrigeration system performance. Implementing these strategies has the potential to enhance energy efficiency and overall system performance, contributing to the development of more sustainable cooling solutions.

To initiate an experiment on the test rig, the primary focus lies in establishing the desired mass flow rate of water for both the evaporator and condenser of the main cycle. This is accomplished by carefully adjusting the control valve and utilizing the by-pass valve as

necessary. By effectively regulating these valves, the appropriate mass flow rate can be achieved, thus setting the foundation for the experiment to proceed smoothly. Mass flow rate of water for evaporator is less which means a lesser amount of loads is given on evaporator. During all the experiments the mass flow rate of water at evaporator and condenser are kept at 3.48 LPM & 8.10 LPM, respectively.

7.5.1 Analysis of simple VCR system with DMS-VCR system for Set 1 & Set 2:

In the experimentation of a simple VCR system without a dedicated subcooling cycle, the system's performance was evaluated resulting a suction pressure of 9 bar and an inlet temperature of 13^{o}C. Notably, the system showed a clear decrease in the temperature of the external fluid, going from 35.2^{o}C to 13.9^{o}C. Further examination revealed a substantial cooling capacity of 5.17 kW and a compressor work input of 1.49 kW, calculated based on the energy meter and impulse counts. The achieved results highlighted a Coefficient of Performance (COP) of 3.46, emphasizing the system's performance. These findings provide valuable insights forming the basis for subsequent discussions.

For this combination of mass flow rate of water, two capillary set are used for observation of system’s performance. The results of capillary sets are given below.

Set - 1: Capillary 1 & 3

In the examination of the VCR system with a subcooler cycle (i.e. DMS-VCR system), focusing on Set-1 with Capillary 1 & 3, with a condenser temperature of 39.2°C and a pressure of 25.8 bar. The net Coefficient of Performance (COP) for this configuration is determined to be 3.69. This increased COP is due to higher refrigerating effect, measuring 5.99 kW, primarily resulting from a degree of subcooling (4.7°C), of the refrigerant after leaving the main cycle condenser-1. Additionally, the compressor work for the subcooler cycle was notably low, specifically by 0.13 kW. The detailed error analysis of the above results is given in Appendix A

Set – 2: Capillary 1 & 4

In testing the DMS VCR system with capillary 1 & 4 in Set-2, using a condenser temperature of 39°C and a pressure of 25.5 bar, the system showed a good performance with a net Coefficient of Performance (COP) of 3.54. This increase in COP results due to an improved refrigerating effect of 6.24 kW, mainly because the refrigerant is subcooled by 5.5°C after leaving the condenser-1. Further, the compressor work for the subcooler cycle is 0.18 kW. It's

worth noting that, in this set, increasing the length of the capillary from 8 to 12 feet led to a slightly decreased performance compared to Set-1 (see Figure 7.5 and Figure 7.6).

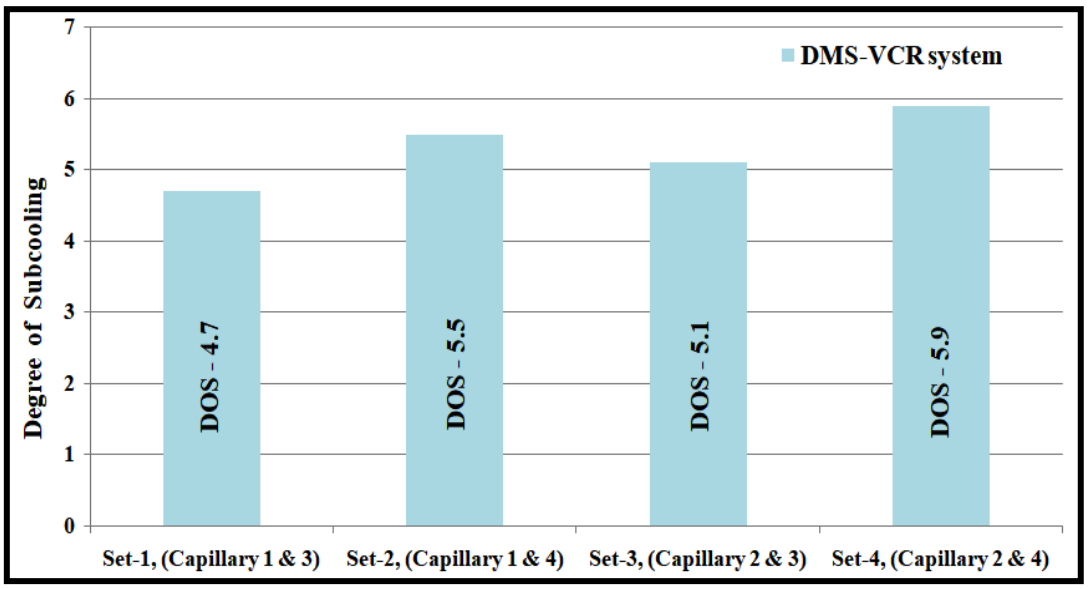

Figure 7.5 Degree of subcooling comparison for different combination of capillaries

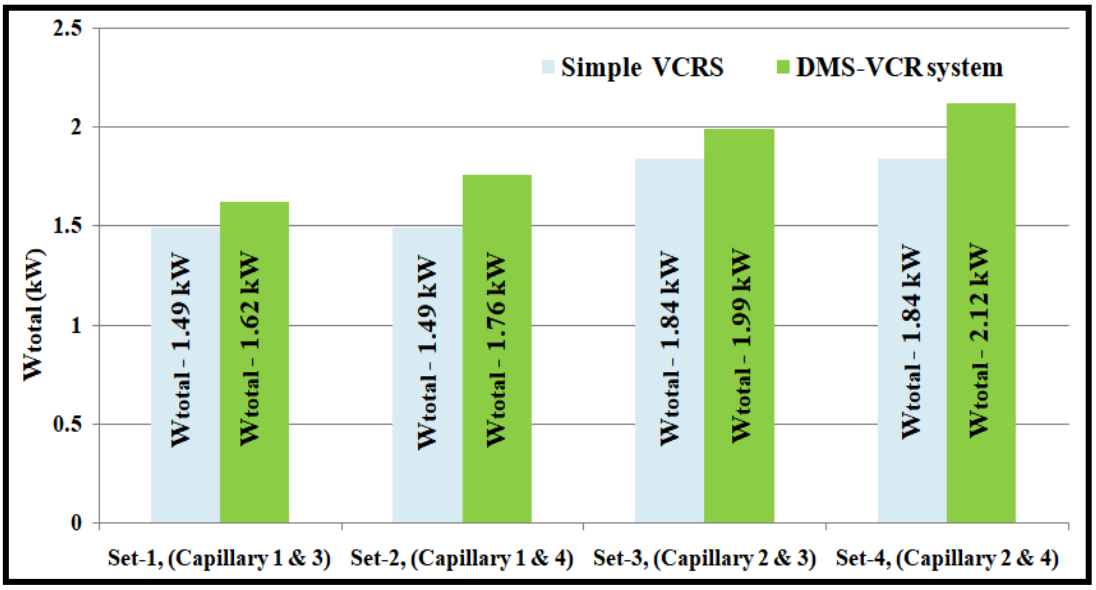

Figure 7.6 Power consumption comparison for different combination of capillaries

7.5.2 Analysis of simple VCR system with DMS-VCR system for Set 3 & Set 4:

In analyzing a simple VCR system without a dedicated subcooling cycle, that assessed its performance with capillary 2, for a suction pressure of 7.9 bar and an inlet temperature of 10.8°C. Notably, the system exhibited a noticeable decrease in the temperature of the external fluid, reducing from 35.1°C to 12.6°C. Further investigation shows a considerable cooling capacity of 5.46 kW and a compressor work input of 1.84 kW, computed using the energy

meter and impulse counts. The outcomes yield a Coefficient of Performance (COP) of 2.96, offering valuable insights for subsequent discussions on effect of decreased diameter of capillary tube. The results of two capillary Sets (Set 3 and Set 4) with same mass flow rates of water are given below.

Set - 3: Capillary 2 & 3

In Set-3, the DMS-VCR system is tested with capillary 2 & 3. With a condenser temperature of 40.6°C and a pressure of 24 bar, the system exhibits a net Coefficient of Performance (COP) of 3.10. This high COP is achieved through an enhanced refrigerating effect of 6.17 kW, accompanied by a subcooling degree of 5.1°C after leaving the condenser-1. Additionally, the compressor work for the subcooler cycle is measured as 0.15 kW. Notably, a decrease in the capillary diameter from 0.7 mm to 0.6 mm in this set led to a significant decrease in performance compared to sets 1 and 2.

Set - 4: Capillary 2 & Capillary 4

In Set-4, the results of DMS-VCR system with capillary 2 & 4, operating with a condenser temperature of 40.5°C and a pressure of 23.5 bar exhibits better performance, showcasing a net COP of 3.05. This enhanced COP, compared to the simple VCR system, is attributed to an improved refrigerating effect of 6.48 kW, primarily due to the refrigerant being subcooled by 5.9°C after leaving the condenser-1. Additionally, the compressor work for the subcooler cycle measured 0.20 kW. It's worth noting that in this set, increasing the capillary length from 8 to 12 feet and reducing the capillary diameter from 0.70 mm to 0.60 mm results in a decrease in performance compared to Set-1, Set-2, and Set-3 (see Figure 7.5 to Figure 7.8).

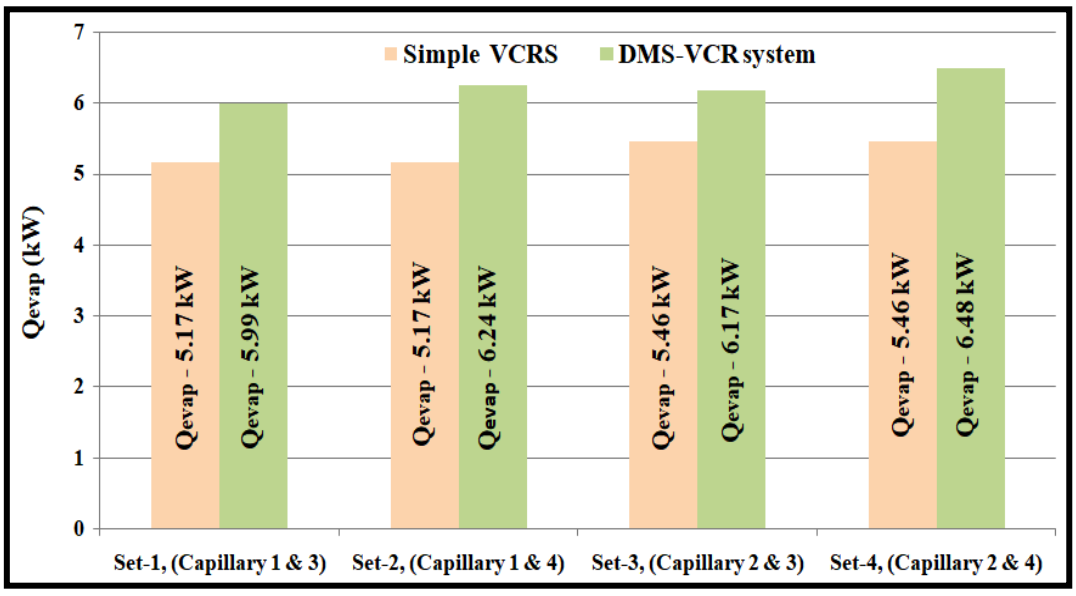

Figure 7.7 Cooling capacity comparison for different combination of capillaries

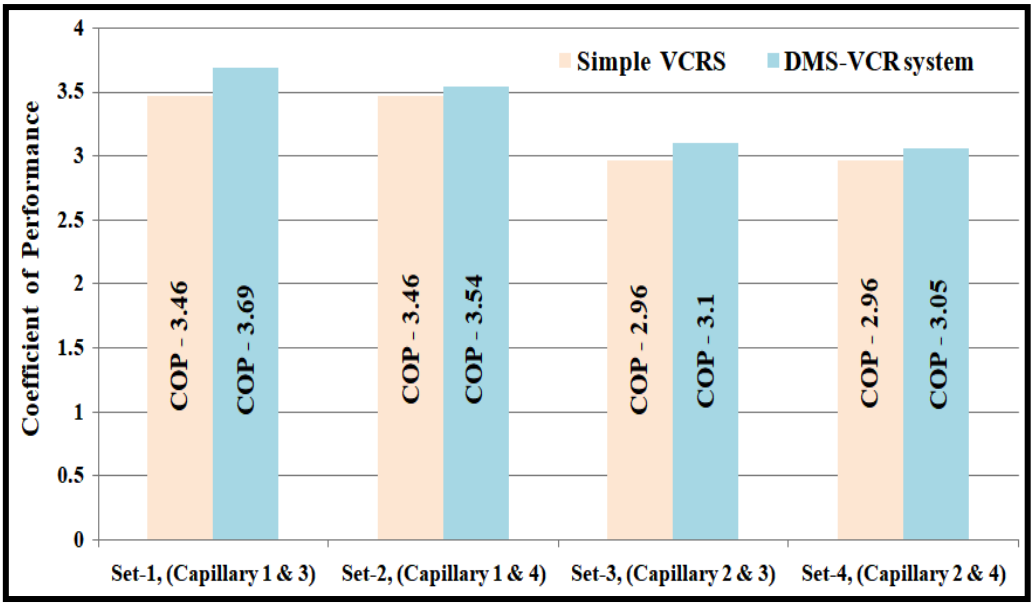

Figure 7.8 Coefficient of performance comparison for different combination of capillaries

In exploring the intricate dynamics within refrigeration systems, the Darcy-Weisbach equation is used to compute head loss due to friction in pipes, which relates head loss in a pipe to factors like diameter, velocity, and friction factor, changes in the diameter of the capillary tube in a refrigeration system have significant effects on system performance. As the diameter decreases, the flow area for the refrigerant reduces, resulting in an increase in flow velocity. According to the Darcy-Weisbach equation, the head loss due to friction is proportional to the square of the velocity. When that expression further modified it is noted that the head loss due to friction is inversely proportional to fifth power of the diameter of pipe. Consequently, a decrease in diameter leads to higher velocity, making the impact of head loss more significant. The same trend was observed in the experimental analysis. This increased head loss due to higher velocity, in conjunction with the decreased diameter, further contribute pressure drop in the capillary tube. This, in turn, requires the compressor to perform more work because of the increased pressure ratio across compressor, resulting in higher energy consumption. As a result, the overall performance of the refrigeration system is compromised, leading to a decrease in the Coefficient of Performance (COP).

7.6 CONCLUSIONS

The design and development of an experimental setup for a dedicated mechanical subcooled vapor compression refrigeration system represent a crucial attempt in the pursuit of energy-efficient and environmentally responsible refrigeration solutions. This comprehensive exploration has delved into the background, objectives, challenges, research methodology,

and expected contributions of the proposed experimental setup. As the refrigeration industry undergoes transformative changes driven by technological advancements and sustainability imperatives, the integration of subcooling mechanisms stands out as a promising possibility for improvement. Through systematic theoretical analysis, careful component design, and rigorous experimental testing, the research aims to provide valuable insights that can shape the future of refrigeration technology. By addressing challenges related to refrigerant selection, heat exchanger design, control strategies, and system modeling, the experimental setup strives to overcome obstacles that hinder the widespread adoption of subcooled vapor compression systems. The anticipated contributions in terms of performance improvement, enhanced cooling capacity, sustainability, and practical insights for industry stakeholders underscore the significance of this research in the broader context of refrigeration system. In conclusion, the journey of designing and developing an experimental setup for a dedicated mechanical subcooled vapor compression refrigeration system is not just a scientific pursuit; it is a commitment to advancing technology for a more sustainable and energy efficient future. The experimental analysis of the DMS-VCR system revealed that dedicated mechanical subcooling significantly improved the coefficient of performance (COP). Optimal performance was achieved with high mass flow rates in the main cycle and low rates in the subcooler cycle. Increasing subcooler length and maintaining specific temperature differentials further enhanced system efficiency. The study emphasizes the importance of managing mass flow rates and optimizing subcooling levels for superior refrigeration system performance, with potential benefits for energy efficiency and sustainable cooling solutions.

CHAPTER 8

OVERALL CONCLUSIONS AND RECOMMENDATIONS

8.1 MAJOR FINDINGS

The conclusion of this thesis represents a comprehensive exploration into vapor compression refrigeration systems, integrating theoretical insights with experimental investigations to advance the field. Through an extensive literature survey and a series of empirical studies, valuable insights have been gained regarding the energy and exergy performance, environmental impact, and economic feasibility of these systems.

Energy and Exergy Analysis:

1. Comparative analysis between DMS-VCR and VCR systems for water chiller applications revealed significant improvements with the former.
2. Optimal subcooling levels of 19°C for the DMS-VCR system led to an 11.67% increase in COP and a 10.45% reduction in compressor power consumption compared to the VCR system.
3. Exergy analysis demonstrated a 15.71% decrease in total irreversibility and a 10.38% increase in exergetic efficiency for the DMS-VCR system.
4. Parametric analysis highlighted the influence of evaporator and condenser temperatures on system performance, with optimal values identified at 1°C and 44°C, respectively.
5. Degree of overlap and degree of subcooling significantly influenced system performance, with modest overlap and a subcooling value of 19°C recommended for optimal performance.

Environment and Economic Analysis:

1. Environmental and economic assessments showcased the superiority of the DMS-VCR system over conventional VCR systems.
2. A 10.45% reduction in power consumption and a decrease in CO_2 emissions from 124 to 110 tons/year were observed with the adoption of the DMS-VCR system.
3. The DMS-VCR system contributed to an 11.30% reduction in the cost of environmental damage, highlighting its environmental benefits.

4. Parametric analysis underscored the importance of optimal system configurations for achieving cost-effectiveness while minimizing environmental impact.
5. The overall annual cost of operating the DMS-VCR system was found to be 6.72% more cost-effective compared to an equivalent VCR system.

Energy, Exergy, and CSB Analysis:

1. Analysis employing energy, exergy, and CSB approaches reaffirmed the energy efficiency and optimization potential of the DMS-VCR system.
2. Improved COP and exergetic efficiency, along with reduced irreversibility rates, highlighted the benefits of dedicated mechanical subcooling.
3. Parametric optimization recommendations emphasized the importance of low condenser temperature, high evaporator temperature, and low degree of overlap for optimal system performance.

Advanced Exergy Analysis:

1. Advanced exergy analysis provided valuable insights into system performance, identifying avoidable irreversibility rates for system components.
2. Improvements in component parameter efficiency led to significant reductions in irreversibility and enhanced overall system performance.
3. The DMS-VCR system emerged as a potential energy-efficient cooling solution with sustainability at its foundation, offering promising avenues for further research and development.

In summary, this research has advanced the understanding of vapor compression refrigeration systems, emphasizing the importance of integrating theoretical insights with practical experimentation. The findings underscore the significance of considering energy, exergy, economic, and environmental aspects in system design and optimization. Through meticulous parametric optimization and innovative design strategies, the DMS-VCR system emerges as a promising solution for achieving optimal performance, cost-effectiveness, and environmental sustainability. The development of experimental setups and the application of advanced exergy analysis represent significant strides towards advancing refrigeration technology for a more sustainable and energy-efficient future. As the refrigeration industry continues to evolve, the insights gained from this research will serve as a valuable foundation for future endeavours and industry innovations, ultimately contributing to a more sustainable and resilient global cooling infrastructure.

8.2 RECOMMENDATIONS FOR FUTURE WORK

Based on the conclusions drawn from the thesis, several recommendations for future work can be made to further advance research in the field of vapor compression refrigeration systems:

1. Experimental Validation and Parametric Analysis: Conduct experimental studies to validate the findings of the theoretical analysis conducted in the thesis. Additionally, perform more extensive parametric analysis to investigate the effects of varying system parameters such as evaporator temperature, condenser temperature, degree of subcooling, and degree of overlap on system performance.
2. Integration of Renewable Energy Sources: Investigate the integration of renewable energy sources, such as solar energy or waste heat recovery, into vapor compression refrigeration systems. Analyze the feasibility and performance implications of integrating these sources to improve system efficiency and reduce environmental impact.
3. Optimization of Subcooling Mechanisms: In present analysis there is only one subcooler of 630mm of length in present test rig. However, future development could involve the construction of a test rig with multiple subcoolers of varying lengths. Explore advanced optimization techniques to further optimize the design and operation of dedicated mechanical subcooled vapor compression refrigeration systems. Focus on maximizing system efficiency while minimizing energy consumption and environmental impact.
4. Comparative Studies with Alternative Refrigerants: In present work R134a and R410A refrigerants are used in theoretical and experimental analysis, in future the test rig can be used to conduct comparative studies to evaluate the performance of vapor compression refrigeration systems using alternative refrigerants with lower global warming potential (GWP) and ozone depletion potential (ODP). Compare their energy efficiency, environmental impact, and economic feasibility relative to traditional refrigerants.
5. Development of Smart Control Strategies: Develop and implement smart control strategies using advanced control algorithms and machine learning techniques to optimize the operation of vapor compression refrigeration systems in real-time. Explore adaptive control strategies that can dynamically

adjust system parameters based on changing operating conditions and external factors.

By addressing these recommendations, future research endeavours can contribute to the advancement of vapor compression refrigeration technology, leading to more efficient, sustainable, and environmentally friendly cooling solutions.

LIST OF PUBLICATIONS

The work presented in the thesis has partially appeared as publications in International Journals and National/International Conferences, as listed below:

International Journals (SCI Journals)

1. Naveen Solanki, Akhilesh Arora and Raj Kumar Singh, "Advance exergy and coefficient of structural bond analysis of dedicated mechanical subcooled vapor compression refrigeration system", *International Journal of Refrigeration,* 153 (2023), 266-280.

2. Naveen Solanki, Akhilesh Arora and Raj Kumar Singh, "A comprehensive parametric and structural bond analysis of an actual vapor compression refrigeration system with dedicated mechanical subcooled system", *Journal of Mechanical Science & Technology,* 38(1), 2024.

3. Naveen Solanki, Akhilesh Arora and Raj Kumar Singh, "A comprehensive energy, exergy, environmental and economic analysis of dedicated mechanical subcooled vapor compression refrigeration system", *Journal of Thermal Analysis and Calorimetry*, Volume 149, pages 1141–1154, (2024).

International Journals (eSCI Journals)

4. Naveen Solanki, Akhilesh Arora and Raj Kumar Singh, "Performance enhancement and environmental analysis of vapor compression refrigeration system with dedicated mechanical subcooling", *International Journal of air conditioning and refrigeration*, 31(2023), 26.

International Conferences

5. Naveen Solanki, Akhilesh Arora and Raj Kumar Singh, "Comparative performance study of vapor compression refrigeration system with dedicated mechanical subcooling using R134a, R600a, and R1234yf", 2nd International Conference on "Energy Resources and Technologies for Sustainable Development, ICERTSD-2023, Paper Id: 224, 27th – 28th April 2023 at Indian Institute of Engineering Science and Technology (IIEST), Shibpur, Howrah, West Bengal, India.

6. Naveen Solanki, Akhilesh Arora and Raj Kumar Singh, "Energy and exergy destruction analysis of vapor compression refrigeration system with dedicated mechanical subcooling using refrigerant R134a and R410A", 4th International Conference on Recent Advancements in Mechanical Engineering (ICRAME-2023) Paper ID: - 197, 03rd – 05th February 2023 at Department of Mechanical engineering, National Institute of Technology, Silchar – 788010, Assam, India.

7. Naveen Solanki, Akhilesh Arora and Raj Kumar Singh, "Performance Comparison of Refrigerants Hfo1234yf and Hfo1234ze In a Vapor Compression Refrigeration System Operating Under Fouled Conditions", *4th International conference on emerging trends in mechanical and Industrial engineering* (ICETMIE-2019), Paper no. 2019ICETMIE11TH, 10th -11th Oct-2019, The NorthCap University, Haryana, Gurugram, India.

8. Naveen Solanki, Akhilesh Arora and Raj Kumar Singh, "Performance Evaluation of Fouled Evaporator Vapor Compression System", *International conference on recent advances in mechanical engineering* (RAME-2016), Paper no. 39, Oct-2016, DTU, Delhi, India, ISBN-978-194523970-0.

References

[1] Z. jiu Chen and W. han Lin, "Dynamic simulation and optimal matching of a small-scale refrigeration system", *Int. J. Refrig.*, vol 14, no 6, bll 329–335, 1991, doi: 10.1016/0140-7007(91)90028-F.

[2] X. Wang, Y. Hwang, and R. Radermacher, "Investigation of potential benefits of compressor cooling", *Appl. Therm. Eng.*, vol 28, no 14–15, bll 1791–1797, Okt 2008, doi: 10.1016/j.applthermaleng.2007.11.010.

[3] A. Arora and S. C. Kaushik, "Theoretical analysis of a vapour compression refrigeration system with R502, R404A and R507A", *Int. J. Refrig.*, vol 31, no 6, bll 998–1005, 2008, doi: 10.1016/j.ijrefrig.2007.12.015.

[4] J. ur R. Khan and S. M. Zubair, "Design and performance evaluation of reciprocating refrigeration systems", *Int. J. Refrig.*, vol 22, no 3, bll 235–243, 1999, doi: 10.1016/S0140-7007(98)00034-6.

[5] J. Winkler, V. Aute, and R. Radermacher, "Comprehensive investigation of numerical methods in simulating a steady-state vapor compression system", *Int. J. Refrig.*, vol 31, no 5, bll 930–942, 2008, doi: 10.1016/j.ijrefrig.2007.08.008.

[6] R. Cabello, J. Navarro, and E. Torrella, "Simplified steady-state modelling of a single stage vapour compression plant. Model development and validation", *Appl. Therm. Eng.*, vol 25, no 11–12, bll 1740–1752, 2005, doi: 10.1016/j.applthermaleng.2004.10.012.

[7] C. Aprea and A. Greco, "Performance evaluation of R22 and R407C in a vapour compression plant with reciprocating compressor", *Appl. Therm. Eng.*, vol 23, no 2, bll 215–227, 2003, doi: 10.1016/S1359-4311(02)00160-6.

[8] V. S. Chakravarthy, R. K. Shah, and G. Venkatarathnam, "A review of refrigeration methods in the temperature range 4-300 K", *J. Therm. Sci. Eng. Appl.*, vol 3, no 2, bll 1–19, 2011, doi: 10.1115/1.4003701.

[9] Y. Yao, W. Wang, and M. Huang, "A state-space dynamic model for vapor compression refrigeration system based on moving-boundary formulation", *Int. J. Refrig.*, vol 60, bll 174–189, 2015, doi: 10.1016/j.ijrefrig.2015.07.027.

[10] T. K. Nunes, J. V. C. Vargas, J. C. Ordonez, D. Shah, and L. C. S. Martinho, "Modeling, simulation and optimization of a vapor compression refrigeration system dynamic and steady state response", *Appl. Energy*, vol 158, bll 540–555, 2015, doi: 10.1016/j.apenergy.2015.08.098.

[11] H. Sayyaadi and M. Nejatolahi, "Multi-objective optimization of a cooling tower assisted vapor compression refrigeration system", *Int. J. Refrig.*, vol 34, no 1, bll 243–256, 2011, doi: 10.1016/j.ijrefrig.2010.07.026.

[12] R. Selbaş, Ö. Kizilkan, and A. Şencan, "Thermoeconomic optimization of subcooled and superheated vapor compression refrigeration cycle", *Energy*, vol 31, no 12, bll 2108–2128, 2006, doi: 10.1016/j.energy.2005.10.015.

[13] C. Park, H. Lee, Y. Hwang, and R. Radermacher, "Recent advances in vapor

compression cycle technologies", *Int. J. Refrig.*, vol 60, no 2015, bll 118–134, 2015, doi: 10.1016/j.ijrefrig.2015.08.005.

[14] S. Agarwal, A. Arora, and B. B. Arora, *Exergy Analysis of Dedicated Mechanically Subcooled Vapour Compression Refrigeration Cycle Using HFC-R134a, HFO-R1234ze and R1234yf*, vol 36. Springer Singapore, 2020. doi: 10.1007/978-981-13-7557-6_3.

[15] J. Catalán-Gil, R. Llopis, D. Sánchez, L. Nebot-Andrés, and R. Cabello, "Energy analysis of dedicated and integrated mechanical subcooled CO 2 boosters for supermarket applications", *Int. J. Refrig.*, vol 101, bll 11–23, 2019, doi: 10.1016/j.ijrefrig.2019.01.034.

[16] G. B. Wang and X. R. Zhang, "Thermoeconomic optimization and comparison of the simple single-stage transcritical carbon dioxide vapor compression cycle with different subcooling methods for district heating and cooling", *Energy Convers. Manag.*, vol 185, no November 2018, bll 740–757, 2019, doi: 10.1016/j.enconman.2019.02.024.

[17] X. She, Y. Yin, and X. Zhang, "A proposed subcooling method for vapor compression refrigeration cycle based on expansion power recovery", *Int. J. Refrig.*, vol 43, bll 50–61, 2014, doi: 10.1016/j.ijrefrig.2014.03.008.

[18] G. Pottker and P. Hrnjak, "Effect of the condenser subcooling on the performance of vapor compression systems", *Int. J. Refrig.*, vol 50, no 217, bll 156–164, 2015, doi: 10.1016/j.ijrefrig.2014.11.003.

[19] G. Pottker and P. Hrnjak, "Experimental investigation of the effect of condenser subcooling in R134a and R1234yf air-conditioning systems with and without internal heat exchanger", *Int. J. Refrig.*, vol 50, bll 104–113, 2015, doi: 10.1016/j.ijrefrig.2014.10.023.

[20] J. P. Koeln and A. G. Alleyne, "Optimal subcooling in vapor compression systems via extremum seeking control: Theory and experiments", *Int. J. Refrig.*, vol 43, bll 14–25, 2014, doi: 10.1016/j.ijrefrig.2014.03.012.

[21] M. H. Yang and R. H. Yeh, "Performance and exergy destruction analysis of optimal subcooling for vapor-compression refrigeration systems", *Int. J. Heat Mass Transf.*, vol 87, bll 1–10, 2015, doi: 10.1016/j.ijheatmasstransfer.2015.03.085.

[22] L. Yang and C. L. Zhang, "Analysis on energy saving potential of integrated supermarket HVAC and refrigeration systems using multiple subcoolers", *Energy Build.*, vol 42, no 2, bll 251–258, 2010, doi: 10.1016/j.enbuild.2009.08.021.

[23] B. A. Qureshi and S. M. Zubair, "The effect of refrigerant combinations on performance of a vapor compression refrigeration system with dedicated mechanical sub-cooling", *Int. J. Refrig.*, vol 35, no 1, bll 47–57, 2012, doi: 10.1016/j.ijrefrig.2011.09.009.

[24] B. A. Qureshi, M. Inam, M. A. Antar, and S. M. Zubair, "Experimental energetic analysis of a vapor compression refrigeration system with dedicated mechanical sub-cooling", *Appl. Energy*, vol 102, bll 1035–1041, 2013, doi: 10.1016/j.apenergy.2012.06.007.

[25] B. A. Qureshi and S. M. Zubair, “Mechanical sub-cooling vapor compression systems: Current status and future directions”, *Int. J. Refrig.*, vol 36, no 8, bll 2097–2110, 2013, doi: 10.1016/j.ijrefrig.2013.07.026.

[26] N. A. Ansari, A. Arora, Samsher, and K. Manjunath, *The Effect of Eco-friendly Refrigerants on Performance of Vapor Compression Refrigeration System with Dedicated Mechanical Subcooling*, vol 36. Springer Singapore, 2020. doi: 10.1007/978-981-13-7557-6_4.

[27] R. Llopis, G. Toffoletti, L. Nebot-Andrés, and G. Cortella, “Experimental evaluation of zeotropic refrigerants in a dedicated mechanical subcooling system in a CO_2 cycle”, *Int. J. Refrig.*, vol 128, bll 287–298, 2021, doi: 10.1016/j.ijrefrig.2021.05.028.

[28] P. D’Agaro, M. A. Coppola, and G. Cortella, “Effect of dedicated mechanical subcooler size and gas cooler pressure control on transcritical CO_2 booster systems”, *Appl. Therm. Eng.*, vol 182, bl 116145, 2021, doi: 10.1016/j.applthermaleng.2020.116145.

[29] L. Nebot-Andrés, D. Sánchez, D. Calleja-Anta, R. Cabello, and R. Llopis, “Experimental determination of the optimum working conditions of a commercial transcritical CO_2 refrigeration plant with a R-152a dedicated mechanical subcooling.”, *Int. J. Refrig.*, vol 121, bll 258–268, 2021, doi: 10.1016/j.ijrefrig.2020.10.002.

[30] E. Chen, Z. Li, J. Yu, Y. Xu, and Y. Yu, “Experimental research of increased cooling output by dedicated subcooling”, *Appl. Therm. Eng.*, vol 154, no February, bll 9–17, 2019, doi: 10.1016/j.applthermaleng.2019.03.071.

[31] J. W. Thornton, S. A. Klein, and J. W. Mitchell, “Dedicated mechanical subcooling design strategies for supermarket applications”, *Int. J. Refrig.*, vol 17, no 8, bll 508–515, 1994, doi: 10.1016/0140-7007(94)90026-4.

[32] R. Llopis, L. Nebot-Andrés, D. Sánchez, J. Catalán-Gil, and R. Cabello, “Subcooling methods for CO_2 refrigeration cycles: A review”, *Int. J. Refrig.*, vol 93, bll 85–107, 2018, doi: 10.1016/j.ijrefrig.2018.06.010.

[33] R. Llopis, R. Cabello, D. Sánchez, and E. Torrella, “Energy improvements of CO_7transcritical refrigeration cycles using dedicated mechanical subcooling”, *Int. J. Refrig.*, vol 55, bll 129–141, 2015, doi: 10.1016/j.ijrefrig.2015.03.016.

[34] R. Llopis, L. Nebot-Andrés, R. Cabello, D. Sánchez, and J. Catalán-Gil, “Évaluation expérimentale d’une installation frigorifique transcritique au CO_2 avec un sous-refroidissement mécanique dédié”, *Int. J. Refrig.*, vol 69, bll 361–368, 2016, doi: 10.1016/j.ijrefrig.2016.06.009.

[35] G. V. Ochoa, “Design of a mechanical subcooling system device for increasing a low temperature refrigeration system’s capacity”, *Prospectiva*, vol 11, no 2, bl 13, 2014, doi: 10.15665/rp.v11i2.33.

[36] F. De Monte, “Calculation of thermodynamic properties of R407C and R410A by the Martin-Hou equation of state - Part I: Theoretical development”, *Int. J. Refrig.*, vol 25, no 3, bll 306–313, 2002, doi: 10.1016/S0140-7007(01)00028-7.

[37] E. U. Küçüksille, R. Selbaş, and A. Şencan, “Data mining techniques for thermophysical properties of refrigerants”, *Energy Convers. Manag.*, vol 50, no 2, bll 399–412, 2009, doi: 10.1016/j.enconman.2008.09.002.

[38] A. Arora and H. L. Sachdev, “Thermodynamic analysis of R422 series refrigerants as alternative refrigerants to HCFC22 in a vapour compression refrigeration system”, *Int. J. Energy Res.*, vol 33, no 8, bll 753–765, Jun 2009, doi: 10.1002/er.1508.

[39] J. M. Calm, “The next generation of refrigerants - Historical review, considerations, and outlook”, *Int. J. Refrig.*, vol 31, no 7, bll 1123–1133, 2008, doi: 10.1016/j.ijrefrig.2008.01.013.

[40] M. O. Mclinden, M. Thol, and E. W. Lemmon, “Thermodynamic Properties of Measurements of Density and Vapor Pressure and a Comprehensive Equation of State”, *Proc. Thirteen. Int. Refrig. Air Cond. Conf. Purdue*, bl PaperID: 1041, 2010.

[41] P. Reasor, V. Aute, and R. Radermacher, “Refrigerant R1234yf Performance Comparison Investigation”, *Int. Refrig. Air Cond. Conf. Purdue*, bll 1–7, 2010.

[42] A. Pearson, “Carbon dioxide - New uses for an old refrigerant”, *Int. J. Refrig.*, vol 28, no 8, bll 1140–1148, 2005, doi: 10.1016/j.ijrefrig.2005.09.005.

[43] K. M. Karber, O. Abdelaziz, and E. A. Vineyard, “Experimental Performance of R-1234yf and R-1234ze as Drop-in Replacements for R-134a in Domestic Refrigerators”, *Int. Refrig. Air Cond. Conf. Purdue, West Lafayette, IN, USA, July 16-19, 2012*, no July, bll 1–10, 2012.

[44] B. Saleh and M. Wendland, “Screening of pure fluids as alternative refrigerants”, *Int. J. Refrig.*, vol 29, no 2, bll 260–269, 2006, doi: 10.1016/j.ijrefrig.2005.05.009.

[45] J. S. Brown, C. Zilio, and A. Cavallini, “The fluorinated olefin R-1234ze(Z) as a high-temperature heat pumping refrigerant”, *Int. J. Refrig.*, vol 32, no 6, bll 1412–1422, 2009, doi: 10.1016/j.ijrefrig.2009.03.002.

[46] J. S. Brown, C. Zilio, and A. Cavallini, “Thermodynamic properties of eight fluorinated olefins”, *Int. J. Refrig.*, vol 33, no 2, bll 235–241, 2010, doi: 10.1016/j.ijrefrig.2009.04.005.

[47] P. Makhnatch and R. Khodabandeh, “The role of environmental metrics (GWP, TEWI, LCCP) in the selection of low GWP refrigerant”, *Energy Procedia*, vol 61, bll 2460–2463, 2014, doi: 10.1016/j.egypro.2014.12.023.

[48] J. E. Mora R, C. Pérez T, F. F. González N, and J. D. D. Ocampo D, “Thermodynamic properties of refrigerants using artificial neural networks”, *Int. J. Refrig.*, vol 46, bll 9–16, 2014, doi: 10.1016/j.ijrefrig.2014.07.007.

[49] A. G. Deveciotlu and V. Oruç, “Characteristics of Some New Generation Refrigerants with Low GWP”, *Energy Procedia*, vol 75, bll 1452–1457, 2015, doi: 10.1016/j.egypro.2015.07.258.

[50] A. Y. Sulaiman, D. Cotter, C. Arpagaus, and N. Hewitt, “Theoretical evaluation of energy, exergy, and minimum superheat in a high-temperature heat pump with low GWP refrigerants”, *Int. J. Refrig.*, vol 153, no May, bll 99–109, 2023, doi: 10.1016/j.ijrefrig.2023.06.001.

[51] G. Tsatsaronis and M. H. Park, “On avoidable and unavoidable exergy destructions and investment costs in thermal systems”, *Energy Convers. Manag.*, vol 43, no 9–12, bll 1259–1270, 2002, doi: 10.1016/S0196-8904(02)00012-2.

[52] T. Morosuk and G. Tsatsaronis, “A new approach to the exergy analysis of absorption refrigeration machines”, *Energy*, vol 33, no 6, bll 890–907, 2008, doi: 10.1016/j.energy.2007.09.012.

[53] S. Kelly, G. Tsatsaronis, and T. Morosuk, “Advanced exergetic analysis: Approaches for splitting the exergy destruction into endogenous and exogenous parts”, *Energy*, vol 34, no 3, bll 384–391, 2009, doi: 10.1016/j.energy.2008.12.007.

[54] T. Morosuk and G. Tsatsaronis, “Advanced exergetic evaluation of refrigeration machines using different working fluids”, *Energy*, vol 34, no 12, bll 2248–2258, 2009, doi: 10.1016/j.energy.2009.01.006.

[55] A. H. Mosaffa, L. Garousi Farshi, C. A. Infante Ferreira, and M. A. Rosen, “Advanced exergy analysis of an air conditioning system incorporating thermal energy storage”, *Energy*, vol 77, bll 945–952, 2014, doi: 10.1016/j.energy.2014.10.006.

[56] S. Gong and K. Goni Boulama, “Parametric study of an absorption refrigeration machine using advanced exergy analysis”, *Energy*, vol 76, bll 453–467, 2014, doi: 10.1016/j.energy.2014.08.038.

[57] F. A. Boyaghchi and H. Molaie, “Sensitivity analysis of exergy destruction in a real combined cycle power plant based on advanced exergy method”, *Energy Convers. Manag.*, vol 99, bll 374–386, 2015, doi: 10.1016/j.enconman.2015.04.048.

[58] D. Colorado, “Advanced exergy analysis applied to a single-stage heat transformer”, *Appl. Therm. Eng.*, vol 116, no January, bll 584–596, 2017, doi: 10.1016/j.applthermaleng.2017.01.109.

[59] G. Liao, J. E, F. Zhang, J. Chen, and E. Leng, “Advanced exergy analysis for Organic Rankine Cycle-based layout to recover waste heat of flue gas”, *Appl. Energy*, vol 266, no February, bl 114891, 2020, doi: 10.1016/j.apenergy.2020.114891.

[60] R. D. Misra, P. K. Sahoo, and A. Gupta, “Thermoeconomic optimization of a LiBr/H 2O absorption chiller using structural method”, *J. Energy Resour. Technol. Trans. ASME*, vol 127, no 2, bll 119–124, 2005, doi: 10.1115/1.1830049.

[61] D. Boer, M. Medrano, and M. Nogués, “Exergy and structural analysis of an absorption cooling cycle and the effect of efficiency parameters”, *ECOS 2005 - Proc. 18th Int. Conf. Effic. Cost, Optim. Simulation, Environ. Impact Energy Syst.*, vol 8, no 4, bll 337–344, 2005.

[62] T. Tekin and M. Bayramoğlu, “Exergy and structural analysis of raw juice production and steam-power units of a sugar production plant”, *Energy*, vol 26, no 3, bll 287–297, 2001, doi: 10.1016/S0360-5442(00)00068-2.

[63] C. Nikolaidis and D. Probert, “Exergy-method analysis of a two-stage vapour-compression refrigeration-plants performance”, *Appl. Energy*, vol 60, no 4, bll 241–256, 1998, doi: 10.1016/S0306-2619(98)00030-0.

[64] A. Arora, B. B. Arora, B. D. Pathak, and H. L. Sachdev, “Exergy analysis of a Vapour Compression Refrigeration system with R-22, R-407C and R-410A”, *Int. J. Exergy*, vol 4, no 4, bll 441–454, 2007, doi: 10.1504/IJEX.2007.015083.

[65] J. U. Ahamed, R. Saidur, and H. H. Masjuki, “A review on exergy analysis of vapor compression refrigeration system”, *Renew. Sustain. Energy Rev.*, vol 15, no 3, bll 1593–1600, 2011, doi: 10.1016/j.rser.2010.11.039.

[66] F. Molés, J. Navarro-Esbrí, B. Peris, A. Mota-Babiloni, and Á. Barragán-Cervera, “Theoretical energy performance evaluation of different single stage vapour compression refrigeration configurations using R1234yf and R1234ze(E) as working fluids”, *Int. J. Refrig.*, vol 44, bll 141–150, 2014, doi: 10.1016/j.ijrefrig.2014.04.025.

[67] T. Menlik, A. Demircioğlu, and M. G. Özkaya, “Energy and exergy analysis of R22 and its alternatives in a vapour compression refrigeration system”, *Int. J. Exergy*, vol 12, no 1, bll 11–30, 2013, doi: 10.1504/IJEX.2013.052568.

[68] P. K. Nag, “Basic And Applied Thermodynamics by PK Nag: Thermodynamics by PK Nag”. bl 781, 2002.

[69] M. Aminyavari, B. Najafi, A. Shirazi, and F. Rinaldi, “Exergetic, economic and environmental (3E) analysis, and multi-objective optimization of a CO_2/NH_3 cascade refrigeration system”, *Appl. Therm. Eng.*, vol 65, no 1–2, bll 42–50, 2014, doi: 10.1016/j.applthermaleng.2013.12.075.

[70] S. Agarwal, “Thermodynamic Performance Analysis of Dedicated Mechanically Subcooled Vapour Compression Refrigeration System”, *J. Therm. Eng.*, vol 5, no 4, bll 222–233, 2019, doi: 10.18186/thermal.581741.

[71] B. A. Qureshi and S. M. Zubair, “Cost optimization of heat exchanger inventory for mechanical subcooling refrigeration cycles”, *Int. J. Refrig.*, vol 36, no 4, bll 1243–1253, 2013, doi: 10.1016/j.ijrefrig.2013.02.011.

[72] V. Zare, S. M. S. Mahmoudi, M. Yari, and M. Amidpour, “Thermoeconomic analysis and optimization of an ammonia-water power/cooling cogeneration cycle”, *Energy*, vol 47, no 1, bll 271–283, 2012, doi: 10.1016/j.energy.2012.09.002.

[73] B. Dai, “Evaluation of transcritical CO_2 heat pump system integrated with mechanical subcooling by utilizing energy, exergy and economic methodologies for residential heating”, *Energy Convers. Manag.*, vol 192, no March, bll 202–220, 2019, doi: 10.1016/j.enconman.2019.03.094.

[74] B. Dai, “Energetic, exergetic and exergoeconomic assessment of transcritical CO_2 reversible system combined with dedicated mechanical subcooling (DMS) for residential heating and cooling”, *Energy Convers. Manag.*, vol 209, no February, bl 112594, 2020, doi: 10.1016/j.enconman.2020.112594.

[75] B. Dai, “Environmental and economical analysis of transcritical CO_2 heat pump combined with direct dedicated mechanical subcooling (DMS) for space heating in China”, *Energy Convers. Manag.*, vol 198, no October 2018, bl 111317, 2019, doi: 10.1016/j.enconman.2019.01.119.

[76] A. Z. Miran, A. Nemati, and M. Yari, “Performance analysis and exergoeconomic evaluation of a TRC system enhanced by a dedicated mechanical subcooling”, *Energy Convers. Manag.*, vol 197, no May, bl 111890, 2019, doi: 10.1016/j.enconman.2019.111890.

[77] K. Golbaten Mofrad, S. Zandi, G. Salehi, and M. H. Khoshgoftar Manesh, “4E analysis and multi-objective optimization of cascade refrigeration cycles with heat recovery system”, *Therm. Sci. Eng. Prog.*, vol 19, bl 100613, 2020, doi: 10.1016/j.tsep.2020.100613.

[78] D. Tsimpoukis *et al.*, “Energy and environmental investigation of R744 all-in-one configurations for refrigeration and heating/air conditioning needs of a supermarket”, *J. Clean. Prod.*, vol 279, bl 123234, 2021, doi: 10.1016/j.jclepro.2020.123234.

[79] B. Bakhtiari, L. Fradette, R. Legros, and J. Paris, “A model for analysis and design of H_2O-LiBr absorption heat pumps”, *Energy Convers. Manag.*, vol 52, no 2, bll 1439–1448, 2011, doi: 10.1016/j.enconman.2010.09.037.

[80] S. Sanaye and H. R. Malekmohammadi, “Thermal and economical optimization of air conditioning units with vapor compression refrigeration system”, *Appl. Therm. Eng.*, vol 24, no 13, bll 1807–1825, 2004, doi: 10.1016/j.applthermaleng.2003.12.017.

[81] Ö. Kizilkan, A. Şencan, and S. A. Kalogirou, “Thermoeconomic optimization of a LiBr absorption refrigeration system”, *Chem. Eng. Process. Process Intensif.*, vol 46, no 12, bll 1376–1384, 2007, doi: 10.1016/j.cep.2006.11.007.

[82] V. Jain, G. Sachdeva, and S. S. Kachhwaha, “NLP model based thermoeconomic optimization of vapor compression-absorption cascaded refrigeration system”, *Energy Convers. Manag.*, vol 93, bll 49–62, 2015, doi: 10.1016/j.enconman.2014.12.095.

[83] KOTAS "the-exergy-method-of-thermal-plant-analysis", Page - 198 for CSB Explanation.

[84] X. H. Han, Y. Qiu, P. Li, Y. J. Xu, Q. Wang, and G. M. Chen, “Cycle performance studies on HFC-161 in a small-scale refrigeration system as an alternative refrigerant to HFC-410A”, *Energy Build.*, vol 44, no 1, bll 33–38, 2012, doi: 10.1016/j.enbuild.2011.10.004.

[85] S. M. Hojjat Mohammadi and M. Ameri, “Energy and exergy comparison of a cascade air conditioning system using different cooling strategies”, *Int. J. Refrig.*, vol 41, bll 14–26, 2014, doi: 10.1016/j.ijrefrig.2013.06.015.

[86] B. A. Qureshi and S. M. Zubair, “The impact of fouling on performance of a vapor compression refrigeration system with integrated mechanical sub-cooling system”, *Appl. Energy*, vol 92, bll 750–762, 2012, doi: 10.1016/j.apenergy.2011.08.021.

[87] Y. Commercial and I. Hvac, “YORK ® Commercial & Industrial HVAC 2018”, 2018.

[88] V. Jain, G. Sachdeva, and S. S. Kachhwaha, “Comparative performance study and advanced exergy analysis of novel vapor compression-absorption integrated refrigeration system”, *Energy Convers. Manag.*, vol 172, no May, bll 81–97, 2018, doi: 10.1016/j.enconman.2018.06.116.

[89] L. Nebot-Andrés, D. Sánchez, D. Calleja-Anta, R. Cabello, and R. Llopis,

"Experimental determination of the optimum working conditions of a commercial transcritical CO_2 refrigeration plant with a R-152a dedicated mechanical subcooling.", *Int. J. Refrig.*, vol 121, bll 258–268, 2021, doi: 10.1016/j.ijrefrig.2020.10.002.

[90] K. Sumeru, M. F. Sukri, T. P. Pramudantoro, E. Erham, and R. Muliawan, "Experimental evaluation on a centralized air conditioning system embedded with a split-type air conditioner as a dedicated subcooler", *J. Build. Eng.*, vol 43, no November 2020, bl 102585, 2021, doi: 10.1016/j.jobe.2021.102585.

[91] A. Kilicarslan, "An experimental investigation of a different type vapor compression cascade refrigeration system", *Appl. Therm. Eng.*, vol 24, no 17–18, bll 2611–2626, 2004, doi: 10.1016/j.applthermaleng.2004.04.004.

[92] M. Ozsipahi, H. A. Kose, H. Kerpicci, and H. Gunes, "Experimental study of R290/R600a mixtures in vapor compression refrigeration system", *Int. J. Refrig.*, vol 133, bll 247–258, Jan 2022, doi: 10.1016/j.ijrefrig.2021.10.004.

[93] S. G. Kim and M. S. Kim, "Experiment and simulation on the performance of an autocascade refrigeration system using carbon dioxide as a refrigerant", *Int. J. Refrig.*, vol 25, no 8, bll 1093–1101, 2002, doi: 10.1016/S0140-7007(01)00110-4.

[94] Y. Xuan and G. Chen, "Experimental study on HFC-161 mixture as an alternative refrigerant to R502", *Int. J. Refrig.*, vol 28, no 3, bll 436–441, 2005, doi: 10.1016/j.ijrefrig.2004.04.003.

[95] B. Niu and Y. Zhang, "Experimental study of the refrigeration cycle performance for the R744/R290 mixtures", *Int. J. Refrig.*, vol 30, no 1, bll 37–42, 2007, doi: 10.1016/j.ijrefrig.2006.06.002.

[96] V. Venkatramanamurthy and P. Senthil Kumar, "Experimental Comparative energy, exergy flow and second law efficiency analysis of R22, R436b vapour compression refrigeration cycles", *Int. J. Eng. Sci. Technol.*, vol 2, no 5, bll 1399–1412, 2010.

[97] J. Navarro-Esbrí, J. M. Mendoza-Miranda, A. Mota-Babiloni, A. Barragán-Cervera, and J. M. Belman-Flores, "Experimental analysis of R1234yf as a drop-in replacement for R134a in a vapor compression system", *Int. J. Refrig.*, vol 36, no 3, bll 870–880, 2013, doi: 10.1016/j.ijrefrig.2012.12.014.

[98] A. Chesi, F. Esposito, G. Ferrara, and L. Ferrari, "Experimental analysis of R744 parallel compression cycle", *Appl. Energy*, vol 135, bll 274–285, 2014, doi: 10.1016/j.apenergy.2014.08.087.

[99] G. Yan, Y. Feng, and L. Peng, "Experimental analysis of a novel cooling system driven by liquid refrigerant pump and vapor compressor", *Int. J. Refrig.*, vol 49, bll 11–18, 2015, doi: 10.1016/j.ijrefrig.2014.09.017.

[100] J. Gill and J. Singh, "Experimental Analysis of R134a/LPG as Replacement of R134a in a Vapor-Compression Refrigeration System", *Int. J. Air-Conditioning Refrig.*, vol 25, no 2, bll 1–13, 2017, doi: 10.1142/S2010132517500158.

[101] S. Anand and S. K. Tyagi, "Exergy analysis and experimental study of a vapor compression refrigeration cycle: A technical note", *J. Therm. Anal. Calorim.*, vol 110, no 2, bll 961–971, 2012, doi: 10.1007/s10973-011-1904-z.

APPENDIX A

ERRORS AND UNCERTAINTIES

A.1. SOURCES OF ERROR

In the experimental analysis of a dedicated mechanical subcooled vapor compression refrigeration system, errors and uncertainties can occur from different sources, potentially impacting the correctness and consistency of the results. The various sources of error are as specified below:

1. **Instrument errors:** Some errors are inherent in instrument systems and may result from inadequate design or construction. Factors such as errors in graduated scale divisions, unevenness in balance arms, or irregular tension in springs can contribute to such inaccuracies. To mitigate instrument errors, one can: (i) choose an appropriate instrument for the specific application, (ii) apply corrections after quantifying the instrument error, and (iii) calibrate the instrument against an appropriate standard.
2. **Measurement Errors**: Errors can occur during the measurement process due to limitations in the accuracy and precision of the instruments used. For instance, temperature sensors, pressure gauges, flow meters, and other measuring devices may have inherent inaccuracies.
3. **Round off error:** It refers to the value that needs to be added to the finite representation of a computed number to make it an accurate representation of that number.This error also exists in the present work. However the order of this error is about 0.0001.
4. **Truncation error:** It is the quantity which must be added to the true representation of the quantity in order that the result is exactly equal to the quantity, which is seeking to generate. This error is a result of the approximate formulae used which are based in truncated series.
5. **Calibration Errors**: Inaccurate calibration of instruments can lead to systematic errors in the measurements. It's crucial to regularly calibrate all equipment to ensure reliable data collection.
6. **Human Factors:** Errors made by experimenters, such as misreading instruments or improper data recording, can contribute to uncertainties in the results.
7. **Environmental Effects:** Fluctuations in ambient conditions, such as temperature and humidity, can affect system performance and introduce uncertainties.

8. **Uncertainties in Properties:** Variations in properties of the working fluid, such as refrigerant properties, can introduce uncertainties. Factors like temperature and pressure can influence these properties, and small deviations from expected values can affect system performance.
9. **Data Processing Errors**: Errors can occur during the processing and analysis of experimental data. Incorrect data manipulation or interpretation can lead to misleading conclusions.
10. **Improper application of the instrument**: These errors occur when instruments are utilized in conditions that deviate from their intended operating parameters. Factors such as intense vibrations, mechanical shocks, or interference from electrical noise can introduce substantial errors, rendering the test data unreliable. In such situations, it's imperative to pause the experiment until the disruptive elements responsible for these significant errors are identified and rectified.

To minimize errors and uncertainties, researchers typically employ rigorous experimental procedures, calibrate instruments regularly, conduct multiple trials, and apply appropriate data analysis techniques, such as error propagation analysis. Additionally, sensitivity analysis can help identify which parameters have the most significant impact on the results, allowing researchers to focus their efforts on reducing uncertainties in those areas.

A.2. ERRORS AND UNCERTAINTIES ASSOCIATED IN PRESENT WORK

The various performance parameters of instruments are determined through specific tests tailored to their type and intended use. Certain key static performance parameters undergo periodic evaluation via static calibration. During this process, consistent 'known' inputs are applied, and the resulting output is observed. However, it experience difficulty in obtaining known constant values of the input quantity. Further, it is also come across the following difficulties:

i) Changes in instrument sensitivity resulting from certain disturbances can affect all output values, typically to the same degree. These changes may occur due to factors such as worn-out parts or environmental fluctuations affecting both the equipment and the user.

ii) When an instrument fails to produce consistent output for repeated applications of a specific input value, it leads to scatter in output values within a defined range. This scattering effect arises from random variations in the parameter or the measurement system itself.

Every measurement inherently carries some degree of inaccuracy and imprecision. Hence, understanding the different types of errors and uncertainties associated with a measurement system is crucial (refer to Table A-1). Additionally, knowing how these errors propagate is essential. Detecting errors enables their elimination or adjustment through suitable corrections. Conversely, unrecognized errors challenge the reliability of experimental data.

The work presented in Chapter 7 is an experimental one. However in some of the Chapters, for validation of the computer model, the results obtained from the computation model are compared with the reported experimental and theoretical results.

In present experiment test rig various measuring instruments have been mounted/installed at the inlet and outlet of different components of the system to measure the thermophysical properties of working fluid, like temperature, pressure and mass flow rates.

Table A-1 Errors/ uncertainties in various measuring instruments

S. No.	Property	Error/Uncertainty (Instrument)
1	Temperature (T)	± 0.1 K
2	Pressure (P)	± 0.001 bar
3	Power consumption (W)	± 0.01 kWh
4	Mass flow rate of refrigerant ($\dot{m}_{ref}$)	± 0.001 LPM
5	Mass flow rate of water ($\dot{m}_{water}$)	± 0.001 LPM

A.3. UNCERTAINTY ANALYSIS

Propagation of Uncertainties in compound quantities

To determine the total uncertainty resulting from the combined effects of uncertainties in various variables, let's examine the following equation in its most general form:

$$y = f(x_1, x_2 \ldots\ldots\ldots x_i \ldots\ldots\ldots\ldots x_n) \quad \text{(A1)}$$

where y is a parameter that depends on independent variables $x_1, x_2 \ldots\ldots\ldots x_i \ldots\ldots\ldots\ldots x_n$.

Writing above equation in differential form, we get,

$$dy = \frac{\partial y}{\partial x_1} dx_1 + \frac{\partial y}{\partial x_2} dx_2 + \ldots\ldots\ldots \frac{\partial y}{\partial x_i} dx_i + \ldots\ldots\ldots \frac{\partial y}{\partial x_n} dx_n \quad \text{(A-2)}$$

If the quantities dy, dx_1, dx_2,……dx_i……dx_n are considered to be uncertainties Uy, Ux_1, Ux_2,……Ux_i……Ux_n in quantities y, x_1, x_2,…….x_i……..x_n respectively, then from Eq. (A-2) we get,

$$Uy = \frac{\partial y}{\partial x_1}(Ux_1) + \frac{\partial y}{\partial x_2}(Ux_2) + \ldots\ldots\frac{\partial y}{\partial x_i}(Ux_i) + \ldots\ldots\frac{\partial y}{\partial x_n}(Ux_n) \quad \text{(A-3)}$$

In the worst-case scenario, the maximum uncertainty value in y, denoted as Uy_{max}, occurs when all uncertainties happen to have the same sign.

$$\text{i.e. } Uy_{max} = \left|\frac{\partial y}{\partial x_1}(Ux_1)\right| + \left|\frac{\partial y}{\partial x_2}(Ux_2)\right| + \ldots\ldots + \left|\frac{\partial y}{\partial x_i}(Ux_i)\right| + \ldots\ldots + \left|\frac{\partial y}{\partial x_n}(Ux_n)\right| \quad \text{(A-4)}$$

However, the possibility of such an occurrence is quite low. Therefore, a more practical approach is to square both sides of Equation (A-3), which ensures equal consideration for both positive and negative values of uncertainties. Thus, squaring Equation (A-3), we get:

$$Uy^2 = \left\{\left(\frac{\partial y}{\partial x_1}\right)^2 (Ux_1)^2 + \left(\frac{\partial y}{\partial x_2}\right)^2 (Ux_2)^2 + \cdots \left(\frac{\partial y}{\partial x_i}\right)^2 (Ux_i)^2 + \cdots \left(\frac{\partial y}{\partial x_n}\right)^2 (Ux_n)^2\right\} +$$

$$\left\{\left(\frac{\partial y}{\partial x_1}\right)\left(\frac{\partial y}{\partial x_2}\right)(Ux_1)(Ux_2) + \cdots \left(\frac{\partial y}{\partial x_i}\right)\left(\frac{\partial y}{\partial x_j}\right)(Ux_i)(Ux_j) + \cdots\right\} \quad \text{(A-5)}$$

Because of the random nature of uncertainties,Ux_1, Ux_2,……..Ux_i……..Ux_n, there is an equal chance of these uncertainties being either positive or negative. Accordingly, the term in the second bracket of Equation (A-5) tends to be a small quantity and can be ignored.

Therefore, Equation (A-5) simplifies to:

$$Uy = \pm\left\{\left(\frac{\partial y}{\partial x_1}\right)^2 (Ux_1)^2 + \left(\frac{\partial y}{\partial x_2}\right)^2 (Ux_2)^2 + \cdots \left(\frac{\partial y}{\partial x_i}\right)^2 (Ux_i)^2 + \cdots \left(\frac{\partial y}{\partial x_n}\right)^2 (Ux_n)^2\right\}^{1/2} \quad \text{(A-6)}$$

Hence, Uy represents the uncertainty in y resulting from the combined effects of various variables.

Uncertainty analysis of COP for a DMS-VCR system

The uncertainty in the value of COP_{net} is calculated as explained below:

$$COP_{net} = \frac{\dot{Q}_{evap}}{\dot{W}_t} = \frac{\dot{Q}_{evap}}{\dot{W}_{comp1} + \dot{W}_{comp2}} \quad \text{(A-7)}$$

where,

$$\dot{Q}_{evap} = (\dot{m}_{water} * C_p)_{evap}(T_{11} - T_{12}) \quad \text{(A-8)}$$

$$\dot{W}_t = \dot{W}_{comp1} + \dot{W}_{comp1} \quad \text{(A-9)}$$

Putting the values of $\dot{Q}_{evap}$, $\dot{W}_{comp1}$ and $\dot{W}_{comp2}$ the COP_{net} is given by

The uncertainty in the value of COP_{net} is calculated as explained below:

$$COP_{net} = \frac{(\dot{m}_{water} * C_p)_{evap}(T_{11} - T_{12})}{\dot{W}_{comp1} + \dot{W}_{comp2}} \quad \text{(A-10)}$$

Applying the principle explained above, the uncertainty in COP can be expressed as,

$$U_{COP} = \pm \left[\left(\frac{\partial COP}{\partial \dot{m}_{water}}\right)^2 (U\dot{m}_{water})^2 + \left(\frac{\partial COP}{\partial C_p}\right)^2 (UC_p)^2 + \left(\frac{\partial COP}{\partial T_{11}}\right)^2 (UT_{11})^2 + \left(\frac{\partial COP}{\partial T_{12}}\right)^2 (UT_{12})^2 + \left(\frac{\partial COP}{\partial \dot{W}_{comp1}}\right)^2 (U\dot{W}_{comp1})^2 + \left(\frac{\partial COP}{\partial \dot{W}_{comp2}}\right)^2 (U\dot{W}_{comp2})^2 \right]^{1/2} \quad \text{(A-11)}$$

where

$$\left(\frac{\partial COP}{\partial \dot{m}_{water}}\right) = \frac{C_p * (T_{11} - T_{12})}{\dot{W}_{comp1} + \dot{W}_{comp2}} \quad \text{(A-12)}$$

$$\left(\frac{\partial COP}{\partial C_p}\right) = \frac{\dot{m}_{ref1} * (T_{11} - T_{12})}{\dot{W}_{comp1} + \dot{W}_{comp2}} \quad \text{(A-13)}$$

$$\left(\frac{\partial COP}{\partial T_{11}}\right) = \frac{(\dot{m}_{ref1} * C_p)}{\dot{W}_{comp1} + \dot{W}_{comp2}} \quad \text{(A-14)}$$

$$\left(\frac{\partial COP}{\partial T_{12}}\right) = \frac{-(\dot{m}_{ref1} * C_p)}{\dot{W}_{comp1} + \dot{W}_{comp2}} \quad \text{(A-15)}$$

$$\left(\frac{\partial COP}{\partial \dot{W}_{comp1}}\right) = \frac{-(\dot{m}_{ref1} * C_p) * (T_{11} - T_{12})}{(\dot{W}_{comp1} + \dot{W}_{comp2})^2} \quad \text{(A-16)}$$

$$\left(\frac{\partial COP}{\partial \dot{W}_{comp2}}\right) = \frac{-(\dot{m}_{ref1} * C_p) * (T_{11} - T_{12})}{(\dot{W}_{comp1} + \dot{W}_{comp2})^2} \quad \text{(A-17)}$$

The partial derivatives of COP with respect to other variables are computed based on the following operating conditions of the DMS-VCR system:

T_{11}= 35^{o}C T_{12} = 10.3^{o}C, mass flow rate of water = 0.058 ltr/s, specific heat capacity for water Cp = 4.187 kJ/kg.K (corresponding to the values of Set-1). The values are

$\left(\frac{\partial COP}{\partial \dot{m}_{water}}\right) =$ 63.84 $\left(\frac{\partial COP}{\partial C_p}\right) = 0$ $\left(\frac{\partial COP}{\partial T_{11}}\right) = 0.1499$

$\left(\frac{\partial COP}{\partial T_{12}}\right) =$ - 0.1499 $\left(\frac{\partial COP}{\partial W_{comp1}}\right) =$ -2.286 $\left(\frac{\partial COP}{\partial W_{comp2}}\right) =$ -2.286

$U\dot{m}_{water}$ = 0.001 $UC_p = 0$ $UT_{11} = 0.1$

$UT_{12} =$ 0.1 $U\dot{W}_{comp1}$= 0.01 $U\dot{W}_{comp2}$ = 0.01

The uncertainty values of the temperature, pressure, power consumption, mass flow rate of refrigerant and water have already been mentioned in Table A-1 and the same is utilized for calculating the uncertainty in COP. Using these values, uncertainty in COP has been found to be 3.698 ±0.07463

Similar to above the uncertainty analysis for other parameters of DMS-VCR system is also carried out and it is found that uncertainty in $\dot{W}_t$ and $\dot{Q}_{evap}$ are 1.62 ± 0.01414 kW and 5.998 ± 0.109 kW respectively.

ABOUT THE AUTHOR

Mr. Naveen Solanki is currently working as an Assistant Professor in the Department of Mechanical Engineering at Maharaja Agrasen Institute of Technology, affiliated with Guru Gobind Singh Indraprastha University, Delhi, India. He completed his Masters in Engineering (Specialization-Thermal Engineering) from Delhi College of Engineering (DCE), Delhi University, in 2012. He is actively involved with undergraduate projects and academic activities.

He is a Life-Time Member of The India Society of Technical Education (ISTE), and a member of the International Association of Engineers (IAENG). He also actively involved in both, Indian Society of Heating Refrigerating & Air-Conditioning Engineers – ISHRAE, and the American Society of Heating Refrigerating & Air-Conditioning Engineers – ASHRAE.

Additionally, he is a research scholar from Delhi Technological University, formerly known as Delhi College of Engineering, specializing in the field of Refrigeration and Air-conditioning. He has made significant contributions to this field through his extensive research work. His research endeavours have been recognized through publications in various national and international journals and conferences.